

**UNIVERSIDAD DE CHILE**

**FACULTAD DE MEDICINA**

**ESCUELA DE POSTGRADO**



**THESIS FOR APPLYING FOR THE DEGREE OF Ph.D IN  
BIOMEDICAL SCIENCES**

**“Modulation of regulatory B cells through differential activation of  
iNKT cells with glycolipids contained in liposomes”**

**RICHARD GARCÍA BETANCOURT**

Una firma manuscrita en tinta azul sobre un fondo blanco.

**Thesis advisor**

**Leandro Javier Carreño Márquez, Ph.D**

Una firma manuscrita en tinta azul sobre un fondo blanco.

**UNIVERSIDAD DE CHILE  
FACULTAD DE MEDICINA  
ESCUELA DE POSTGRADO**

**INFORME DE APROBACION TESIS DE  
DOCTORADO EN .....**

Se informa a la Comisión de Grados Académicos de la Facultad de Medicina, que la Tesis de Doctorado en .....presentada por el candidato

**NOMBRE CANDIDATO/A**

ha sido aprobada por la Comisión Informante de Tesis como requisito para optar al Grado de **Doctor en Ciencias** ..... en Examen de Defensa de Tesis rendido el día ..... de ..... de 2021.

**Prof. ....**  
**Director de Tesis**  
**Dpto.**  
**Facultad de ....., Universidad de Chile**

**COMISION INFORMANTE DE TESIS**

**PROF. DR. ....**

**PROF. DR. ....**

**PROF. DR. ....**

**PROF. DRA. ....**  
Presidente Comisión de Examen

*Esta tesis va dedicada a:  
mis padres, mis amigos,  
mis profesores, y mis alumnos.*

*"Yo soy un hombre sincero  
De donde crece la palma,  
Y antes de morirme quiero  
Echar mis versos del alma.*

*Yo vengo de todas partes,  
Y hacia todas partes voy:  
Arte soy entre las artes,  
En los montes, monte soy."*

**José Martí**

## Agradecimientos

Lo más hermoso de lograr triunfos en la vida es poder compartirlos con todas las personas que de una manera u otra contribuyeron a que estos pudieran concretarse. Por lo anterior, es para mí un gran placer dedicarme un tiempo para agradecer a todas las personas que me ayudaron a lo largo de este viaje profesional y personal.

Primeramente, quisiera agradecer al Dr. Leandro Carreño, mi director de tesis. Usted, profesor, hace vivas las palabras de José Martí: "Educar es depositar en cada hombre toda la obra humana que le ha antecedido". Muchas gracias por ser un guía, por sus consejos, y porque nunca dejó de creer en mí. Para usted mi eterna gratitud. Por otra parte, quisiera agradecer a mis padres, los grandes luchadores de los cuales aprendí a ser una persona resiliente y empática. Muchas gracias por todo su amor y cariño desde mis primeros minutos de vida.

En otro orden, quisiera agradecer a los doctores que formaron parte de mi Comisión de Tesis Doctoral: Dr. Rolando Vernal, Dr. Arturo Borzutzky y Dr. Felipe Oyarzún; muchas gracias por todos sus consejos durante este período. Quisiera agradecer de modo especial a la Dra. María Carmen Molina, muchas gracias profe por su apoyo, análisis constructivo y gran disposición a ayudarme en todo lo que necesite. Agradezco además a María Cecilia Carter, la secretaria Docente del Programa de Doctorado en Ciencias Biomédicas. Gracias Ceci por tu ayuda, por tus palabras de aliento, por siempre estar ahí para nosotros.

Durante este doctorado he tenido el privilegio de trabajar con excelentes personas. Quisiera agradecer a mis compañeros de laboratorios: Daniela Schneider, Pablo Palacios, Álvaro Santibáñez, Carolina Schäfer y Cristián Gutiérrez. Amigos míos, hemos crecido juntos, hemos aprendido a amarnos y tolerarnos como una gran familia. En cada resultado que muestro en esta tesis hay su granito de arena. Siéntanse parte de mis logros, desde ya ocupan un lugar especial en mi corazón. Además, agradezco a los tesisistas de pregrado en los que de una manera u otra he contribuido a su formación: Sebastián Andrés González, Fernanda Denisse Antilén y Gary Flores. Gracias Chichos, ustedes fueron mis manos, siempre estuvieron presentes hasta el último momento.

Además, agradezco al Dr. David Montero, gracias, amigo, compañero, eres un fiel ejemplo para seguir. Te felicito por tus éxitos y espero que volvamos a trabajar juntos.

Por otro lado, quisiera agradecer a las lindas personas que trabajan en el Programa de Inmunología, de la Facultad de Medicina. Le doy gracias al personal técnico Rut Mora y Nancy Fabres, personas con un gran corazón de las cuales aprendí y su ayuda fue clave en las actividades experimentales de esta tesis. También, le agradezco a Dra. Karen Toledo, Dra. Bárbara Pesque, Dr. Felipe Flores, Amarilis Pérez, Romina Falcón, Dominique Fernández, los tesistas Francisco y Daniel. Mis queridos compañeros, amigos, muchas gracias por siempre ayudarme cuando lo necesite y por transmitirme siempre la buena vibra durante todos estos años. También, agradezco a mis amigos y profesores que conocí en la Universidad de Valparaíso: Dr. Emerson Carmona, Juan José Alvear, Dra. Javiera Villar; Dra. Karen Castillo, y Dr. Ramón La Torre. Gracias, a todos por darme la cálida bienvenida a este país, en el que siento como en casa.

Hay personas que de una manera indirecta contribuyeron a la realización de este trabajo. Quisiera agradecer a todas las personas que me han hecho sentir de Chile, mi hogar. Doy las gracias a Marcelo Fredericksen por todo el apoyo brindado al inicio de mi doctorado, gracias por ser mi familia, en los momentos en que más los necesitaba. También, agradezco al Dr. Francisco Mura, “mi querido Pancho”, gracias por tu apoyo y por tu hermosa compañía durante todo este tiempo. Por otra parte, reconozco cuanto apoyo he recibido de mis queridos amigos: María Belén Borgonovo, Diana de Alcántara, Rosa Scala, Isdani Morales, Yaremis Suárez, Arturo Elías, Dayesi López, Diana Rosa Rodríguez y Lisandra Móral. ¡A todos ellos gracias infinitas!

Finalmente, agradezco a mi maestra de ballet Sharon Márquez por adentrarme en el hermoso mundo de la danza. Además, doy gracias infinitas al Dr. Juan Pablo Osorio, por su gran ayuda en los momentos más difíciles. No puedo dejar de agradecer a todos mis estudiantes de la Universidad del Alba. Ustedes han sido mi compañía, mi familia, el motivo de mis alegrías. No hay dicha mayor que la de transmitir conocimientos y prepararlos para la vida.

**FUNDING:**

FONDECYT Project 1160336, Millennium Institute of Immunology and Immunotherapy

P09 / 016-F and CONICYT-PFCHA/Doctorado Nacional/2017-21170084 to R.G.

## ABSTRACT

Invariant NKT (iNKT) cells, a subpopulation of NKT cells, have attracted attention because of their ability to be activated by glycolipid antigens. Once activated, iNKT cells can secrete various cytokines to modulate immune responses. The activation of iNKT cells (mainly NKT10 cells, an iNKT cell population capable of secreting IL-10) with the  $\alpha$ -galactosylceramide ( $\alpha$ -GalCer) can contribute to the recruitment and suppressive effect of regulatory B and T cells (Breg and Treg). Nevertheless, the strong activation of iNKT cells elicited by  $\alpha$ -GalCer exhibit limited therapeutic efficacy in asthma and allergies, mainly due to the induction of a mixed pro- and anti-inflammatory cytokine response. However, there have been developed multiple structural analogs of  $\alpha$ -GalCer that elicit more selectively cytokine responses by iNKT cells. Thus, it would be highly relevant to determine whether  $\alpha$ -GalCer analogs will increase interaction between iNKT cells and B reg cell types during allergic inflammation. We propose the following hypothesis: *"The differential activation of iNKT cells with  $\alpha$ -GalCer analogs, which expand NKT10 cells and elicit the regulatory- skewed response, increases the expansion of Breg cells during allergic inflammation"*. Firstly, we identified NKT10 cells in hCD1d-KI mice (a partially humanized murine model for NKT cell responses). Hence, we evaluated different experimental conditions, such as immunization schemes, glycolipid activators of iNKT cells, and the uses of glycolipid delivery systems. We observed a significant expansion of NKT10 cells only in hCD1d-KI mice treated with  $\alpha$ -GalCer at seven days, like the proliferation of NKT10 cells reported during the immunization scheme of 30 days. In addition, we obtained glycolipid-contained liposomes. It was observed that incorporating the glycolipid ligands into liposomes remarkably increased the expansion of NKT10 cells. We evaluated the anti-allergic effect of liposomes containing the glycolipids ( $\alpha$ -GalCer and AH10-7) in a prophylactic and therapeutic scenery. Our results demonstrated that liposomes containing AH10-7 and OVA (Lp/OVA/AH10-7) induced an anti-allergic effect in BALB/c mice with OVA-induced allergy in a prophylactic scenery. Particularly, we observed a significant decrease in the inflammatory score and the number of mucus-producing cells in the lungs of mice with allergic induction treated with Lp/OVA/AH10-7. Besides, we could not appreciate an expansion of IL-10-producing regulatory B cells (B10 cells) in mediastinal lymph nodes (MLN) from mice with OVA-induced allergy and treated with Lp/OVA/AH10-7 in a therapeutic scenery. Since this expansion was not statistically significant, future experiments must verify the proliferation of B10 cells induced by Lp/OVA/AH10-7. On the other hand, we observed, a complete decrease in lung inflammation and goblet cell hyperplasia in mice with OVA-induced allergy treated with two regimens of doses of liposomes containing OVA the  $\alpha$ -GalCer. Finally, we could appreciate that it is tricky to induce an OVA model in hCD1d-KI mice (C57BL/6J background). Additionally, we didn't obtain a severe allergic response in the lung and the BAL of mice challenged with HDM. Consequently, it is necessary to improve the obtention of the HDM induced-allergic model in hCD1D-KI mice.



## INDEX

<i>INTRODUCTION</i> .....	11
iNKT Cells: main properties and role in immunity.....	11
How iNKT cells fit in the current model of allergic asthma?.....	13
Glycolipid iNKT cells ligand: refining strategies to specify iNKT-based immunotherapy.....	15
The interaction between NKT cells and regulatory T and B cells. ....	18
<i>HYPOTHESIS</i> .....	23
<i>GENERAL AIM:</i> .....	23
<i>SPECIFIC AIMS:</i> .....	23
<i>METHODS</i> .....	24
<i>RESULTS</i> .....	35
Incorporation of glycolipids contained into liposomes.....	35
Physicochemical characterization of liposomes. ....	35
$\alpha$ -GalCer analogs contained into liposomes or OVA-contained liposomes activate human iNKT cells and splenocytes from OT1 mice.....	41
Induction of NKT10 cell in hCD1d-KI mice .....	43
Expansion of NKT10 cells in hCD1d-KI mice with $\alpha$ -GalCer or $\alpha$ -GalCer analogs (OCH and AH10-7) with different schemes of immunizations.....	46
Expansion of NKT10 cells in hCD1d-KI mice with $\alpha$ -GalCer or $\alpha$ -GalCer analogs that induce Th1- type cytokine response (AH10-7, AH10-3, AH10-1).....	49
Expansion of NKT10 cells in hCD1d-KI mice with $\alpha$ -GalCer or $\alpha$ -GalCer analogs (OCH and AH10-7) contained into liposomes. ....	52
Obtention of OVA induced-allergic mice and antiallergic effect of liposomes containing $\alpha$ GalCer analogs. ....	58
Determination of the antiallergic effect of a-GalCer analogs contained into liposomes in a therapeutic scenery.....	66
Determination of the anti-inflammatory effect of a-GalCer analogs contained into liposomes, in a therapeutic scenery, two treatment regimens. ....	72

Obtention of OVA induced-allergic hCD1d-KI mice.....	84
Obtention of HDM induced-allergic hCD1d-KI mice .....	86
<i>DISCUSSION</i> .....	88
<i>CONCLUSIONS</i> .....	100
<i>PUBLICATIONS &amp; PARTICIPATION IN SCIENTIFIC MEETINGS</i> .....	101
<i>REFERENCES</i> .....	102
<i>APPENDIX</i> .....	109
<i>Certificate of the Institutional Animal Care and Use Committee</i> .....	109

## INTRODUCTION

### **iNKT Cells: main properties and role in immunity.**

Natural killer T cells (NKT) represent a heterogeneous and specialized subset of T cells characterized by the expression of T cell receptors (TCR) together with multiple receptors associated with natural killer cells (NK), such as CD161/NK1.1, NKG2D, and members of the Ly-49 family [1-6]. Invariant natural killer T cells (iNKT) are an NKT subset that expresses an invariant TCR  $\alpha$ -chain (V $\alpha$ 14J $\alpha$ 18 in mice and V $\alpha$ 24J $\alpha$ 18 in humans) that is paired with a semi-invariant  $\beta$  TCR chain (V $\beta$ 8, V $\beta$ 7, V $\beta$ 2 in mice and mostly V $\beta$ 11 in humans) [7-9]. These semi-invariant TCRs recognize lipids presented by CD1d, a non-polymorphic major histocompatibility complex (MHC) class I-like antigen-presenting molecule [10-12]. CD1d-binding lipid antigens from various commensal and pathogenic microorganisms have been well characterized [13-16]; however, iNKT cells are also self-reactive, and several self-lipid antigens have been reported as well [14, 16-19].

Antigenic stimulation of iNKT cells results in the rapid production of both anti- and pro-inflammatory cytokines, including interferon- $\gamma$  (IFN- $\gamma$ ), tumor necrosis factor- $\alpha$  (TNF- $\alpha$ ), interleukin (IL)-4, IL-5, IL-13, IL-17A, IL-22, granulocyte macrophage colony-stimulating factor (GM-CSF), IL-21, among others [2, 20-22]. Because of the association of these cytokines with T helper type (Th) 1-, Th2-, Th17-, and Th Follicular -type responses, it is common to refer to iNKT subsets as NKT1, NKT2, NKT17, and follicular helper NKT cells. Functional iNKT subsets can also be distinguished based on their expression of different transcription factors [21]. For instance, NKT2 cells express the most

considerable amount of the transcription factor promyelocytic leukemia zinc finger (PLZF); NKT1 cells express the smallest amount of PLZF; NKT17 cells express PLZF at levels between those of NKT2 and NKT1 cells [23-25]. Recently, a subset of iNKT cells (NKT10) was found to be enriched in adipose tissue, showing a unique transcriptional program (they lacked PLZF but expressed the transcription factor E4BP4) and producing regulatory cytokines (IL-2 and IL-10) [22, 26, 27], which expands even further the potential of iNKT cell stimulation for immunomodulation. One of the major outcomes of iNKT cell activation is their rapid secretion of effector cytokines after TCR engagement. It seems to be due to their constitutive expression of preformed mRNA transcripts for cytokines such as IFN- $\gamma$  and IL-4 [28]. Thus, iNKT cells are said to constitutively display a partially activated phenotype, like conventional memory T cells. However, in the case of iNKT cells, this is independent of previous antigen exposure [4, 29].

The rapid secretion of cytokines upon iNKT cell activation induces the subsequent activation of multiple other cell types, such as dendritic cells (DC), NK cells, B cells and CD4<sup>+</sup>, and CD8<sup>+</sup> T cells, in a process known as transactivation [7, 30-33]. This endows iNKT cells with a remarkable ability to bridge innate and adaptive immune responses or even to participate in the innate response [21]. The transactivation induced by iNKT cells can significantly amplify their cytokine responses and profoundly affect the cytokine milieu during the initiation of an adaptive immune response [6]. The capacity of iNKT to influence quickly and differently other cell types allows the involvement of iNKT cells in the enhancement of anti-tumor immunity [34], the protection against infectious organisms [35] (including bacteria [36, 37] and viruses [38]), the regulation

of allograft rejection [39-41], and autoimmunity [42-44]. On the other hand, there are situations where iNKT cells seem pathogenic, such as atherosclerosis, allergy, and skin disorders [45]. iNKT cells can exacerbate lung inflammation without infection, as in the case of allergic asthma [46].

### **How iNKT cells fit in the current model of allergic asthma?**

The lungs' primary function is the process of gas exchange called respiration. But also, they are an essential immune site. They filter the air we breathe, repulsing invaders and repairing injuries. However, these robust immune responses can overreact, causing diseases such as asthma [47]. The immunological events during asthma can be divided into three phases (Fig. 1). The first phase is initiated with the first contact with an allergen, which induces the activation, differentiation, and clonal expansion of naive T cells to Th2 cells specific for the allergen, capable of producing Th2 cytokines (such as IL-4 and IL-13). Allergen-specific Th2 cells induce immunoglobulin class switching to IgE and clonal expansion of naive IgE<sup>+</sup> memory B cells [48, 49].

The second phase is the type 1 hypersensitivity reaction (The immediate step of the allergic reaction). This stage is triggered when there is a re-exposure to the allergen, and recognition by IgE bound to the high-affinity receptor for IgE (FcεRI) of mast cells and basophils [50]. This signal leads to the release of vasoactive amines (mainly histamine), lipid mediators (prostaglandins and cysteinyl leukotrienes), chemokines (such as CC- chemokine ligand 3 and CC- chemokine ligand 5), and other cytokines (such as IL-4, IL-5, and IL-13) [51]. IgE also binds to FcεRI on the surface of DC and monocytes, this process increases the uptake of allergen by these antigen presenting

cells and the subsequent presentation from allergen-derived peptides to specific CD4<sup>+</sup> T cells [52].

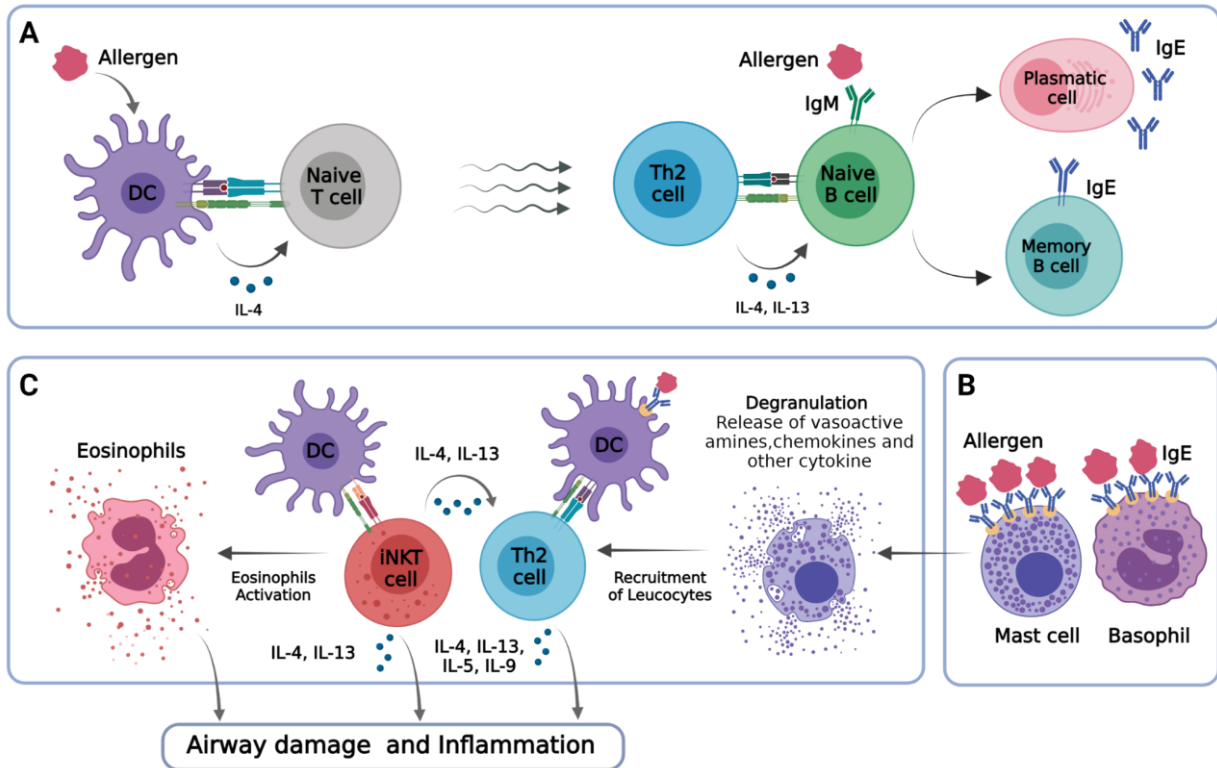


**Figure 1. Mechanisms of allergic reactions.** (A) The first phase is the allergen sensitization and development of allergen-specific memory B cells. T cell activation in the presence of IL-4 increases the differentiation into Th2 cells. (B) The second phase is the type 1 hypersensitivity reaction. IgE secreted by plasma cells binds to the high-affinity IgE receptor on basophils and mast cells. (C) The third phase is allergic inflammation. IgE is cross-linked by antigen, then basophils and mast cells release a wide variety of biologically active proteins and other chemical mediators that condition the recruitment of lymphocytes (such as Th2 cells and iNKT cells) and neutrophils that secrete a range of highly toxic granule proteins and other inflammatory mediators that favors the airway damage and inflammation [53].

The third stage is allergic inflammation (the late stage of allergic reaction). During this stage, the release of vasoactive amines, lipid mediators, chemokines, and cytokines induces the migration of allergen-specific T cells to sites of exposure to allergens; these

T cells reactivate and expand clonally [54]. There is also an activation of eosinophils and the release of proinflammatory mediators, chemokines, and cytokines. Eosinophils are one of the primary inflammatory cells (constituting up to 50% of the cellular infiltrate) in the lungs of asthmatic individuals [55]. Interestingly, NKT cells have been found to have shown the ability to exacerbate inflammation in the lungs in the case of allergic asthma (iNKT cells secrete IL-4 and IL-13 and increase airway inflammation) [56]. For this reason, possible therapies that target iNKT cells to treat allergic inflammation are highly relevant.

### **Glycolipid iNKT cells ligand: refining strategies to specify iNKT-based immunotherapy.**

An important discovery for the study of iNKT cells and the development of specific lipid activators was that extracts of  $\alpha$ -galactosylceramide ( $\alpha$ -GalCer) from the marine sponge *Agelas mauritanus* are potent activators for iNKT cells [11]. This discovery quickly scaled up to developing a synthetic form of  $\alpha$ -GalCer, also known as KRN7000, that can activate iNKT cells [57, 58]. However, the treatment with  $\alpha$ -GalCer has been problematic, as it induces pro-inflammatory, anti-inflammatory, and regulatory cytokine responses that may lead to conflicting effects [59]. Thus, the mixed cytokine response induced by  $\alpha$ -GalCer is probably not ideal for precisely targeted immunotherapy. For instance, in the Ovalbumin (OVA)-induced asthma model,  $\alpha$ -GalCer administration significantly augmented the inflammatory responses, including elevated inflammatory cell infiltration in the lung and bronchoalveolar lavage (BAL), increased levels of IL-4, IL-5, IL-10, IL-13, and IFN- $\gamma$ , and increased serum levels of OVA-specific IgE [60-62].

In order to obtain glycolipid activators of iNKT cells with more restricted patterns of cytokine expression, an extensive range of  $\alpha$ -GalCer derivatives containing different chemical modifications has been synthesized and tested (Fig. 2) [4, 6, 59, 63, 64]. In general,  $\alpha$ -GalCer analogs that elicit the expression of IFN- $\gamma$  and other Th1-type cytokines after iNKT cell activation have been associated with favorable therapeutic effects in mouse models of cancer and infectious diseases [65-67]; as well as, Th2-biased analogs may be more suitable for the treatment of autoimmune diseases or inflammatory conditions [68, 69].

Among the analogs inducing markedly pro-inflammatory cytokine responses are those in which the sugar has been modified by C6"-substituted amides, carbamates, and ureas [70-72]. For instance, AH10-7 incorporates a C6" hydrocinnamoyl ester and lacks the C4'-OH of the sphingoid base, vigorously promoting pro-inflammatory and anti-tumor iNKT cell responses [72]. Conversely,  $\alpha$ GalCer analogs inducing Th2-type cytokine responses have been synthesized by N-acyl and sphingosine modifications [73]. For example, OCH (an  $\alpha$ -GalCer analog with truncated acyl and sphingosine chains) induces an anti-inflammatory response through a predominant production of IL-4 by iNKT cells, leading to suppression of experimental autoimmune encephalomyelitis (EAE) [69]. Finally, it was recently reported that a group of Th1-biased analogs (C-Gly, EF77, SMC124, and DB06-1) shared the ability to expand *in vivo* NKT10 cells [74, 75]. Through the production of IL-10, expanded NKT10 cells protect mice against EAE [22]. Overall, all the evidence demonstrates how  $\alpha$ -GalCer analogs can modulate iNKT cells' immune response differently. Nevertheless, there is no evidence about the use of  $\alpha$ -GalCer analogs to restrict the cytokine-expression profile of iNKT cells during asthma.



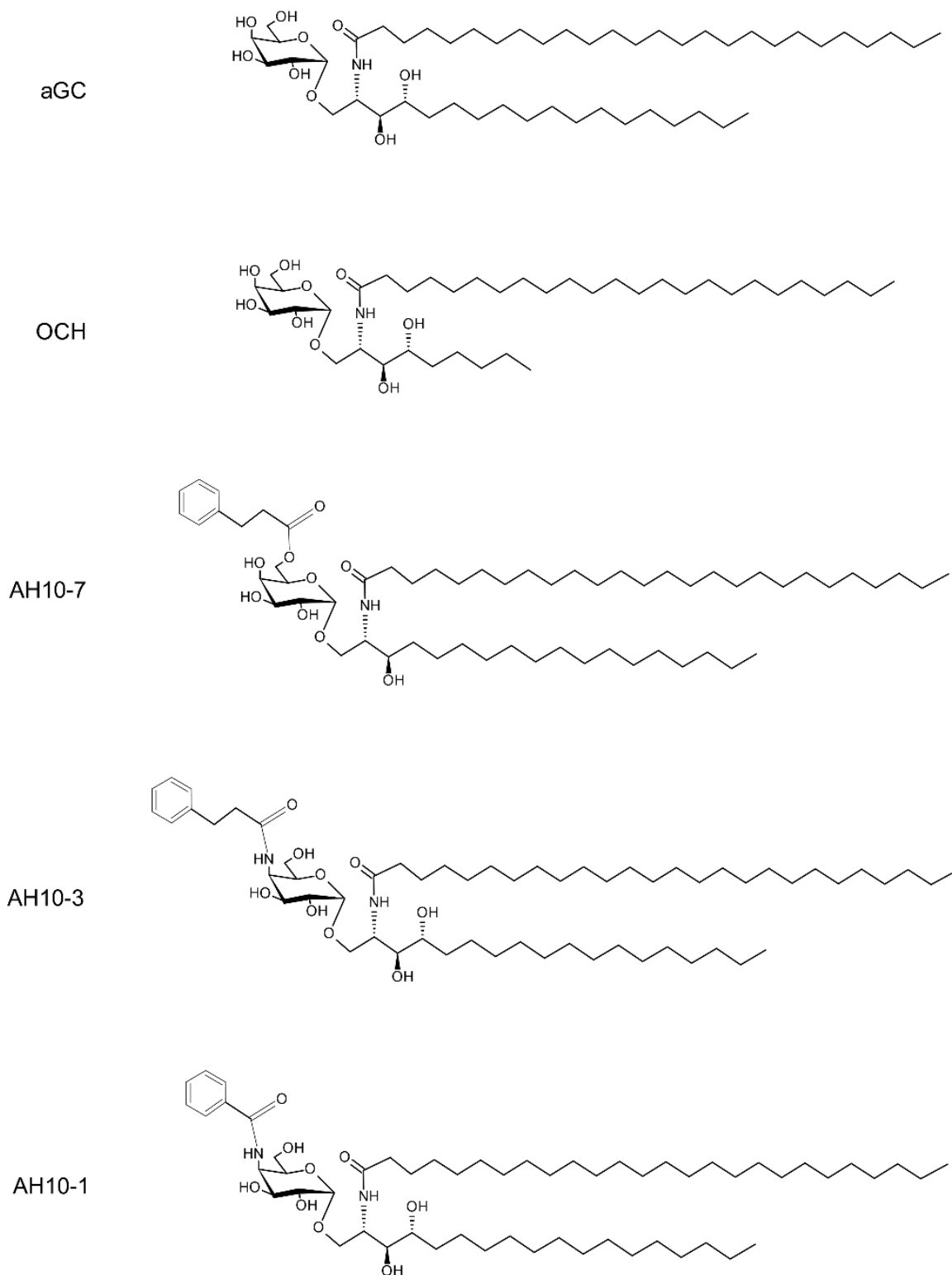


**Figure 2. Glycolipid structure of  $\alpha$ -GalCer and some  $\alpha$ -GalCer analogs.**  $\alpha$ -GalCer ( $\alpha$ -GC) is the prototypical antigen for iNKT cells. The compounds OCH, AH10-7, AH10-3, and AH10-1 are  $\alpha$ -GalCer derivatives previously described [72, 76].

Despite the great potential of NKT cells for immunomodulation, their relatively low frequency in the blood, lymphoid organs, and tissues has hindered their study in humans. On the other hand, mice display much higher frequencies of total NKT cells, different tissue distribution, and altered ratios of NKT cell subsets compared to humans, making them a useful but imperfect model for their human counterparts [6, 77]. Although human and mouse iNKT cells display conserved phenotypic and functional features, the differences observed in conventional mouse models limits their predictive utility for humans. In some attempts to overcome this problem, non-human primates have been used to model *in vivo* the iNKT cells' response since such animals generally have amounts of NKT cells closer than in humans [67, 78]. However, such studies are limited by sample size, available tools, high costs, and the inability to perform genetic manipulations. These limitations promote the development of humanized mice models, such as the reported human CD1d knock-in mouse (hCD1d-KI), which displays NKT cells' frequencies and tissue distribution similar to human [79]; hCD1d-KI also retain NKT cells' substantial immunomodulatory functions in a variety of *in vitro* and *in vivo* assays [79, 80]. Humanized mice are highly tentative for designing and applying preventive or curative NKT cell-based immunotherapies.

### **The interaction between NKT cells and regulatory T and B cells.**

It has been demonstrated that iNKT cells can contribute to the maintenance of immune tolerance [81, 82]. This is related to anti-inflammatory or regulatory cytokines expressed by iNKT cells [83, 84] that profoundly influence other regulatory cell types. Regulatory T cells (Treg) are essential for maintaining immune tolerance, preventing autoimmune diseases, and limiting chronic inflammatory diseases [85]. One of the

critical populations of Treg cells studied in asthma is CD25<sup>hi</sup>Foxp3<sup>+</sup> CD4<sup>+</sup>Tregs. A deficiency in the number or function of this subset is typical in patients with allergic diseases [86]. The basic mechanisms used by Treg cells are the production of the immunosuppressive cytokines such as IL-10 and the transforming growth factor-beta (TGF- $\beta$ ), the reduction in the ability of antigen-presenting cells to stimulate T cells, and the consumption of IL-2 because of the high level of expression of IL-2 receptor  $\alpha$ - chain (CD25) [85].

IL-2 is a critical factor in the activation and maintenance of Treg [87, 88]. Although the peripheral expansion of Treg seems to require IL-2 [89-91], the source of IL-2 for Treg expansion is still unknown in several cases [92]. In a previous study, the activation of iNKT cells by  $\alpha$ -GalCer protected mice from the experimental model of the autoimmune disease *myasthenia gravis* (EAMG), which was correlated with the peripheral expansion of Treg and the Treg cells' potency to inhibit *in vitro* proliferation of autoreactive T cells. Interestingly, the depletion of CD25<sup>+</sup> cells or neutralization of IL-2 reduced the therapeutic effect of  $\alpha$ -GalCer in this model [93]. Besides, in wild-type mice treated with  $\alpha$ -GalCer, NKT10 cells controlled the number, proliferation, and suppressor function of adipose Treg cells by producing IL-2 [27]. In other words, the cytokines produced by  $\alpha$ -GalCer- stimulated iNKT cells (mainly NKT10 cells) can create favorable conditions for the recruitment and expansion of Treg cells (Fig. 3).

The second regulatory cell type, which appears to have a beneficial role in responses in the case of autoimmunity or allergy diseases, is a heterogeneous population of regulatory B cells (Breg) [94, 95]. Breg can suppress immune responses through the production of IL-10 [96]. Additional Breg-mediated suppression includes TGF- $\beta$  [97],

IL-35 [98] release, and PD-L1 expression [99]. Although a partial consensus regarding the effector function of Breg cells has been reached, a unified view concerning their phenotype is still missing. In mice, multiple subsets of Breg cells have been described, including CD19<sup>+</sup>CD1d<sup>hi</sup>CD5<sup>+</sup>IL-10<sup>+</sup> (B10 cells) associated with allergic airway inflammation [100]. While  $\alpha$ -GalCer presentation by B cells to iNKT cells results in the differentiation of antibody-producing B cells by a feedback mechanism [101, 102], whether the Breg by interacting with iNKT cells condition their responses remains less explored.

Recent studies evidence an active interaction between Breg cells and iNKT cells (Fig. 3). Almishri *et al.* (2015) concluded that  $\alpha$ -GalCer stimulation of iNKT cells produces the recruitment of an MZ Breg subset to the liver, suppressing hepatic inflammation [103]. On the other hand, Oleinika *et al.* (2018) demonstrated that CD1d-lipid presentation by Breg induces IFN- $\gamma$  secretion by iNKT cells, partially contributing (Fig. 3) to the downregulation of Th1 and Th17 immune responses and ameliorating experimental arthritis. In this sense, they showed that mice lacking CD1d expressing B cells develop a more exacerbated disease than wild-type mice and fail to respond to treatment with  $\alpha$ -GalCer. They also demonstrated that suppression of arthritis by the T2-MZP Breg subset requires iNKT cells. Since T2-MZP cells were isolated from wild-type mice in remission from arthritis and adoptively transferred into CD1d-KO mice (mice that lack iNKT cells), they were unable to reduce the frequency and absolute number of IFN- $\gamma$ <sup>+</sup> and IL-7<sup>+</sup> CD4<sup>+</sup> T cells in iNKT cell-deficient mice with arthritis induction [44].

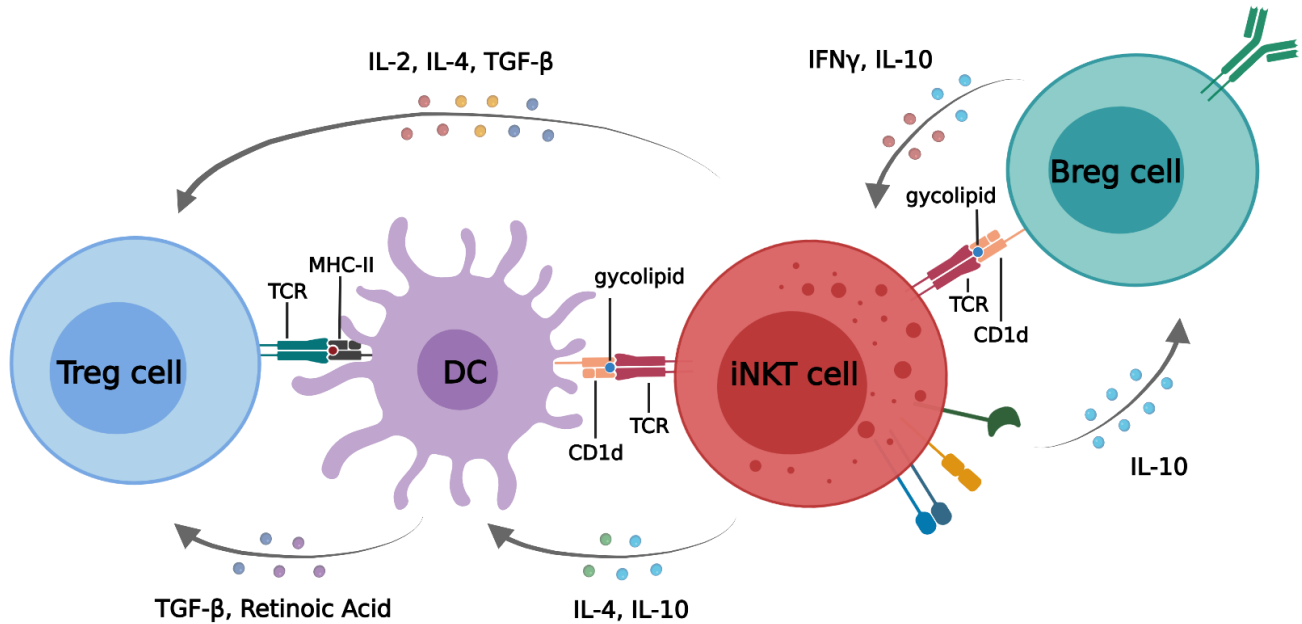


**Figure 3. Proposed interaction between iNKT cells and regulatory T and B cells.**

The activation of iNKT cells with glycolipids can promote the function of Treg cells by secreting cytokines, including IL-2, IL-4, and TGF-β). Additionally, iNKT cells can promote immature DC to become tolerogenic DC, which, in turn, can promote the activation of Tregs [40, 92, 93, 104]. On the other hand, the CD1d-dependent Breg interaction with iNKT cells is critical for differentiating iNKT cells with suppressive capacity. That interaction is mediated by the secretion of cytokines, including IFNγ and IL-10 [44, 105].

The antecedents showed that activating iNKT cells with α-GalCer can contribute to the recruitment and suppressive effect of regulatory cell types (Breg and Treg), which protect against autoimmunity or inflammatory diseases. However, iNKT cell activation elicited by α-GalCer exhibit limited therapeutic efficacy in asthma and allergies, mainly due to the induction of a mixed cytokine response [46, 61, 62, 106]. Because of this, multiple structural analogs of α-GalCer that elicit more selective cytokine responses by iNKT cells have been developed. Thus, it would be highly relevant to determine *which α-GalCer analogs potentiate the interaction between iNKT cells and regulatory B cell*

*during allergic inflammation.* This work would increase the knowledge regarding the possible mechanisms associated with the interaction between activated iNKT cells and regulatory B cell types. Additionally, it would open new approaches to immunomodulation of iNKT cells during asthma and allergies to restrict the cytokine-expression profile of iNKT cells and enhance the immunological tolerance required in therapies for allergic inflammation, which are ineffective (do not change the chronic course of the disease) and limited at controlling symptoms.

## **HYPOTHESIS**

***“The differential activation of iNKT cells with  $\alpha$ -GalCer analogs, which expand NKT10 cells and elicit a regulatory-skewed response, increases the expansion of regulatory B cells, leading to the prevention or reduction of allergic asthma.”***

## **GENERAL AIM:**

To evaluate if the expansion of Breg cells promoted by the differential activation of iNKT cells with  $\alpha$ -GalCer analogs contained in liposomes will prevent or suppress the airway hyperreactivity in murine models of allergic asthma.

## **SPECIFIC AIMS:**

1. To induce differential activation of iNKT cells (mainly NKT10 cells) with  $\alpha$ -GalCer analogs contained in liposomes, in a partially humanized murine model for NKT cell responses (hCD1d-KI C57BL6).
2. To determine if the differential activation of iNKT cells with different  $\alpha$ -GalCer analogs in liposomes will increase the expansion of Breg, leading to the prevention or reduction of allergic asthma in BALB/c mice with induced allergy by the experimental allergen OVA.
3. To determine if the differential activation of iNKT cells with different  $\alpha$ -GalCer analogs in liposomes will increase the expansion of Breg, leading to prevention or reduction of allergic asthma, in hCD1d-KI C57BL6 with induced allergy by the human allergen HDM.

## **METHODS**

### **Mice**

C57BL/6 mice were purchased from the animal facility of the Faculty of Medicine, University of Chile. C57BL/6 hCD1d Knock-in mice were donated from the Albert Einstein College of Medicine, USA. C57BL/6 OT-I mice were donated from the private nonprofit institution Fundación Ciencia & Vida. BALB/c mice were purchased from the Institute of Public Health of Chile. All mice were bred and kept under specific conditions at the animal facility of the Faculty of Medicine, University of Chile. Animals were randomly assigned to experimental groups. Animals were 6–12 weeks of age when entering the experiments. The influence of gender on the experimental results has not been assessed in this study. Studies involving mice were explicitly approved by the Institutional Animal Care and Use Committee of the University of Chile (20342-MED-UCH).

### **Glycolipids and reagents for the synthesis of liposomes**

$\alpha$ -GalCer and OCH were obtained from commercial sources (Avanti Polar Lipids, USA, and Adipogen, USA, respectively). AH10-7, AH10-3, and AH10-1 were kindly provided by Amy R. Howell, PhD. from the University of Connecticut, USA. Egg phosphatidylcholine (EPC), cholesterol (Chol), and 1,2-distearoyl-sn-glycerol-3-phosphoethanolamine-N- [amino (polyethylene glycol) -2000] (DSPE-PEG2000) were purchased from Avanti Polar Lipids, USA. The cell-penetrating peptide stearylated octaarginine (STR-R8) was purchased from Life Tein, USA.



## **Preparation of liposomes incorporating glycolipid ligands of iNKT**

Lipid vesicles were synthesized as described previously [107]. Briefly, 560 nmol of EPC, 240 nmol of Chol, 40 nmol of STR-R8, and 16 nmol of DSPE-PEG200 in chloroform/methanol solution were mixed with 100 µg of the iNKT cell-modulating glycolipid ( $\alpha$ -GalCer, OCH, or AH10-7) was added. The solvent was eliminated by evaporation in a vacuum desiccator overnight. The lipid film was rehydrated with 0.2 mL either of PBS (GIBCO Life Technologies, USA) or OVA (Sigma-Aldrich, USA) dissolved in PBS (in the case of OVA-contained liposomes). Finally, the liposomes were extruded through a polycarbonate membrane with a pore size of 800 nm in a Mini extruder (Avanti Polar Lipids, USA) and stored at 4°C. In the case of OVA-containing liposomes, non-entrapped OVA was removed by washing twice with PBS and centrifuging at 80,000 x g for 30 minutes in an Ultracentrifuge Sorvall™ WX+ (Thermofisher, USA). Pellets were finally resuspended in an appropriated volume of PBS and stored at 4°C.

## **Morphology and physicochemical characterization of liposomes.**

The hydrodynamic diameter (Z-average size), polydispersity index (PDI), and zeta potential of the liposomes were determined by the Dynamic Light Scattering (DLS) technique with the Malvern Zetasizer ZS 3600 (Malvern Instruments, UK), operating with a He-Ne laser at a wavelength of 633 nm, with a scattering angle of 173° at 25°C. The particle size of the liposomes was determined by Nanoparticle Tracking Analysis with a NanoSight NS300 (Malvern Instruments, UK).

The morphology of the liposomes was characterized by scanning transmission electron microscopy performed in a ZEISS EM 109. Once synthesized, the liposomes were centrifuged for 10 minutes at 4,000 RPM to concentrate them. Twenty microliters of each sample were extracted and incubated with 1.5% uranyl acetate solution under a Formvar polymer-coated copper grid, allowing the sample to dry before observation under the transmission electron microscope.

### **Reconstitution of Glycolipids for *in vitro* and *in vivo* Use**

For *in vitro* assays, glycolipid stock solutions were prepared at 100 mM in DMSO (Thermo Fisher Scientific, USA). Immediately before use, these stock solutions were heated for two minutes at 70°C, sonicated for 5 minutes, and then diluted to 1 mM in a prewarmed (37°C) culture medium of RPMI-1640 (GIBCO Life Technologies, USA) with 10% Fetal Bovine Serum (BI Biological Industries, Israel). This preparation was further diluted with a culture medium immediately before adding it to cell cultures to obtain the desired final glycolipid concentrations and a final DMSO concentration of 1% v/v. For mice injections (*in vivo*), glycolipids were first dissolved to 20 mM in DMSO and then further diluted to 200 µM using PBS + 0.5% Tween-20. This solution was diluted at 1:10 with prewarmed (80°C) PBS immediately before injections. Each injection consisted of 200 µL of glycolipid in a vehicle with a final composition of PBS + 0.1% DMSO + 0.05% Tween-20.

### **Antigen-presentation assay**

Bone marrow-derived DCs (BMDC) from C57BL/6J hCD1d-KI mice were generated with GM-CSF [108]. Briefly, bone marrow cells were isolated from femurs and tibias

and cultured in a medium containing 10 ng/mL GM-CSF (PeproTech, USA) for 6 days. BMDC were pulsed with glycolipids or glycolipids-containing liposomes to the desired final glycolipid concentrations ranging from 0.01–1000 nM for 24 hours. Subsequently, pulsed BMDC were co-cultured for 24 hours with iNKT cell hybridoma. BMDC pulsed with glycolipids incorporated in OVA-contained liposomes were co-cultured for 24 hours with iNKT cells hybridoma or splenocytes from OT1 mice. Finally, we detected the activation of iNKT cell hybridoma or splenocytes from OT1 mice by measuring the secretion of IL-2 in the supernatant through ELISA.

#### **Determination of activation of human iNKT cells and splenocytes from OT1 mice by ELISA.**

The quantification of the IL-2 cytokine in the supernatants of the co-cultures described in the previous point was carried out by sandwich-type ELISA. For this, 96-well plates for immunoassay (Nunc, USA) were sensitized with 100  $\mu$ L/well of antibody purified monoclonal anti-mouse IL-2 (clone JES6-1A12; BD Biosciences, USA), dilution 1:400 in PBS (GIBCO Life Technologies, USA), for 12 hours at 4°C. Subsequently, the wells were blocked with 200  $\mu$ L/well of PBS-BSA 1% for one hour with gentle horizontal agitation (SHKA2000 horizontal shaker, Barnstead International, USA) at room temperature. Afterward, the wells were washed with 250  $\mu$ L/well of PBS-Tween 20 0.1% in an ELISA plate washer (HydroFlex, Austria). Next, 10  $\mu$ L of the supernatant of the co-cultures performed in the antigen presentation essays were added, and the volume was made up to 100  $\mu$ L with PBS-BSA 1%, incubating for 12 hours at 4°C. Then, the wells were washed with 250  $\mu$ L/well with PBS-Tween 20 0.1%. Then, 100  $\mu$ L/well of monoclonal anti-mouse IL-2 antibody conjugated to biotin (clone JES6-1A12;

BD Biosciences, USA), diluted 1:700 in PBS BSA 1%, was incubated for 1:30 h, at room temperature. Afterward, the wells were washed, and 100  $\mu$ L/well of streptavidin-horseradish peroxidase (BD Biosciences, USA), dilution 1:1500 in assay buffer, was incubated for one hour at room temperature. Finally, the wells were washed. and the TMB substrate (3,3',5,5'-tetramethylbenzidine; Life Technologies, USA) was added. The reaction was carried out at room temperature for 5 minutes and stopped with 50  $\mu$ L/well of 2M H<sub>2</sub>SO<sub>4</sub>. The colorimetric result was read in an ELISA plate reader (Synergy HT, Bio-Tek, USA) at absorbances of 450 nm and 570 nm to perform the wavelength correction. This subtraction corrects the optical imperfections that can present the plate used.

### **Genotyping PCR**

DNA was verified by polymerase chain reactions (PCR) analysis of tail DNA. Genotyping was done using murine CD1D primers (5': CCTGGGACCAAGGCTTCAG AG, 3': CCTGCTGTTTCTGCTGCT CTG) and human CD1D primers (5': ATATTTGAG GCAGGCTGTACCAGTCGAAAT,3': GAAGCCAGAGACATGACACACCAGCTGCCT) to amplify genomic sequences from tail fragments to verify the presence of *hCD1D* and absence of *mCD1D1* gene in the mice. To analyze the product of the PCR, we performed 4% agarose gel electrophoresis. The PCR product size for murine CD1d should be about 343 bp, and for human CD1d should be about 504 pb. Positive control was blood human, and negative control was a sample without DNA.

### ***In Vivo* Activation of iNKT Cells**

Mice were intravenous (i.v.) injected with 4 µg of one of the next glycolipids: α-GalCer, OCH, AH10-7, AH10-3, AH10-1; or as otherwise indicated. Four weeks after the first glycolipid dose, mice were re-challenged with 1 µg of α-GalCer or indicated otherwise. Ninety minutes after the last injection, splenocytes were harvested.

### **Monoclonal Antibodies and Flow Cytometry**

Cell suspensions were obtained from the tissue of origin in FACS stain buffer (2% of Fetal Bovine Serum and 0.05 % of sodium azide) after removal of erythrocytes by buffer lysis RCB (Biolegend, USA). Cells were incubated with purified rat anti-mouse CD /32 antibody (2.462) to block non-specific binding to FcγR (BD Biosciences, USA). Subsequently, the staining was carried out with the following specific antimouse monoclonal antibodies: TCR β- FITC (H57-597), IL4-PE Cyanine 7 (11B11), CD4-APC Cyanine 7 (GK1.5), CD45R/B220-Pacific Blue (RA3-6B2), MHC-II-FITC (M5/114.15.2), Ly-6G-APC/Cyanine7, CD24-BV605 (M1/69), CD64-BV711 (X54-5/7.1), CD19-PECyanine7 (6D5) (all from Biolegend, USA); IFNγ-Alexa Fluor 700 (XMG 1.2), IL17A-PE, CF594 (TC11-18H10), TNF-BV650 (Mab11), IL-10-APC (JES5-16E3), PLZF-PE CF594 (R17-809), RORγt- BV650 (Q31-378), GATA3-BV711 (L50-823), Tbet-BV786 (O4-46), SiglecF-PE (E50-2440), TCR β APC (H57-597), CD11b-V450 (M1/70), Foxp3-PE-CF594, IL-10-BV650 (JES5-16E3) (all from BD Biosciences, USA); F4/80-PerCP-Cyanine5.5 (BM8), CD45R (B220)-APC (RA3-6B2), and CD25-APC (PC61.5) (all from Thermo Fisher Scientific, USA). For iNKT cell staining, we used the Mouse CD1d Tetramer (α-GalCer loaded)-PE (MBL International Corporation, USA). For intracellular

antigens staining, the cells were permeabilized with Foxp3/Transcription Factor Staining Buffer (Invitrogen, USA). For detection of cytokines expressed in NKT cells, ex vivo stimulation of splenocytes was performed with PMA (50 ng/mL) (Sigma-Aldrich, USA) and Ionomycin (4 µg/mL) (Sigma-Aldrich, USA) for four hours at 37°C in the presence of Monensin (4 µg/mL) (Biolegend, USA), and Brefeldine A (4 µg/mL) (Thermo Fisher Scientific, USA). To analyze the percentage of cytokines expressed in NKT cells, we adjust the gate according to the fluorescence minus one (FMO) control. The flow cytometry assay was performed in an 18-color flow cytometer (BD LSR FORTESSA X-20). The analysis from acquired cells was carried out in the FlowJo V10.

### **Induction and evaluation of OVA or HMD-Allergic Airway Inflammation**

For the acute allergic OVA model, female BALB/c mice were sensitized intraperitoneally (i.p.) with 100 µg OVA in 1 mg Inject<sup>TM</sup> Alum (Thermo Scientific, USA), followed by intranasal (i.n.) challenge with 10 µg of OVA dissolved in PBS at days 21, 24, and 28 post-immunizations. Treatments were administered in a prophylactic and therapeutic scenery. After the treatment, mice received an i.n. re-challenged with 10 µg of OVA dissolved in PBS. Mice were euthanized 24 hours after the last i.n. re-challenged. Bronchoalveolar lavage (BAL) fluid was obtained by flushing the lungs three times with 1 mL of PBS containing 0.5 mmol/L EDTA (Sigma-Aldrich, EUA). The right lung was cut into small pieces and digested for 30 min in RPMI-1640 (GIBCO Life Technologies, USA) containing 20 µg/ml Liberase TM (Roche, USA) and 10 U/ml DNase I (Roche, USA). After enzyme digestion, lung cells were washed and stained with monoclonal antibodies to identify immune cells by flow cytometry. For the establishment of the induced allergy model for HDM, C57BL/6J hCD1d-KI mice were

sensitized i.n. with 1 µg of HDM (Greer Laboratories, USA) in 10 µL of PBS followed by i.n. challenges on days 7 to 11 with 10 µg of HDM in 10 µL of PBS. Mice were euthanized on day 14. The allergic response was evaluated by determining the recruitment of eosinophils through flow cytometry.

### **Histopathological analysis of the lung inflammation**

Before BAL collection, the principal left bronchus of the left lung was clamped using a Kelly hemostatic forceps to perform the histopathology analysis without losing significant tissue architecture. After obtaining the BAL of the right lung, the left lung was fixed with 4% paraformaldehyde and then paraffined embedded using a Leica ASP300 S enclosed, automatic tissue processor (Leica Microsystems, Wetzlar, Germany). Then, 5 µm-thick tissue sections were obtained using a Microm HM 325 Rotary Microtome (Thermo Scientific, USA), mounted, and stained for histopathology analyses using hematoxylin & eosin to identify lung infiltrate.

For hematoxylin & eosin staining, sections were incubated in Mayer's Hematoxylin for 3 minutes, then washed in tap water for 5 minutes and in distilled water for a couple of seconds. After this, the sections were incubated for 5 seconds in aqueous eosin and the sections were immediately washed with distilled water. After this, the sections were dehydrated in four steps of ethanol in increasing concentration (70°, 95°, 100°, 100°) and two steps of xylol for 30 seconds each with agitation. Finally, Entellan® mounting medium was added to the sections; then they were covered with a coverslip.

Histopathological scoring of the lung inflammation was done by a blinded observer. The final scores reflected averages of scores from five representative regions of each

sample × 40 fields per tissue per mouse. Lung inflammation was scored separately for cellular infiltration around blood vessels (perivascular regions) and airways (bronchus and bronchioles) with a scoring system from 0 to 4. Where: 0 = absence of inflammatory cells; 1 = few inflammatory cells; 2 = a ring of inflammatory cells of one deep cell layer; 3 = a ring of inflammatory cells of two or four cell layers deep; 4 = a ring of inflammatory cells more than four cell layers deep. A composite score was determined by adding the inflammatory scores for both perivascular region and airways [109].

### **Identification of goblet cells and mucus production**

For the identification of goblet cells and mucus production, the Periodic Acid-Schiff (PAS) Stain was carried out. For this purpose, the lung sections were treated with a periodic acid solution (1%) for 5 minutes and washed with distilled water for a couple of seconds with agitation. Subsequently, Sections were incubated with Coleman's Schiff's Reagent for 15 minutes and washed in tap water for 10 minutes. Finally, nuclear contracting was performed with Mayer's Hematoxylin for 5 minutes, followed by a washing step in tap water for 5 minutes. After this, the sections were dehydrated in four steps of ethanol in increasing concentration (70°, 95°, 100°, 100°) and two steps of xylol for 30 seconds each with agitation. Finally, Entellan® mounting medium was added to the sections; then they were covered with a coverslip.

To score the degree of goblet cell hyperplasia, the number of PAS-positive goblet cells was manually counted. A scoring system of 0 to 4 was used, where 0 = less than 0.5% are PAS-positive goblet cells, 1 = less than 25% are PAS-positive goblet cells, 2 = 25-50% are positive goblet cells for PAS, 3 = 50-75% are PAS-positive goblet cells and 4



= greater than 75% are PAS-positive goblet cells [110]. Quantification of the PAS-positive goblet cells was expressed as the number of PAS-positive cells per mm of the basement membrane of bronchioles and bronchi to correct for airway size [111]. The length of the basement membrane of bronchioles and bronchi was measured using ImageJ software. The degree of goblet cell hyperplasia was done by a blinded observer in five randomly representative airways regions of each sample, at 40X, without knowing which experimental group the samples belonged to. The images presented were obtained with the MiniVID 5.1 MP 1/2.5" camera (LW Scientific, USA).

### **Detection of OVA-IgE levels by ELISA**

The detection of OVA-IgE levels in the serum OVA induced-allergic mice was carried out by indirect-type ELISA. For this, 96-well plates for immunoassay (Nunc, USA) were sensitized with 50  $\mu$ L/well of 0.5  $\mu$ g OVA (Sigma-Aldrich, USA) in PBS (GIBCO Life Technologies, USA), for 12 hours at 4°C. Afterward, they were washed with 250  $\mu$ L/well of PBS-Tween 20 0.1% in an ELISA plate washer (HydroFlex, Austria). Subsequently, the wells were blocked with 200  $\mu$ L/well of PBS- Skim Milk 1% for 1 hour at 37°C. Afterward, the wells were incubated with diluted serum samples for 12 hours at 4°C. The wells were washed and incubated for 1.5 hours at room temperature with 1  $\mu$ g/mL biotinylated polyclonal rabbit anti-mouse IgE (clone 23G3, Abcam, UK), dilution 1:500 in assay buffer. Additionally, the wells were washed and incubated for 1 hour with streptavidin-horseradish peroxidase (BD Biosciences, USA), dilution 1:1500 in assay buffer. Finally, the TMB substrate (3,3',5,5'-tetramethylbenzidine; Life Technologies, USA) was added. The reaction was carried out at room temperature for 5 minutes and

stopped with 50  $\mu\text{L}$ /well of 2M  $\text{H}_2\text{SO}_4$ . The colorimetric result was read in an ELISA plate reader (Synergy HT, Bio-Tek, USA) at 450 nm and 570 nm absorbances.

### **Statistical analysis**

Statistical analysis was performed using GraphPad Prism 7 (GraphPad Software). Statistical differences were evaluated using parametric tests (Unpaired t test or ANOVA with Dunnett's multiple comparisons test) or nonparametric tests (Mann-Whitney test or Kruskal-Wallis multiple comparisons test). The normal distribution was assessed with the Kolmogorov-Smirnov test. All the experiments were performed in duplicates

.

## RESULTS

***SPECIFIC AIM 1: To induce differential activation of iNKT cells (mainly NKT10 cells) with  $\alpha$ -GalCer analogs contained in liposomes, in a partially humanized murine model for NKT cell responses (hCD1d-KI C57BL6).***

### **Incorporation of glycolipids contained into liposomes.**

As previously mentioned, an effective way of avoiding anergy and liver toxicity in iNKT cells is the incorporation of  $\alpha$ -GalCer in nanoparticles [107, 112]. Therefore, we proposed incorporating  $\alpha$ -GalCer or  $\alpha$ -GalCer analogs (OCH and AH10-7) into stearylated octaarginine-modified liposomes following the method described by Nakamura, *et al.* (2013) [107]. Liposomes were composed with EPC, Chol, DSPE-PEG2000, and STR-R8 in a molar ratio 35:15:1:3. Thus, all the components were initially mixed in chloroform/methanol solution, and 100  $\mu$ g of the iNKT cell-modulating glycolipid ( $\alpha$ -GalCer, OCH, or AH10-7) was then added. The organic solvent was evaporated, generating a lipid film, then rehydrated with 0.2 mL either of PBS or OVA dissolved in PBS (in the case of OVA-contained liposomes). Finally, the liposomes were extruded through 800 nm polycarbonate membrane filters and stored at 4 °C until use.

### **Physicochemical characterization of liposomes.**

There are several methods to determine nanoparticle size and morphology. One of them is scanning transmission electron microscopy (STEM) [113]. In STEM analysis, electrons are emitted by the electron source and are accelerated toward the sample.

SEM creates an image by detecting reflected or knocked-off electrons [114]. Figure 4 shows micrographs obtained from transmission electron microscopy of  $\alpha$ -GalCer or  $\alpha$ -GalCer analogs (OCH and AH10-7) contained in liposomes (or in OVA-contained liposomes). In these micrographs, we can visualize liposomes with a round shape and non-regular edges. Additionally, it was not observed any change in the forms of liposomes when the protein is encapsulated into the liposome. Finally, measuring the size of the liposomes in the stained image gives a range of 100 nm to 200 nm.

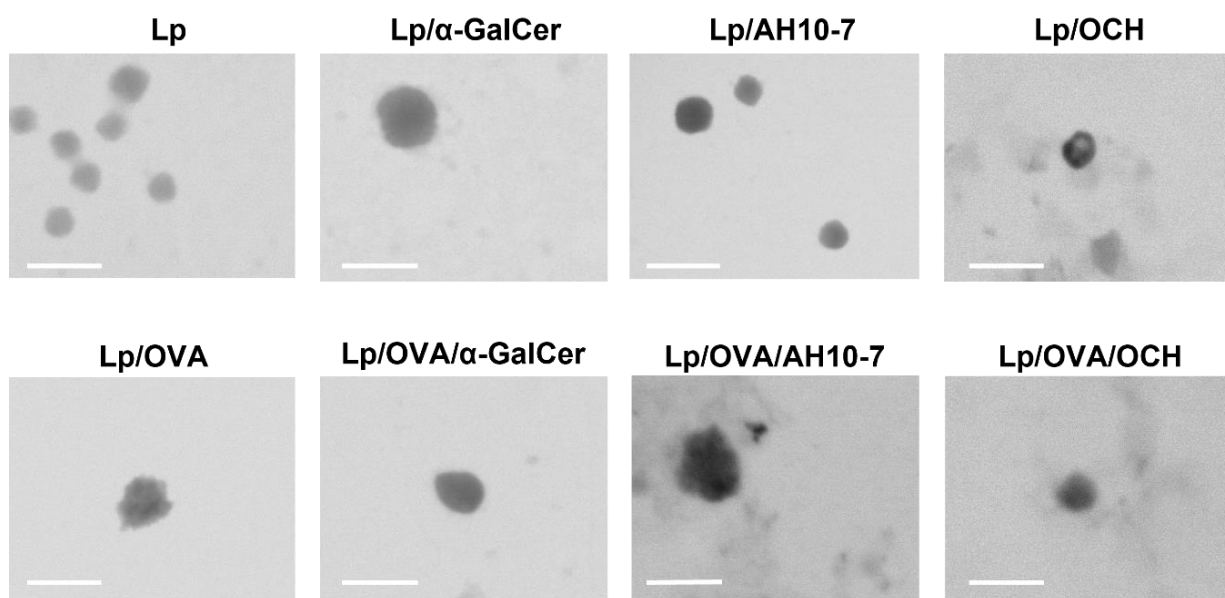


**Figure 4. Morphology of liposomes containing  $\alpha$ -GalCer or  $\alpha$ -GalCer analogs (OCH and AH10-7) incorporated into the liposomes (or in OVA-contained liposomes).** Representative image obtained from STEM of liposomes (**Lp**), OVA-contained liposomes (**Lp/OVA**),  $\alpha$ -GalCer into liposomes (**Lp/  $\alpha$ -GalCer**),  $\alpha$ -GalCer into OVA-contained liposomes (**Lp/OVA/ $\alpha$ -GalCer**), AH10-7 into liposomes (**Lp/AH10-7**) and AH10-7 into OVA-contained liposomes (**Lp/OVA/AH10-7**), OCH into liposomes (**Lp/OCH**) and OCH into OVA-contained liposomes (**Lp/OVA/OCH**). White scale bars represent 100 nm.

STEM is a powerful tool for studying the morphology of molecular ultra-structures. However, STEM analysis requires the nanoparticle sample to be dried on a substrate

[115, 116]. Under these experimental conditions, the particle aggregation of the liposomes caused by the drying step generates less reliable images compared to micrographs in suspension. On the other hand, dynamic light scattering (DLS) and nanoparticle tracking analysis (NTA) are the most used techniques for the particle size analyses of liposomes [117, 118]. Both methods do not require the drying step (avoid drying artifacts) and can be conducted during sizing analysis in the original dispersion state. Hence, research that investigates the aggregation of nanoparticles dispersed in different liquid mediums such as PBS [105], DLS, and NTA can undoubtedly provide more meaningful data than STEM. Figure 5 shows the size of liposomes containing  $\alpha$ -GalCer or  $\alpha$ -GalCer analogs (OCH or AH10-7) determined by NTA using a Nanosight. In most cases, the mode of sizes' liposomes takes values from 100 nm to 200 nm.

The DLS results are often reported as the Z-average size. The Z-average size is the harmonic intensity-averaged hydrodynamic size of the sample particles measured by DLS. In other words, Z-average size is also known as the “cumulant mean” of the size [119]. The Z-average size of  $\alpha$ -GalCer or  $\alpha$ -GalCer analogs (OCH and AH10-7) contained in liposomes took values from 100 nm to 200 nm and differs statistically from  $\alpha$ -GalCer, or  $\alpha$ -GalCer analogs (OCH and AH10-7) included in OVA-contained liposomes (Fig. 6C). Interestingly,  $\alpha$ -GalCer or  $\alpha$ -GalCer analogs (OCH and AH10-7) incorporated in OVA-contained liposomes presented hydrodynamic diameters  $\geq$  500 nm. The term polydispersity index (PDI) describes the degree of non-uniformity of the size distribution of particles [120]. This index is dimensionless and scaled, so values smaller than 0.4 are mainly considered a highly monodisperse size distribution [121]. We observed that the liposomes' PDI values of  $\alpha$ -GalCer or  $\alpha$ -GalCer analogs (OCH

and AH10-7) are smaller or equal to 0.4 (Figure 6D). On the other hand, the PDI values of  $\alpha$ -GalCer or  $\alpha$ -GalCer analogs (OCH and AH10-7) incorporated in OVA-contained liposomes were higher than 0.4. This result indicates that these liposomes were a high polydispersity system. On the other hand, the zeta potential of a particle is the overall electrical potential at the slipping plane generated around the liposome as a compact double layer [122]. A significant difference was observed between the zeta potential of  $\alpha$ -GalCer or  $\alpha$ -GalCer analogs (OCH and AH10-7) contained in the liposomes and the zeta potential of all the glycolipids contained in OVA-liposomes. In the case of  $\alpha$ -GalCer or  $\alpha$ -GalCer analogs (OCH and AH10-7) contained in liposomes, the average zeta potential was  $33.84 \pm 3.84$  mV. On the contrary, glycolipids encapsulated into OVA-contained liposomes had an average zeta potential of  $15.97 \pm 7.15$  mV. (Fig. 6A). Finally, we generated liposomes and OVA-contained liposomes with /or without STR-8, with the purpose to evaluate if the positive charge liposomes and OVA-contained liposomes was due to the inclusion of the cell-penetrating peptide (stearylated octaarginine, STR-8). According to our results, the zeta potential of liposomes and OVA-contained liposomes with STR-8 was positive (zeta potential  $> 0$ ) (Fig. 6B). Contrarily, the liposomes and OVA-contained liposomes without STR-8 had negative zeta potential values. In summary, we obtained a monodisperse liposome size from 100 nm to 250 nm, and a positive zeta potential due to the incorporation of the STR8. If OVA is encapsulated within the liposomes, an increase in polydispersity index was observed, affecting the measurements of Z-average size in the Zetazizer.

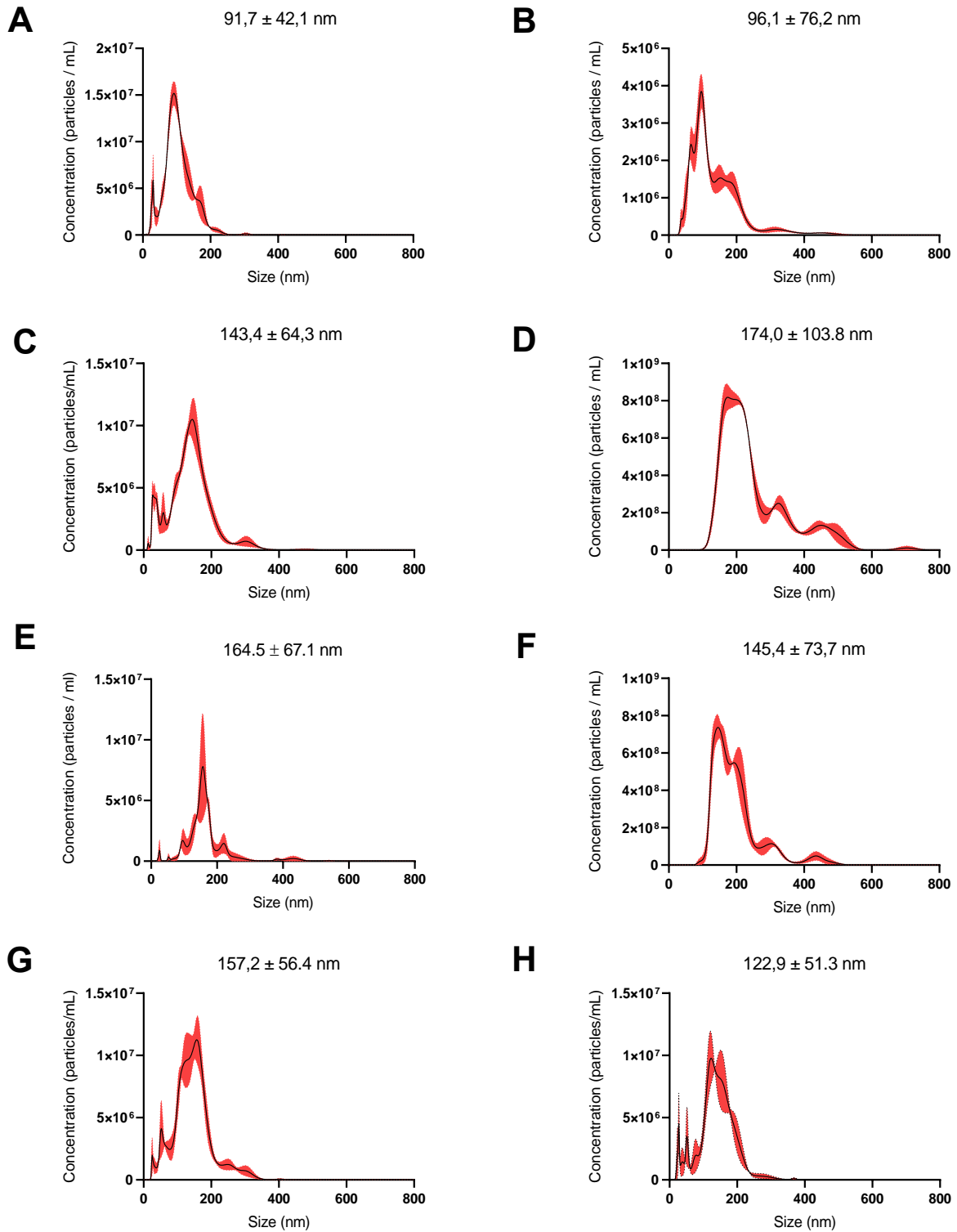


**Figure 5. Nanoparticle size of liposomes containing  $\alpha$ -GalCer or  $\alpha$ -GalCer analogs (AH10-7).** Nanoparticle size and concentration of liposomes (A), OVA-contained liposomes (B),  $\alpha$ -GalCer into liposomes (C),  $\alpha$ -GalCer into OVA-contained

liposomes (**D**), AH10-7 into liposomes (**E**) and AH10-7 into OVA-contained liposomes (**F**), OCH into liposomes (**G**) and OCH into OVA-contained liposomes (**H**) determinate by Nanoparticle Tracking Analysis. The values represent the mode  $\pm$  standard deviation.

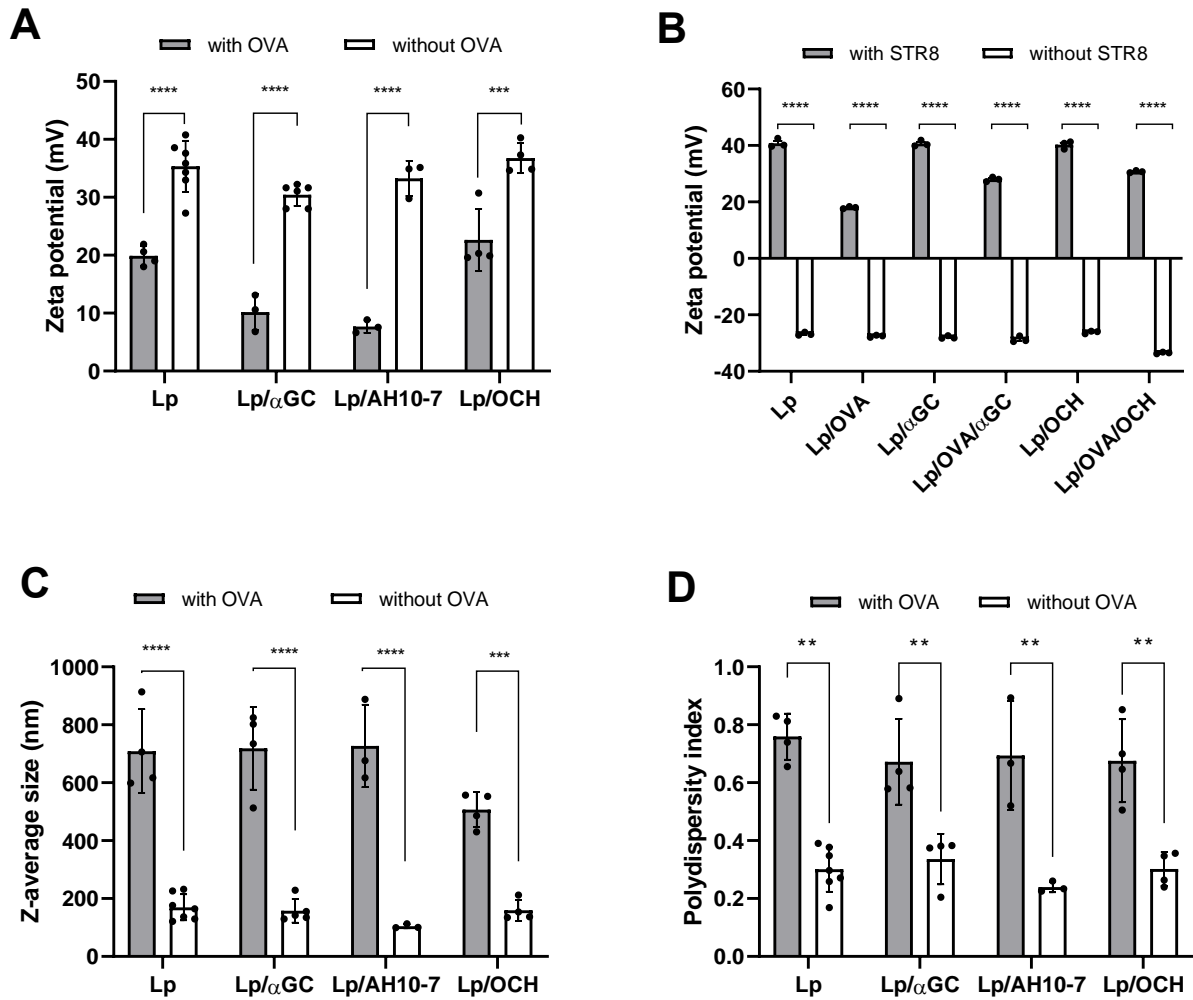


**Figure 6. Physicochemical characterization of  $\alpha$ -GalCer or  $\alpha$ -GalCer analogs (OCH and AH10-7) contained into liposomes (or in OVA-contained liposomes). (A) The Zeta Potential, (B) Nanoparticles' size, and (C) Polydispersity index of liposomes containing  $\alpha$ -GalCer or  $\alpha$ -GalCer analogs (OCH and AH10-7) were measured by electrophoretic mobility and dynamic light scattering, respectively, using a Zetasizer Nano ZS. The graphs represent the mean  $\pm$  standard deviation of at least three independent measurements. In the case of figures, **A**, **B**, and **C**, asterisks indicate significant differences in liposomes containing  $\alpha$ -GalCer or  $\alpha$ -GalCer analogs (OCH and AH10-7) contained into liposomes (or in OVA-contained liposomes). <sup>ns</sup>,  $p > 0.05$ ; \*,**



p <0.5; \*\*, p <0.01; \*\*\*, p<0.001; and \*\*\*\* p<0.0001. (Two-way ANOVA with Sidak's post-test for multiple comparisons).

Liposome	Particle Size (nm)	PDI	Zeta Potential (mV)
Lp	172,2 ± 73,3	0,3 ± 0,08	35 ± 4,4
Lp/αGC	159,9 ± 83,2	0,37 ± 0,1	30 ± 1,9
Lp/AH10-7	167,7 ± 67,1	0,24 ± 0,02	33 ± 3
Lp/OCH	192,9 ± 90,0	0,3 ± 0,06	37 ± 2,6
Lp/OVA	194,1 ± 92,9	0,76 ± 0,08	20 ± 1,7
Lp/OVA/αGC	182,4 ± 82,6	0,67 ± 0,15	15 ± 9,3
Lp/OVA/AH10-7	198,1 ± 73,7	0,69 ± 0,19	7,7 ± 1,1
Lp/OVA/OCH	139,8 ± 51,3	0,68 ± 0,14	23 ± 5,4

**Table 1. Summary of the physicochemical properties of liposomes containing glycolipid antigens.** Data are represented as mean ± standard deviation of at least three independent liposome samples.

**α-GalCer analogs contained into liposomes or OVA-contained liposomes activate human iNKT cells and splenocytes from OT1 mice.**

With the purpose of obtaining glycolipid activators of iNKT cells with more restricted and predictable effects, an extensive range of derivatives of α-GalCer containing different chemical modifications has been synthesized [73]. In this project, we included α-GalCer analogs (OCH and AH10-7) into liposomes as a novel method for delivering glycolipids. Thus, we need to measure the antigenic potency of these compounds in this new formulation. For this purpose, we used a cell-based antigen-presentation assay with bone marrow-derived DC (BMDC) from hCD1d-KI mice as antigen-presenting cells. Briefly, BMDC were pulsed with the glycolipids contained in liposomes for 24 hours. Subsequently, pulsed BMDC were co-culture with iNKT cell hybridoma; then, we detected the activation of iNKT cell hybridoma by measuring the secretion of IL-2 in the supernatant by ELISA. Our results show that BMDC pulsed with glycolipids α-GalCer, OCH and AH10-7 (Fig. 7A) incorporated in liposomes efficiently activated

iNKT cells hybridoma. We found statistical differences between IL-2 secreted from iNKT cells hybridoma activated by BMDC pulsed with the glycolipids ( $\alpha$ -GalCer, OCH or AH10-7) incorporated into liposomes, and IL-2 secreted from iNKT cells hybridoma co-cultured with BMDC pulsed with empty liposomes (negative control).

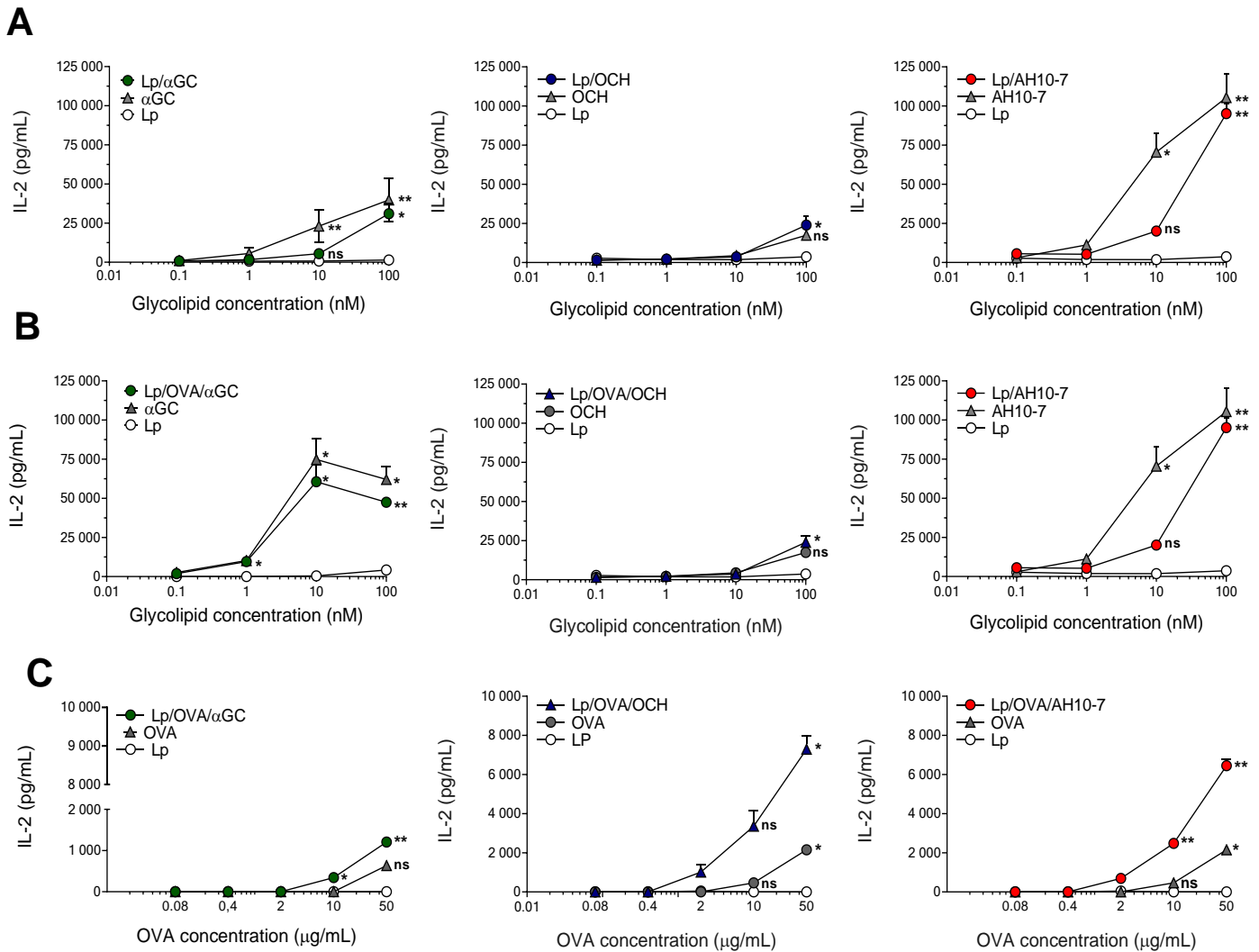


**Figure 7. Bone marrow-derived dendritic cells (BMDC) from C57BL/6J hCD1d-KI mice stimulated with  $\alpha$ -GalCer, or  $\alpha$ -GalCer analogs (OCH and AH10-7) contained into liposomes (or in OVA-contained liposomes) can induce *in vitro* activation of iNKT cells and splenocytes from OT1 mice. Graphs show the concentration of IL-2 released by hybridomas of iNKT cells (A and B), and splenocytes from OT1 mice (C), present in co-culture with BMDC previously stimulated with liposomes containing**

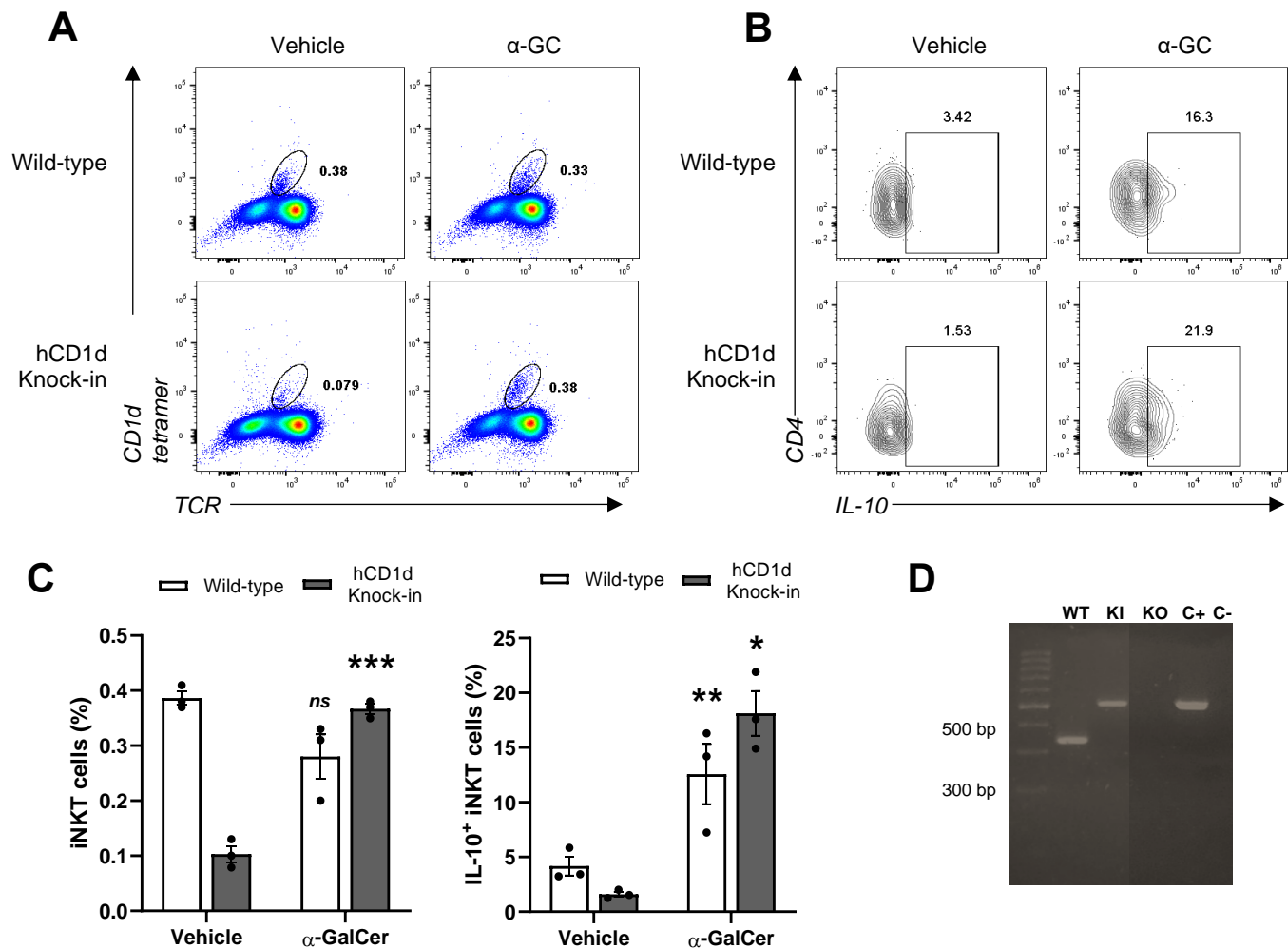
different concentrations of OVA and glycolipids ( $\alpha$ -GalCer, OCH or AH10-7, respectively). The plotted data represent the average of three experiments  $\pm$  standard error of the mean. Asterisks indicate significant differences compared with empty liposomes (Lp). <sup>ns</sup>,  $p > 0.05$ ; \*,  $p < 0.05$ ; \*\*,  $p < 0.01$  (ANOVA with Dunnett post-test for multiple comparisons).

We carried out similar experiments, but in this case, we pulsed BMDC with  $\alpha$ -GalCer, OCH, and AH10-7 in OVA-contained liposomes. Then, we established a co-culture of this pulsed BMDC with iNKT cells hybridoma or splenocytes from OT1 mice (these mice have a transgenic TCR designed to recognize specifically OVA peptide residues in the context of MHC class I) [123]. These results showed that incorporating glycolipids in OVA-contained liposomes does not affect the glycolipid presenting process due to the efficient activation of iNKT cells hybridoma by BMDC pulsed with  $\alpha$ -GalCer, OCH, and AH10-7 (Fig. 7B). Analogous to these results, OT1' splenocytes were efficiently activated by BMDC pulsed with  $\alpha$ -GalCer, OCH, and AH10-7 in OVA-contained liposomes (Fig. 7C). The IL-2 secreted from iNKT cells hybridoma and OT1' splenocytes activated by BMDC pulsed with the glycolipids ( $\alpha$ -GalCer, OCH or AH10-7) incorporated into OVA-contained liposomes were statistically different from the IL-2 secreted from iNKT cells hybridoma and OT1' splenocytes co-cultured with BMDC pulsed with empty liposomes. Then, we can conclude that the inclusion of glycolipid or OVA into this new liposome formulation did not change the antigenic potency of these compounds.

### **Induction of NKT10 cell in hCD1d-KI mice**

Although essentially all iNKT cells recognize  $\alpha$ -GalCer bound to CD1d via their invariant TCR, it became clear in recent years that iNKT cells are not a uniform population [21,

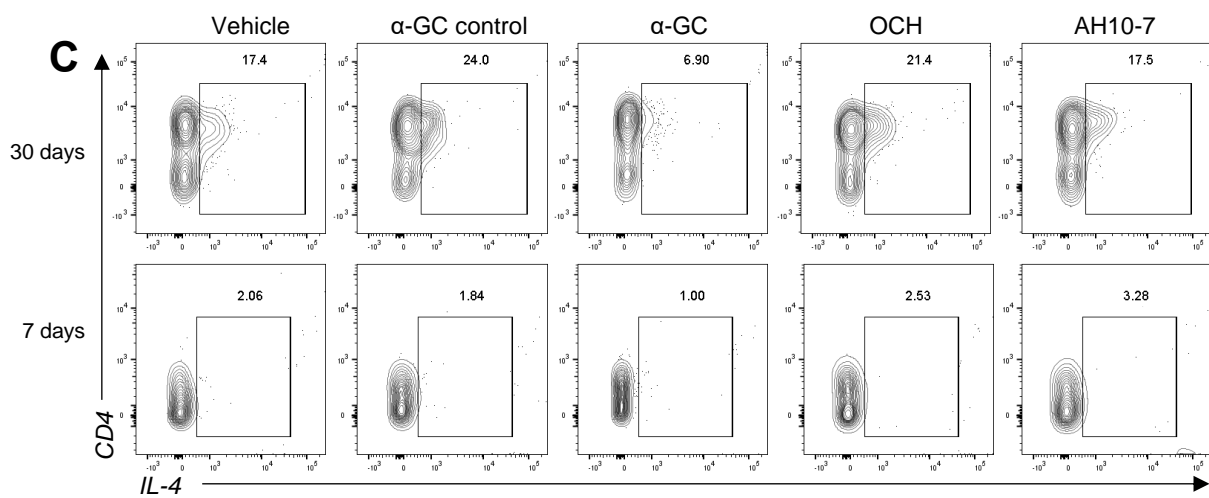
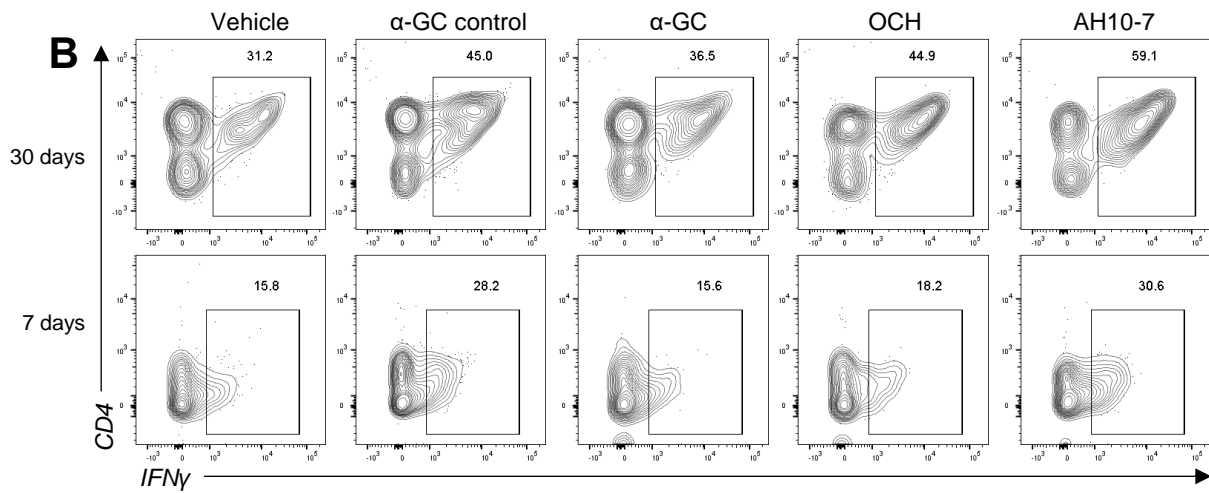
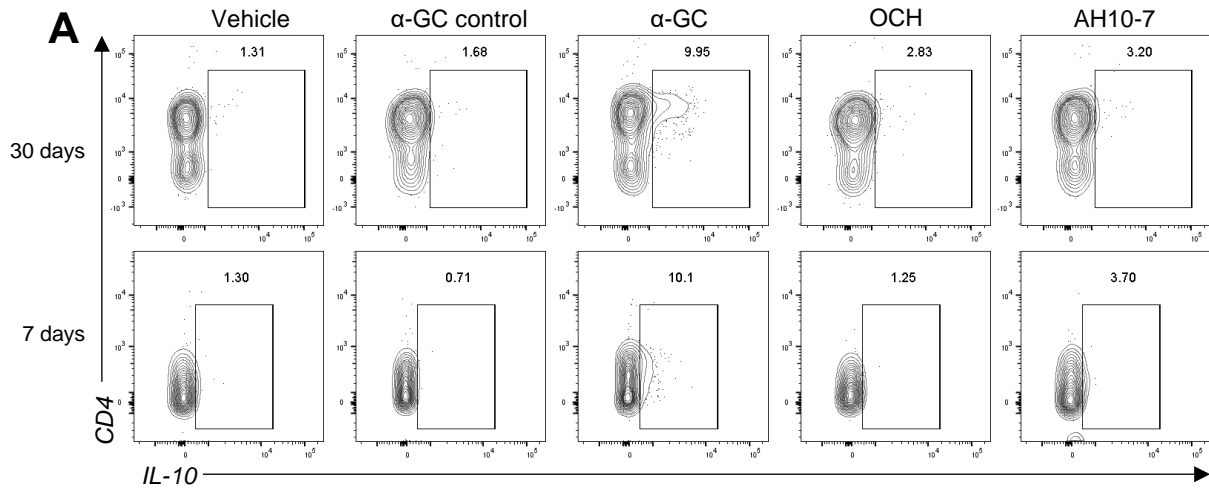
23]. Recently, a novel iNKT cell subset with IL-10-dependent regulatory function was described, termed NKT10 cells [22]. Through this IL-10 production, NKT10 cells could impair anti-tumor immune responses and protect mice against EAE, a mouse model of autoimmune disease. The hCD1d-KI mouse is a mouse model that more accurately replicates features of iNKT cell responses in humans [79, 80]. The generation of hCD1d-KI mice consists of the homologous recombination and integration of the human genomic CD1D gene in the mouse CD1D1 locus [79], which can be easily verified by PCR (Fig. 8D). Nowadays, there is no evidence of NKT10 cells in this model; for this reason, we tried to identify NKT10 cells in hCD1d-KI mice (C57BL/6J background) using the conventional scheme of stimulation of NKT10 cells utilized in wild-type mice. Briefly, we intravenous (i.v.) injected 4  $\mu$ g of  $\alpha$ -GalCer in hCD1d-KI mice and measured the iNKT cell response one month later by rechallenge with 1  $\mu$ g of  $\alpha$ -GalCer. Ninety minutes after the rechallenge, NKT10 cell expansion was measured by intracellular IL-10 labeling in iNKT cells (B220<sup>-</sup>TRC<sup>+</sup>CD1d<sup>+</sup>tetramer). To control that the iNKT cells activation was due to the treatment with  $\alpha$ -GalCer, we administered in one group the vehicle utilized to reconstitute the glycolipids (PBS with 0.05% Tween-20 and 0.1% DMSO). We could observe an expansion of iNKT cells in hCD1d-KI mice treated with  $\alpha$ -GalCer, but not in iNKT from wild-type mice treated with  $\alpha$ -GalCer (Fig. 8A). On the other hand, both wild-type and hCD1d-KI mice treated with  $\alpha$ -GalCer experimented an expansion of NKT10 cells, which was statistically different from the vehicle group (Fig. 8A, 8C). This result was relevant since it was the first time the NKT10 population was identified in hCD1d-KI mice.



**Figure 8. Identification of NKT10 cells in C57BL/6J wild-type and hCD1d-KI mice.** C57BL/6J wild-type (WT) and hCD1d-KI (n = 3) mice were injected with 4  $\mu$ g of  $\alpha$ -GalCer ( $\alpha$ -GC); 30 days later, they were re-stimulated with 1  $\mu$ g of  $\alpha$ -GalCer. NKT10 cell expansion was measured by intracellular IL-10 labeling in iNKT cells (B220<sup>-</sup> TRC<sup>+</sup> CD1d tetramer<sup>+</sup> cells). **(A)** and **(B)** represent flow cytometry showing the iNKT and NKT10 cells' expansion in response to  $\alpha$ -GC, respectively. **(C)** Summary charts of the experiment. The bars represent the mean  $\pm$  standard error of the mean. Asterisks indicate significant differences compared to vehicle. *ns*,  $p > 0.05$ ; \*,  $p < 0.5$ ; and \*\*,  $p < 0.01$  (Unpaired t-test). **(D)** Genotyping PCRs of hCD1d-KI (KI) mice, murine CD1d knock-out (KO) mice, and wild-type (WT) mice. The PCR product size for murine CD1d should be about 343 bp, and for human CD1d should be about 504 pb. Positive control (C+) was blood human, and negative control (C-) was a sample without DNA.

## **Expansion of NKT10 cells in hCD1d-KI mice with $\alpha$ -GalCer or $\alpha$ -GalCer analogs (OCH and AH10-7) with different schemes of immunizations.**

Identifying NKT10 cells in hCD1d-KI mice opened an opportunity to formulate new research questions related to the response of this population in hCD1d-KI mice. Parekh *et. al.* (2005) reported that the iNKT cell population experimented with similar expansion values from seven days to one month [124]. This result leads us to think that we could increase NKT10 cells in hCD1d-KI mice in a short period (at seven days); similarly, we induced NKT10 cells in hCD1d-KI mice with the immunization scheme of one month. Additionally, we would like to test which one of the synthetic  $\alpha$ -GalCer variants (those that induce Th1 or Th2 cytokine response) could be affordable to generate NKT10 cells in hCD1d-KI mice. For this purpose, hCD1d-KI mice were i.v. injected with 4  $\mu$ g of  $\alpha$ -GalCer, OCH, or AH10-7. After 7 or 30 days, iNKT cells were re-stimulated with 1  $\mu$ g of  $\alpha$ -GalCer. To determine if the expansion of NKT10 cells was mediated for the treatment at 7 or 30 days with the glycolipids ( $\alpha$ -GalCer, OCH or AH10-7) after the re-stimulation with  $\alpha$ -GalCer, we incorporated an experimental group of mice, which only received a dose of 1  $\mu$ g of  $\alpha$ -GalCer ( $\alpha$ -GalCer control group). Ninety minutes after the re-stimulation, iNKT cells, and IL-10<sup>+</sup>, IFN $\gamma$ <sup>+</sup>, IL-4<sup>+</sup> iNKT cells were measured. iNKT cell expansion was increased only in mice treated with  $\alpha$ -GalCer at 7 and 30 days (Fig. 9D). On the other hand, we can observe a predominant expansion of NKT10 cells in mice treated with  $\alpha$ -GalCer at 7 and 30 days, which was statistically different from the vehicle group (Fig. 9A, 9E).



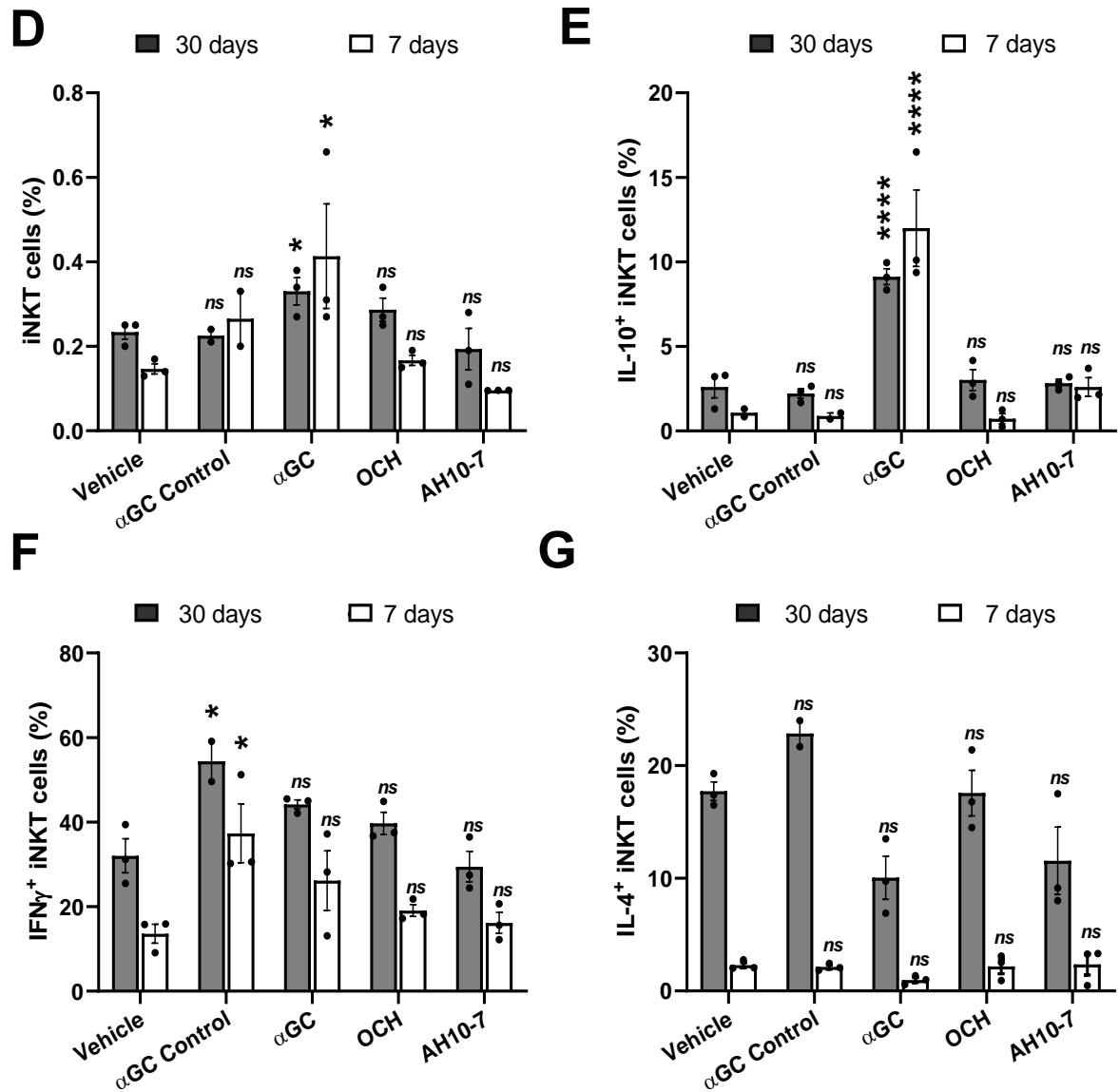


**Figure 9. Expansion of NKT10 cells in hCD1d-KI mice with  $\alpha$ -GalCer or  $\alpha$ -GalCer analogs (OCH and AH10-7) using different schemes of immunizations.** hCD1d-KI mice ( $n = 3$ ) were injected with 4  $\mu$ g of  $\alpha$ -GalCer ( $\alpha$ -GC) OCH or AH10-7. After 7 or 30 days, iNKT cells were re-stimulated with 1  $\mu$ g of  $\alpha$ -GalCer. NKT10 cell expansion was measured by intracellular IL-10 labeling in iNKT cells (B220<sup>-</sup>TRC<sup>+</sup>CD1d<sup>+</sup>tetramer). **(A)**, **(B)** and **(C)** are representative flow cytometry showing IL-10<sup>+</sup>, IFN $\gamma$ <sup>+</sup>, and IL-4<sup>+</sup> iNKT cells, respectively. **(D)**, **(E)**, **(F)**, and **(G)** Summary charts of iNKT cells and IL-10<sup>+</sup>, IFN $\gamma$ <sup>+</sup>, and IL-4<sup>+</sup> iNKT cells expansion, respectively. The bars represent the mean  $\pm$  standard error of the mean. Asterisks indicate significant differences compared with their respective Vehicles. *ns*,  $p > 0.05$ ; \*,  $p < 0.05$ ; and \*\*\*\*  $p < 0.0001$  (ANOVA with Dunnett post-test for multiple comparisons).



The expansion of NKT10 cells in mice treated with OCH and AH10-7 at 7 and 30 days was not well different from the vehicle and  $\alpha$ -GalCer control groups. Only in the group of mice treated with AH10-7 at 7 days we could observe a slight increase of NKT10 cells, but this was not statistically significant. Besides, the expansion of IFN $\gamma$ <sup>+</sup> iNKT cells at 7 or 30 days had the same tendency: a not statistically significant increase in the groups treated with  $\alpha$ -GalCer, OCH, or AH10-7 compared to the vehicle group (Fig. 9B, 9F). Finally, the expansion of IL-4<sup>+</sup> iNKT cells was higher at 30 days of stimulation than the rechallenge on the 7<sup>th</sup> day. At 30 days of re-stimulation between experimental groups, we could observe a decrease of IL-4<sup>+</sup> iNKT cells in mice treated with  $\alpha$ -GalCer and AH10-7 compared to the vehicle group (Fig. 9C, 9G). On the other hand, at 7 days of re-stimulation, considerable differences were not observed in IL-4<sup>+</sup> iNKT cells between experimental groups. These results show that we can effectively activate NKT10 cells with an immunization scheme of two doses (4  $\mu$ g of glycolipid, 1  $\mu$ g of  $\alpha$ -GalCer) separated by seven days.

### **Expansion of NKT10 cells in hCD1d-KI mice with $\alpha$ -GalCer or $\alpha$ -GalCer analogs that induce Th1- type cytokine response (AH10-7, AH10-3, AH10-1).**

Numerous structural analogs of  $\alpha$ -GalCer have been synthesized to understand the structure-function relationship and produce specific iNKT cells ligands with more favorable activity profiles for potential therapeutic applications [76, 125]. The glycolipids AH10-3, AH10-1, and AH10-7 were recently synthesized and categorized as  $\alpha$ -GalCer analogs that induce the expression of IFN- $\gamma$  and other Th1-type cytokines after iNKT cell activation [72, 76]. AH10-3 and AH10-1 have in common that they present variations in the C4'' of galactose bound to sphingosine. On the other hand, AH10-7

presents a modification in the C6" of galactose and a hydroxyl group substitution) in the acyl chain. [72, 76]. Despite these antecedents, it would be necessary to identify which of those Th1-biasing iNKT cells agonists could promote the expansion of NKT10 cells in hCD1d-KI mice in a short period of immunization scheme (at seven days). For this purpose, hCD1d-KI mice were i.v. injected with 4 µg of AH10-3, AH10-1, AH10-7, or α-GalCer (as an internal positive control of each experiment). After 7 days, iNKT cells were re-stimulated with 1 µg of α-GalCer. To determine if the expansion of NKT10 cells is mediated for the treatment at 7 days with the glycolipids (α-GalCer, AH10-3, AH10-1, or AH10-7) after the re-stimulation with α-GalCer, we incorporated an experimental group of mice, which only received a dose of 1 µg of α-GalCer (α-GalCer control group). Ninety minutes after the re-stimulation, iNKT cells, and IL-10<sup>+</sup> iNKT cells were measured. iNKT cell expansion was increased only in mice treated with α-GalCer at 7 days. As previous results, iNKT cell expansion significantly increased only in mice treated with α-GalCer at 7 days (data not showed). On the other hand, we can observe a predominant expansion of NKT10 cells in mice treated with α-GalCer, which was statistically different from the vehicle group (Fig. 10A, 10B, and 10C). The expansion of NKT10 cells in mice treated with AH10-3, AH10-1, and AH10-7 had no statistical difference in comparison to the vehicle and α-GalCer control groups (Fig. 10A, 10B, and 10C). Interestingly, in the group of mice treated with AH10-7 we observe a slight increase in NKT10 cells, but unfortunately non-significant (Fig. 10C).

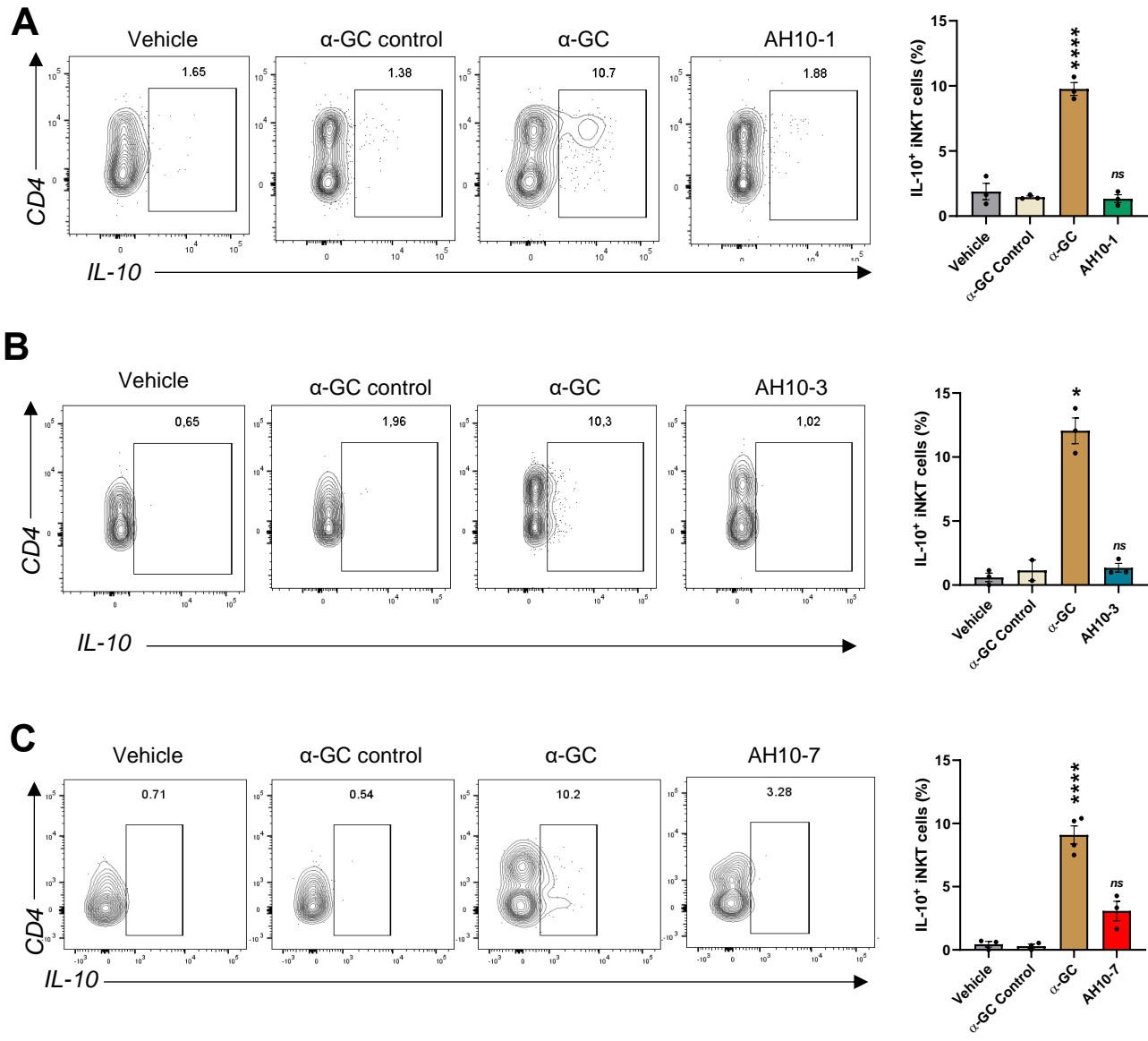


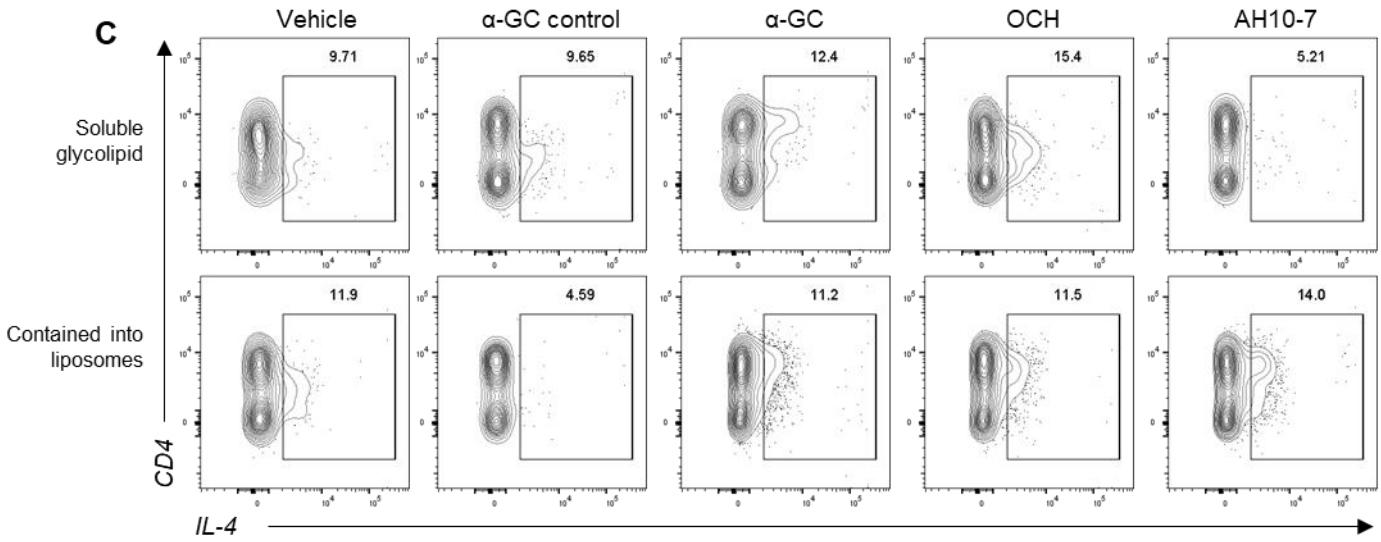
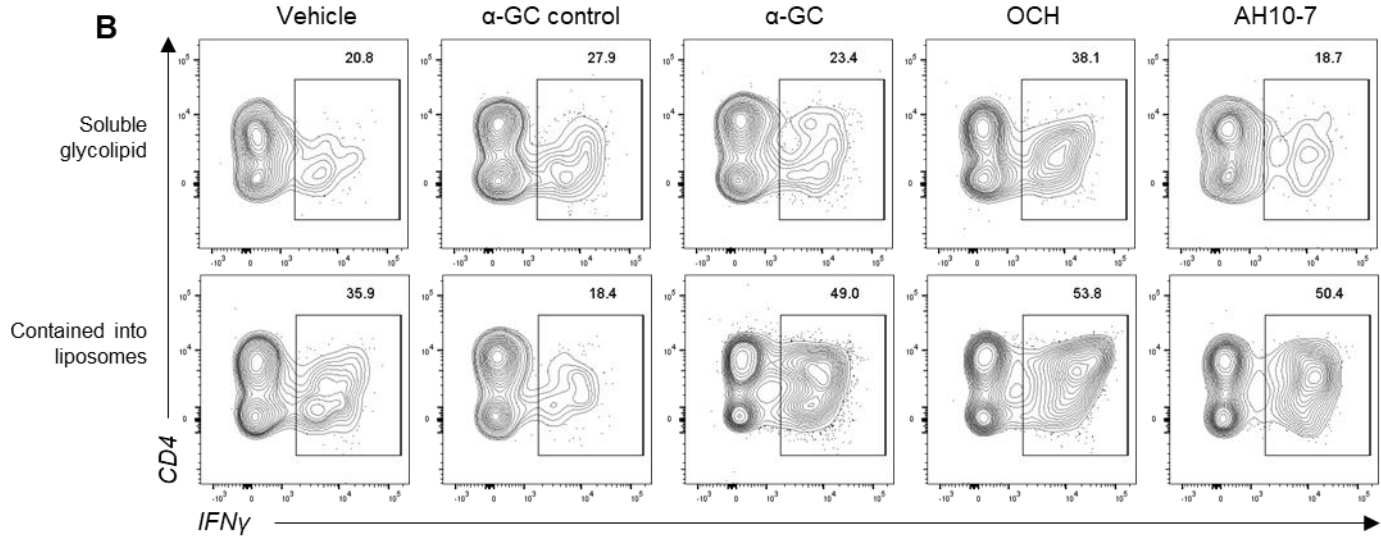
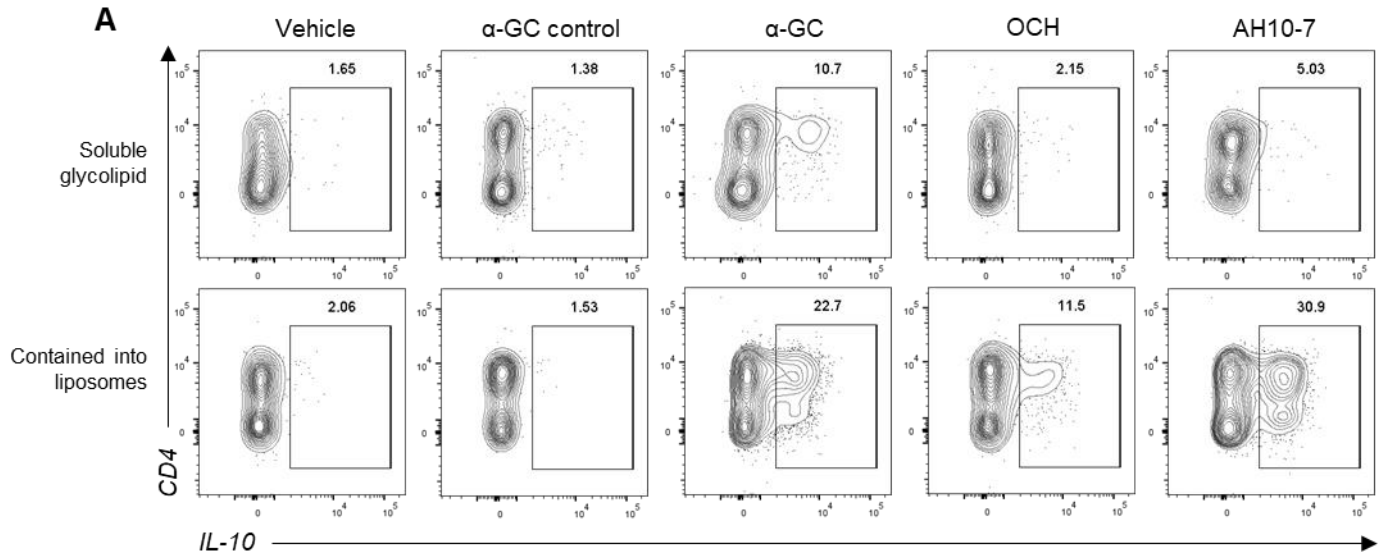
**Figure 10. Expansion of NKT10 cells in hCD1d-KI mice with α-GalCer or α-GalCer analogs (AH10-1, AH10-3, and AH10-7).** hCD1d-KI mice (n = 3) were injected with 4 μg of α-GalCer (α-GC) AH10-1, AH10-3, or AH10-7. After 7 days, iNKT cells were re-stimulated with 1 μg of α-GalCer. NKT10 cell expansion was measured by intracellular IL-10 labeling in iNKT cells (B220<sup>-</sup>TRC<sup>+</sup>CD1d<sup>+</sup>tetramer). **(A)**, **(B)** and **(C)** represent flow cytometry showing IL-10<sup>+</sup> iNKT cells from mice treated with AH10-1, AH10-3, and AH10-7, respectively, in three independent experiments. Also is represented summary charts of IL-10<sup>+</sup> iNKT cells expansion. The bars represent the mean ± standard error of the mean. Asterisks indicate significant differences compared with Vehicles. *ns*, p > 0.05; \*, p < 0.5; \*\*, p < 0.01; \*\*\*, p < 0.001; and \*\*\*\* p < 0.0001 (ANOVA with Dunnet post-test for multiple comparisons).

As previously shown, we can effectively activate NKT10 with the prototypical antigen  $\alpha$ -GalCer cells in an immunization scheme of two doses (4  $\mu$ g of glycolipid, 1  $\mu$ g of  $\alpha$ -GalCer) separated by seven days. On the other hand, it was necessary to improve the activation of NKT10 cells with  $\alpha$ -GalCer analogs, one strategy could be the use of antigen delivery systems, such as liposomes.

**Expansion of NKT10 cells in hCD1d-KI mice with  $\alpha$ -GalCer or  $\alpha$ -GalCer analogs (OCH and AH10-7) contained into liposomes.**

Including  $\alpha$ -GalCer into liposomes is an effective way to enhance iNKT cells response, avoiding both anergy and liver toxicity [124, 126-130]. In this work, we analyzed for the first time the modulation of iNKT cells' cytokine response stimulated with glycolipid encapsulated into liposomes, focusing on the modulation that expands NKT10 cells and elicits a regulatory- skewed response. In this sense, we evaluated the IL-10<sup>+</sup> iNKT cells from hCD1d-KI mice stimulated with  $\alpha$ -GalCer, OCH or AH10-7 contained in liposomes. We applied the immunization scheme of seven days mentioned above. To check if glycolipid ligands incorporated in liposomes would induce a different response than soluble glycolipids, we administered free glycolipids ( $\alpha$ -GalCer, OCH or AH10-7) in three other groups. To control that the iNKT activation was due to the incorporation of glycolipid ligands, we administered in two independent groups empty liposomes, or the vehicle utilized to reconstitute the glycolipids (vehicle groups). Firstly, we observed that incorporating glycolipids into liposomes enhanced the expansion of iNKT cells (Fig. 11D). As in previous results, the proliferation of NKT10 cells was statistically significant when we stimulated with  $\alpha$ -GalCer, not in the case when we stimulated with OCH or AH10-7.

On the contrary, incorporating these glycolipid ligands ( $\alpha$ -GalCer, OCH, and AH10-7) into liposomes increased the expansion of NKT10 cells, which was superior in the group treated with AH10-7 incorporated in liposomes (Fig. 11A, 11E). This result places AH10-7 in liposomes as an excellent candidate for iNKT-based immunotherapy as a substitute for  $\alpha$ -GalCer. On the other hand, the intracellular cytokine staining of iNKT cells showed a different response of iNKT stimulated glycolipid ligands incorporated in liposomes compared to iNKT stimulated soluble glycolipids. In this sense, we observed a not statistically significant increase of IFN $\gamma$ <sup>+</sup> iNKT cells in the groups treated with  $\alpha$ -GalCer, OCH, and AH10-7 incorporated in liposomes (Fig. 11B, 11F). On the contrary, we observed a not statistically significant decrease of IL-17<sup>+</sup> iNKT cells from  $\alpha$ -GalCer, OCH, and AH10-7 incorporated in liposomes treated mice (Fig. 13H). The production of IL-4 and TNF were moderately similar between groups in iNKT stimulated glycolipid ligands incorporated in liposomes compared to iNKT stimulated soluble glycolipids (Fig. 11C, 11G, 11I).



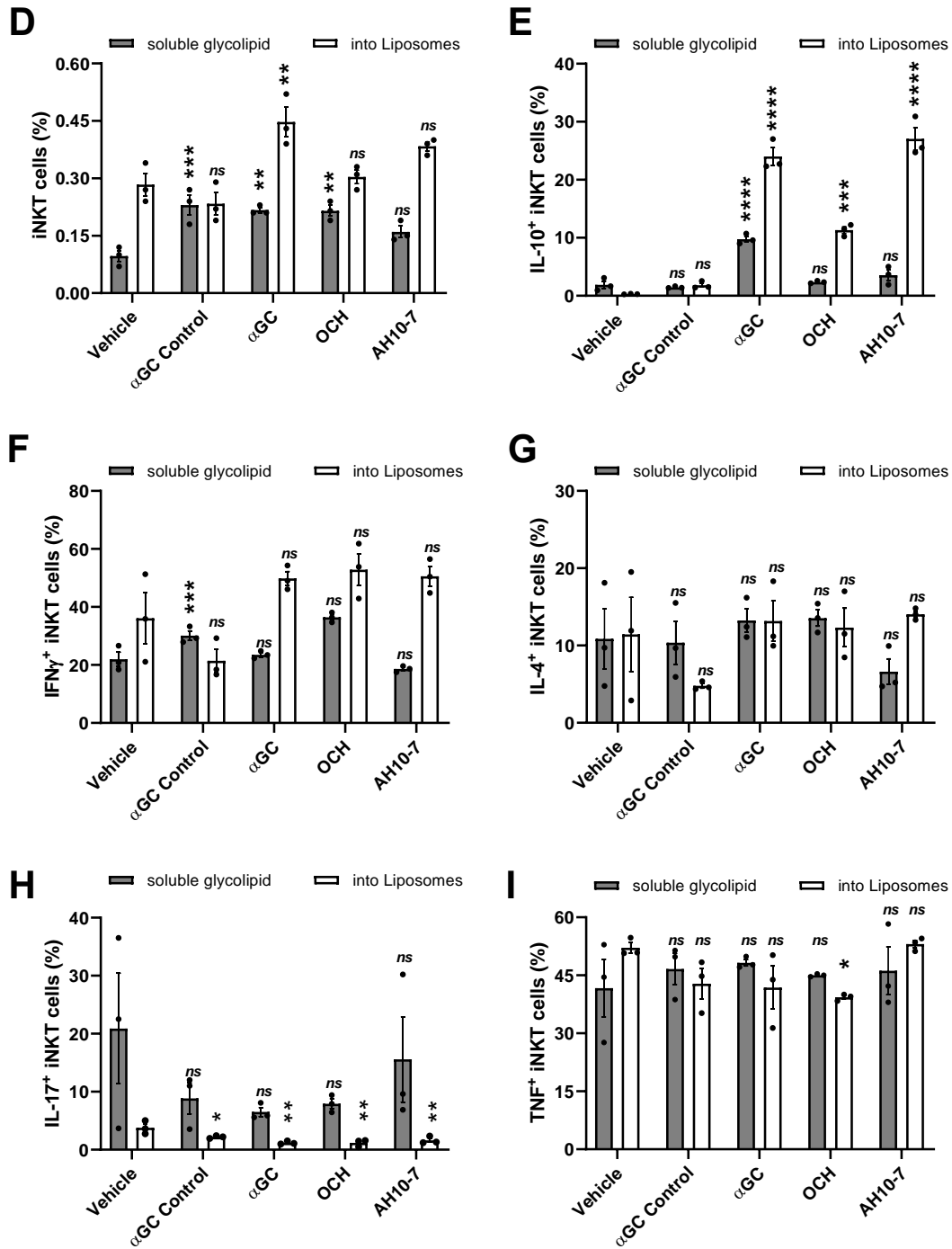
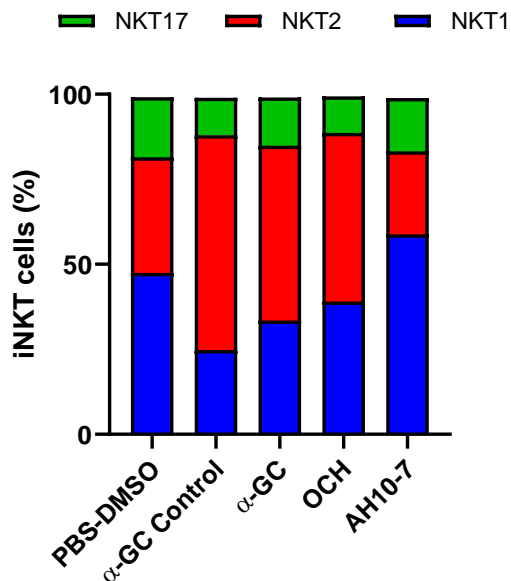


**Figure 11. Expansion of NKT10 cells in hCD1d-KI mice with  $\alpha$ -GalCer or  $\alpha$ -GalCer analogs (OCH and AH10-7) contained or not into liposomes.** hCD1d-KI mice ( $n = 3$ ) mice were injected with 4  $\mu$ g of  $\alpha$ -GalCer ( $\alpha$ -GC) OCH or AH10-7 contained or not into liposomes. After 7 days, iNKT cells were re-stimulated with 1  $\mu$ g of  $\alpha$ -GalCer contained or not into liposomes. NKT10 cell expansion was measured by intracellular

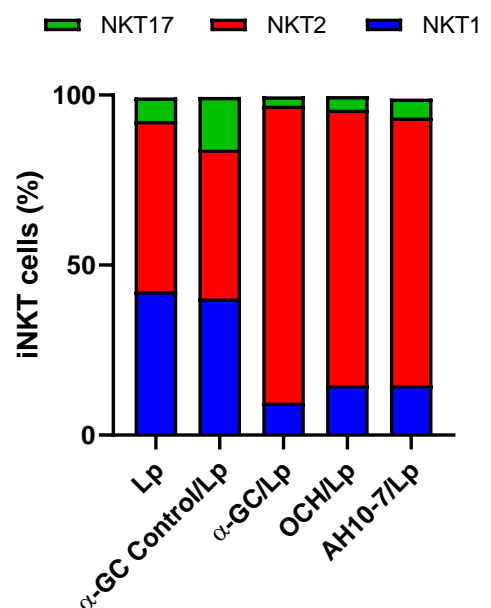
IL-10 labeling in iNKT cells (B220-TRC<sup>+</sup>CD1d<sup>+</sup>tetramer). **(A)**, **(B)** and **(C)** are representatives flow cytometry showing IL-10<sup>+</sup>, IFN $\gamma$ <sup>+</sup> and IL-4<sup>+</sup> iNKT cells, respectively. From **(D)** to **(I)** are summary charts of iNKT cells and IL-10<sup>+</sup>, IFN $\gamma$ <sup>+</sup>, IL-4<sup>+</sup>, IL-17<sup>+</sup> and TNF<sup>+</sup> iNKT cells' expansion, respectively. The bars represent the mean  $\pm$  standard error of the mean. Asterisks indicate significant differences compared with Vehicles. <sup>ns</sup>, p >0.05; \*, p <0.5; \*\*, p <0.01; \*\*\*, p <0.001; and \*\*\*\* p <0.0001 (ANOVA with Dunnet post-test for multiple comparisons).

Finally, we tried to identify other iNKT cells subsets based on the transcriptional factor activated during the stimulation of iNKT cells with  $\alpha$ -GalCer or  $\alpha$ -GalCer analogs (OCH and AH10-7) contained into liposomes (Figure 12). As a result, we observed a predominant activation of the NKT2 subset (PLZF<sup>+</sup>, ROR $\gamma$ t<sup>+</sup>) when we stimulated iNKT cells with  $\alpha$ -GalCer, OCH or AH10-7 contained into liposomes. On the contrary, we appreciated a decrease in the NKT1 subset (PLZF<sup>low</sup>, ROR $\gamma$ t<sup>-</sup>) and a severe reduction of NKT17 subset (PLZF<sup>interm</sup>, ROR $\gamma$ t<sup>+</sup>) under these experimental conditions.

**A**



**B**





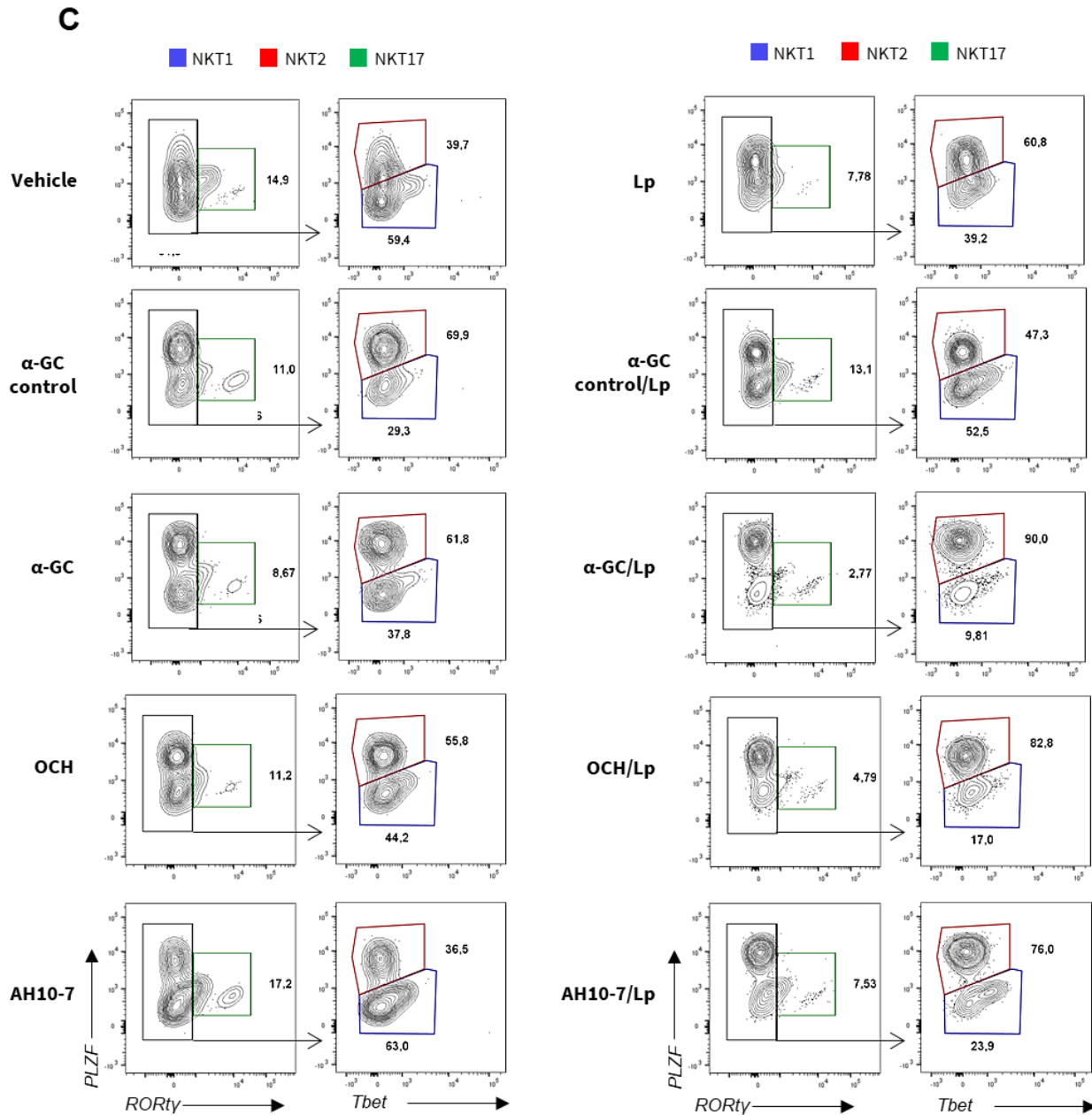
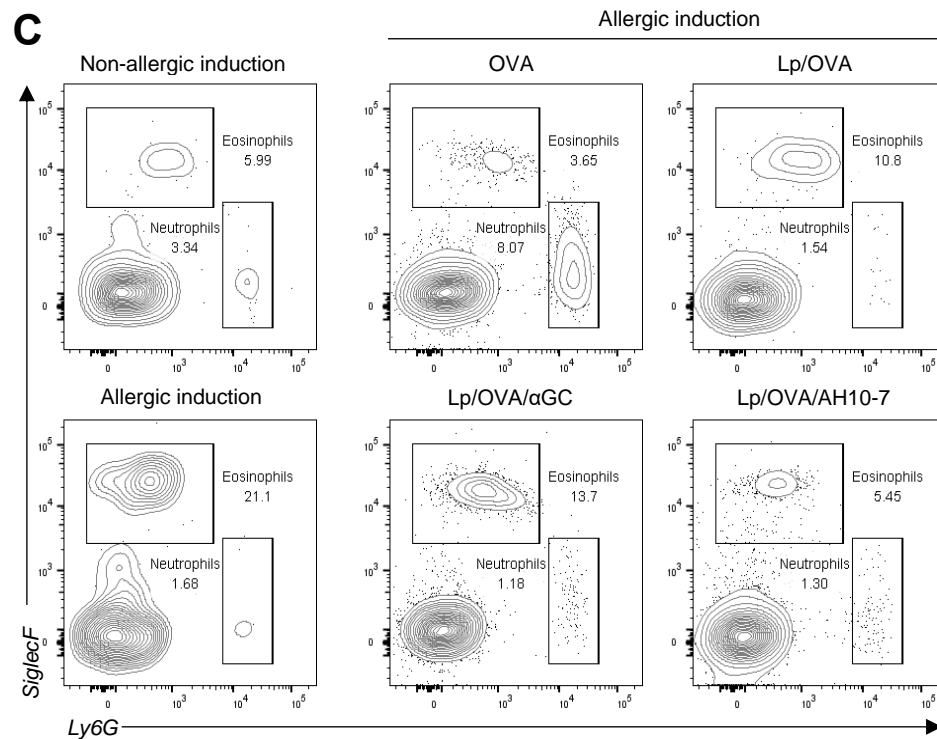
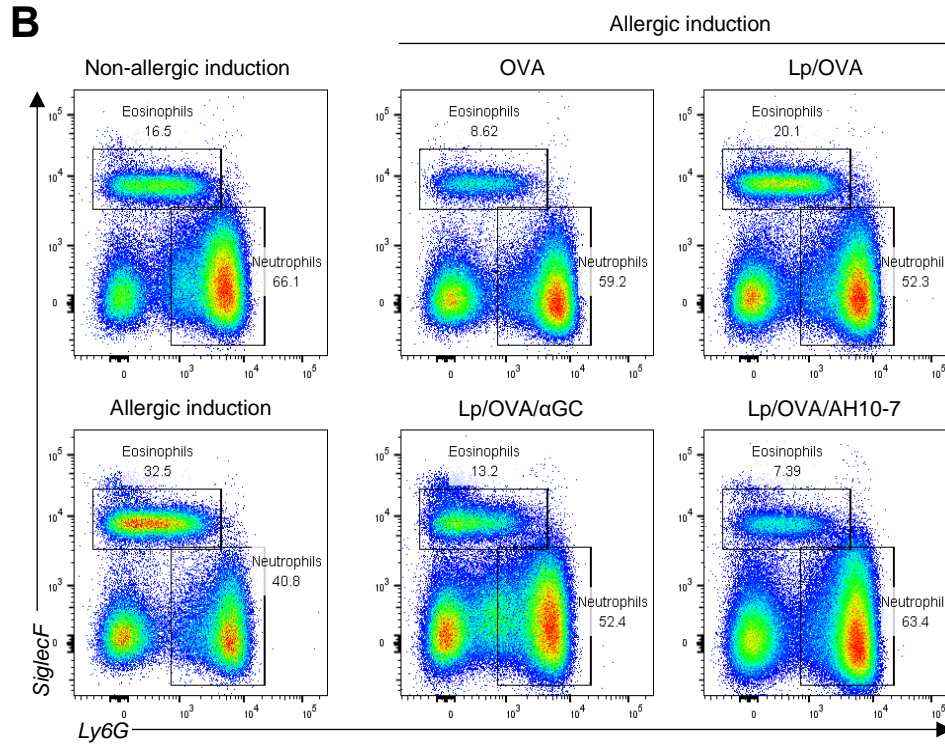
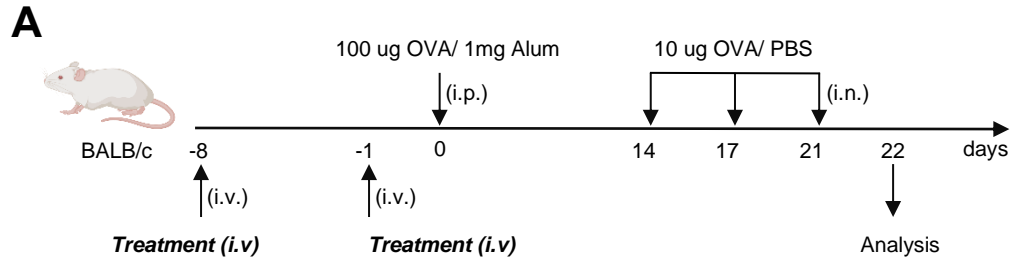


**Figure 12. Analysis of iNKT subsets in hCD1d-KI mice stimulated with  $\alpha$ -GalCer or  $\alpha$ -GalCer analogs (OCH and AH10-7) contained or not into liposomes.** hCD1d-KI mice ( $n = 3$ ) were injected with 4  $\mu$ g of  $\alpha$ -GalCer ( $\alpha$ -GC), OCH or AH10-7 contained or not into liposomes. After 7 days, iNKT cells were re-stimulated with 1  $\mu$ g of  $\alpha$ -GalCer contained or not into liposomes. **(A)** and **(B)** are summary bar graphs of iNKT cells subsets (NKT1, NKT2, and NKT17) in mice stimulated with  $\alpha$ -GalCer or  $\alpha$ -GalCer analogs (OCH and AH10-7) contained or not into liposomes, respectively. **(C)** is a representative flow cytometry plot showing iNKT cells subsets: NKT2 (PLZF<sup>high</sup>, RORyt<sup>-</sup>Tbet<sup>+</sup>), NKT1 (PLZF<sup>low</sup>, RORyt<sup>+</sup>Tbet<sup>+</sup>), and NKT17 (PLZF<sup>interm</sup>, RORyt<sup>+</sup>).

***SPECIFIC AIM 2: To determine if the differential activation of iNKT cells with different  $\alpha$ -GalCer analogs in liposomes will increase the expansion of Breg, leading to the prevention or reduction of allergic asthma in BALB/c mice with induced allergy by the experimental allergen OVA.***

**Obtention of OVA induced-allergic mice and antiallergic effect of liposomes containing  $\alpha$ GalCer analogs.**

First, we needed to obtain a mouse model of asthma to assess this objective. For this purpose, female BALB/c mice were immunized by intraperitoneal injection (i.p.) with 100  $\mu$ g OVA in 1mg Inject<sup>TM</sup>Alum followed by intranasal (i.n.) challenge with 10  $\mu$ g of OVA dissolved in PBS at days 21, 24, and 28 post-immunizations (Fig. 13A). As a control of the mouse model of allergic asthma, we administered in a group of mice i.p and i.n PBS (non-allergic induction group). In addition, we evaluated the antiallergic effect of the glycolipids ( $\alpha$ -GalCer and AH10-7) administered in OVA-contained liposomes. For this reason, the liposomes were i.v. administered at 8 and 1 day before immunization with OVA/Alum described (Fig. 13A). Following the immunization scheme established in this study for NKT10 cell induction (two doses from 4  $\mu$ g of glycolipid and 1  $\mu$ g of  $\alpha$ -GalCer, separated by seven days). To ensure that the antiallergic effect observed was due to the incorporation of glycolipid ligands, we administered i.v. OVA-contained liposomes and soluble OVA in two independent experimental groups. Symptoms of allergic inflammation were evaluated 24 hours after the last i.n. challenge. As a result, we appreciated a significant decrease in the recruitment eosinophil in lungs from mice with allergic induction and treated with liposomes containing OVA and AH10-7 (Lp/OVA/AH10-7) compared to mice with allergic induction (Fig. 13B y D).



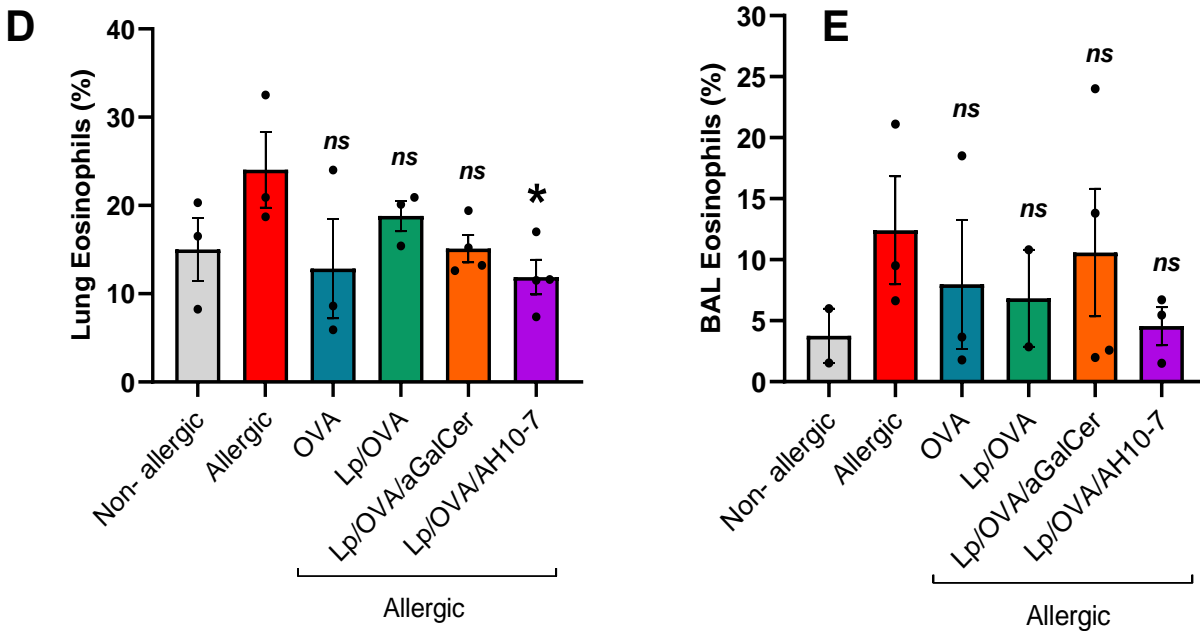


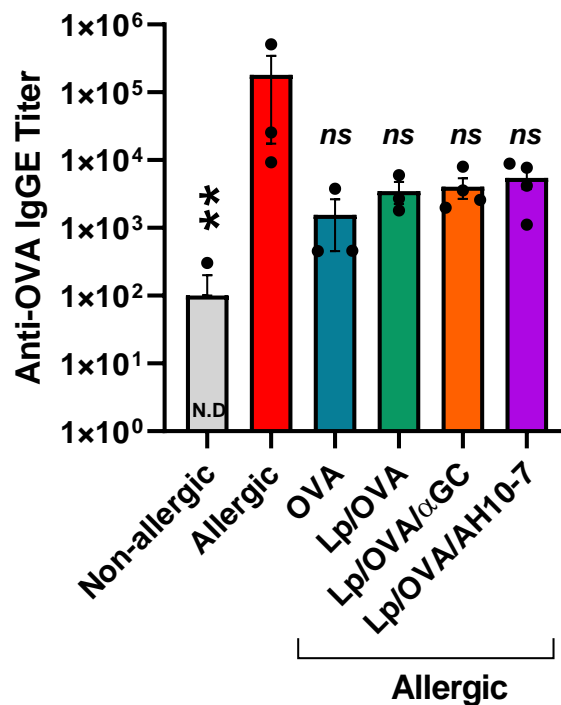
**Figure 13. Eosinophil recruitment in lung and bronchoalveolar lavage (BAL) from mice with OVA-induced allergy treated with liposomes containing OVA and glycolipids ( $\alpha$ -GalCer or AH10-7), in a prophylactic scenery. (A) Protocol for the obtention of mice with OVA-allergic induction and treated liposomes containing glycolipids (Glyc) and OVA. BALB/c mice ( $n = 4$ ) were sensitized with 100  $\mu$ g of OVA in 1mg of Alum. At 21, 24, and 28 days the mice were re-challenge with an intranasal dose of 10  $\mu$ g of OVA in PBS. Liposomal preparations (and controls) were administered at 8 and 1 day before immunization with OVA/ Alum. (B) y (C) Representative flow cytometry graphs with the population of eosinophils ( $CD45^+$ ,  $CD11c^-$ ,  $TCR^-$ ,  $B220^-$ ,  $CD11b^+$ ,  $MHCII^{low}$ ,  $Ly6G^-$  and  $SiglecF^+$  cells) in lungs, and eosinophils ( $CD45^+$ ,  $CD11c^-$ ,  $Ly6G^-$  and  $SiglecF^+$  cells) in BAL. Charts (D) and (E) show the summary of the % of eosinophils in the BAL and lung, respectively. The bars represent the mean  $\pm$  standard error of the mean. Asterisks indicate significant differences compared with the allergic group. <sup>ns</sup>,  $p > 0.05$  and \*,  $p < 0.05$  (Unpaired t-test or Mann-Whitney test).**

However, it was not observed a reduction in the recruitment eosinophil in lungs from mice with allergic induction treated with liposomes containing OVA and  $\alpha$ -GalCer (Lp/OVA/ $\alpha$ -GC), liposomes containing OVA (Lp/OVA), and soluble OVA. Additionally, it was not appreciated a significant decrease in the frequency of eosinophils in the bronchoalveolar lavage (Fig. 13C y E) and the titer of allergen-specific IgE (Fig. 14) from the mice with allergic induction and treated with Lp/OVA/ $\alpha$ -GC, Lp/OVA/AH10-7, Lp/OVA, and soluble OVA.

On the other hand, in allergic mice treated with liposomes containing OVA and AH10-7 we observed a complete recovery of lung morphology: a significant decrease in the degree of lung inflammation and goblet cell hyperplasia (Fig. 15 y 16). In this experimental group, we could see a decrease in inflammatory infiltrate foci in the bronchioles' submucosa. In addition, it was distinguished that the blood vessels were surrounded by a smaller number of foci of inflammatory infiltrate (Fig. 15A). Around both structures (the bronchioles and the blood vessels), the alveolar structures maintain their alveolar spaces well preserved. Increased numbers of goblet cells (goblet cell hyperplasia) is part of airway remodeling in asthma [131]. Thus, we consider as a promising result that it was observed a significant reduction in the number of goblet cells, in allergic mice treated with Lp/OVA/AH10-7 (Fig. 16).

Finally, in allergic mice treated with Lp/OVA/ $\alpha$ GalCer, we observed the presence of foci of inflammatory infiltrate and goblet cells in the submucosal of the bronchioles (Fig. 15A y 16A). In addition, Alveolar structures are identified with reduced alveolar spaces due to red blood cells and inflammatory infiltrate. On the other side, in the groups of allergic mice treated with Lp/OVA and soluble OVA, we observed the presence of foci of

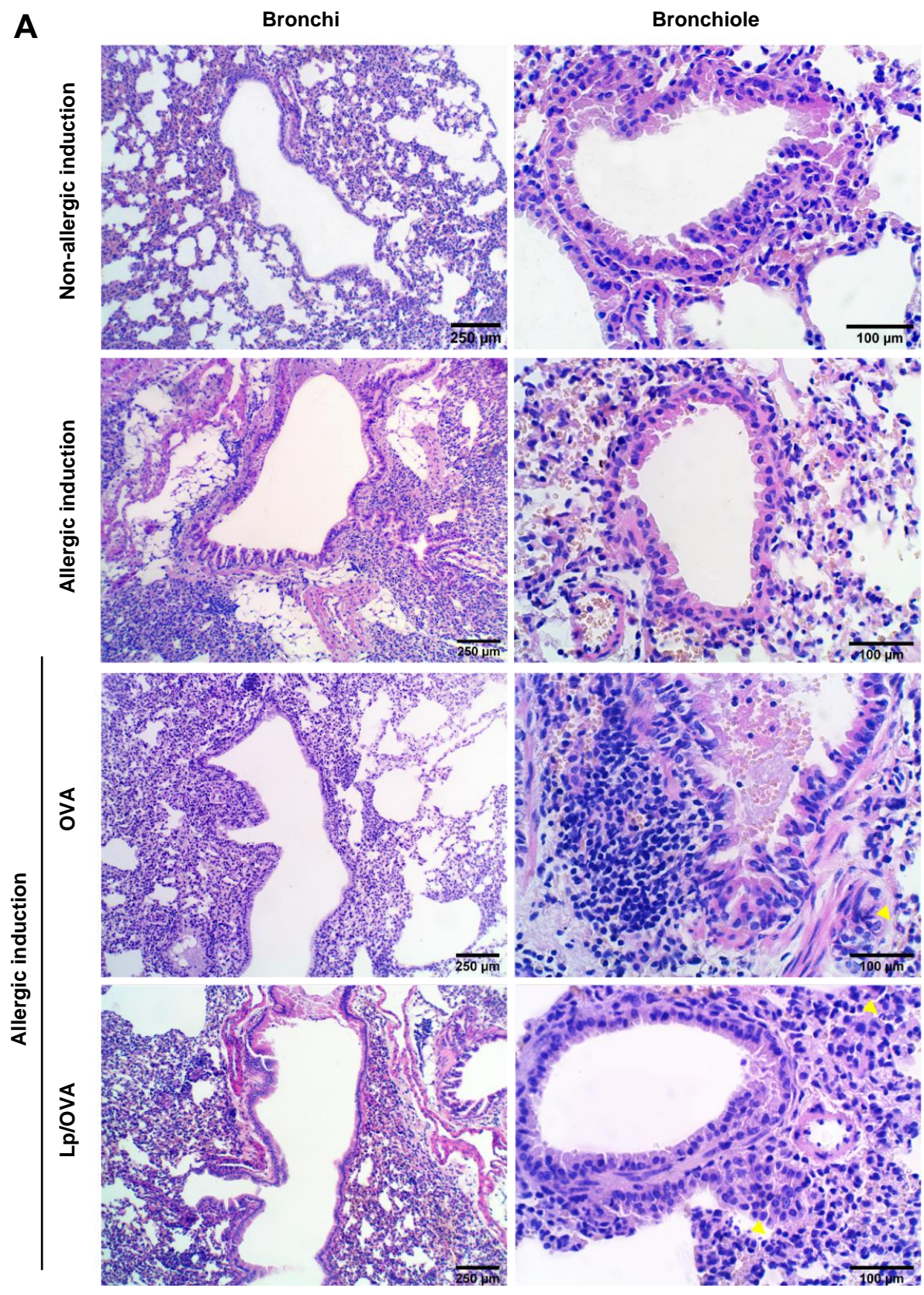
inflammatory infiltrate in the submucosa of the bronchioles, together with a reduction in alveolar spaces due to the presence of inflammatory infiltrate and globules red (Fig. 15A). In addition, these experimental groups had PAS-positive cell levels like allergy-induced mice. Interestingly, both groups had mucous plugging in the bronchial lumen (Fig. 16A).



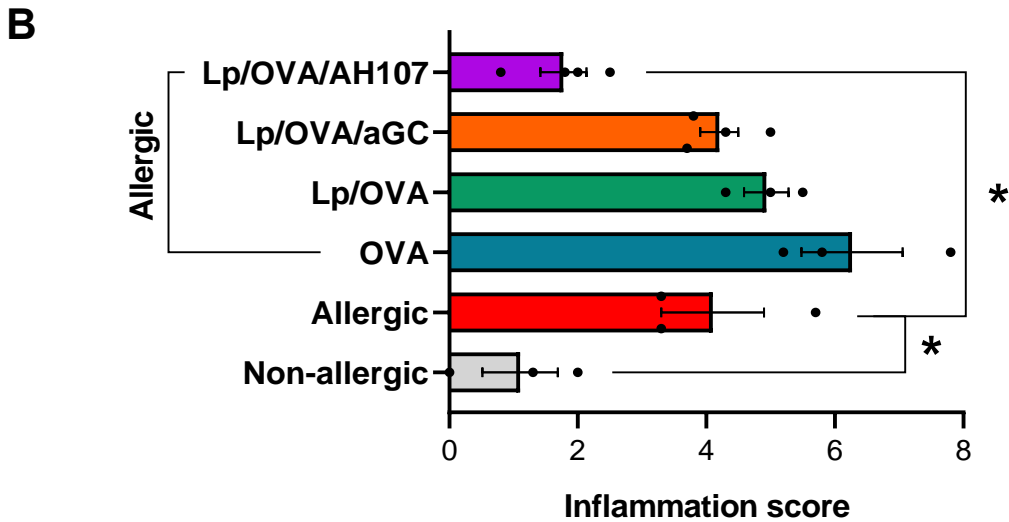
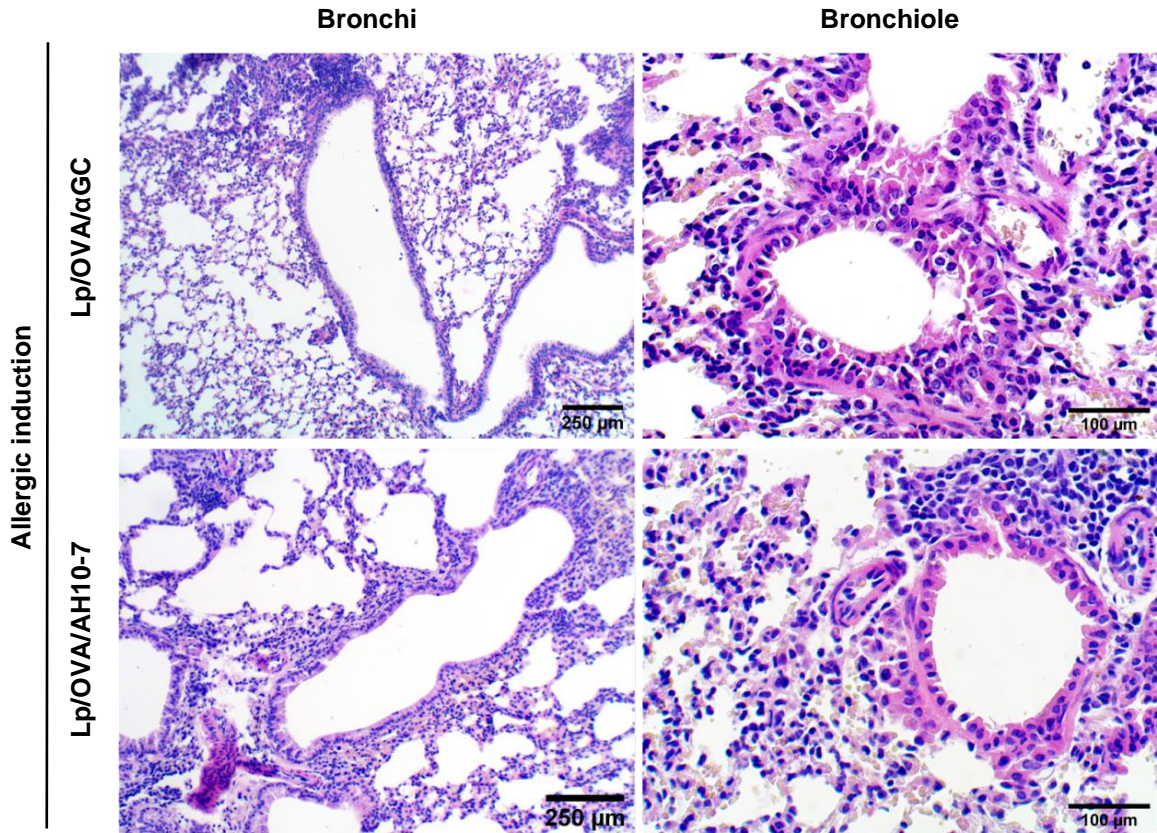
**Figure 14. Levels of allergen-specific IgE in mice with OVA-induced allergy treated with liposomes containing OVA and glycolipids ( $\alpha$ -GalCer or AH10-7), in a prophylactic scenery.** BALB/c mice ( $n = 4$ ) were induced by OVA allergy by sensitizing with 100  $\mu$ g of OVA in 1mg of Alum, after an i.n challenge with 10  $\mu$ g of OVA in PBS at 21, 24, and 28 days. Liposomal preparations and controls were administered at 8 and 1 day before immunization with OVA / Alum. Anti-OVA IgE titer is shown, defined as the cut-off point to determine the titer, twice the absorbance average of the pre-immune group. If the absorbance is below the cut-off point, the titer is considered as not determinable (N.D). Asterisks indicate a statistical difference between allergic induced-mice and treated allergic induced-mice. ns,  $p > 0.05$ ; \*,  $p < 0.05$ ; (Kruskal-Wallis test).



**A**



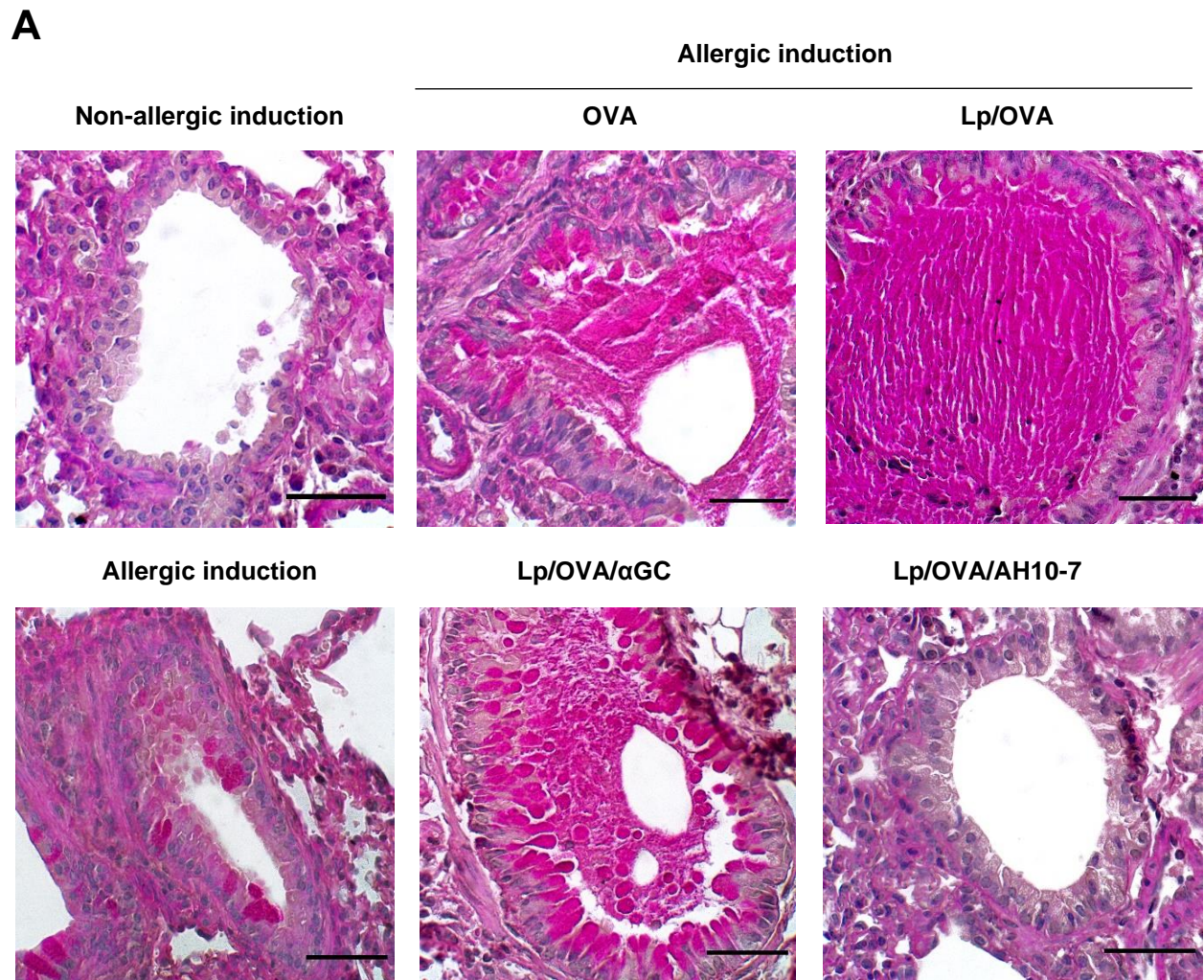




**Figure 15.** Infiltration of inflammatory cells in lung tissue from lungs removed from mice with OVA-induced allergy treated with liposomes containing OVA and glycolipids ( $\alpha$ -GalCer or AH10-7), in a prophylactic scenery. BALB/c mice ( $n = 4$ ) were sensitized with 100  $\mu$ g of OVA in 1mg of Alum. At 21, 24, and 28 days, the mice



were re-challenged with an intranasal dose of 10  $\mu$ g of OVA in PBS. Liposomal preparations and controls were administered at 8 and 1 day before immunization with OVA / Alum. Lungs were collected 24 hours after the last i.n. challenge and stained for histopathology analyses using hematoxylin & eosin to identify lung infiltrate at 40 X. **(A)** Representative microscopic photos of bronchi and bronchioles stained with hematoxylin & eosin. Yellow arrows indicate eosinophils in peribronchial and perivascular inflammatory foci. Black scale bars in the bronchi represent 250  $\mu$ m and in the bronchiole 100  $\mu$ m **(B)**. Inflammation scores. Each point represents results obtained from 1 individual mouse. The bars represent the mean  $\pm$  standard error of the mean. Asterisks indicate a statistical difference between allergic induced-mice and treated allergic induced-mice. ns,  $p > 0.05$ ; \*,  $p < 0.5$ ; (ANOVA with Dunnet post-test for multiple comparisons).



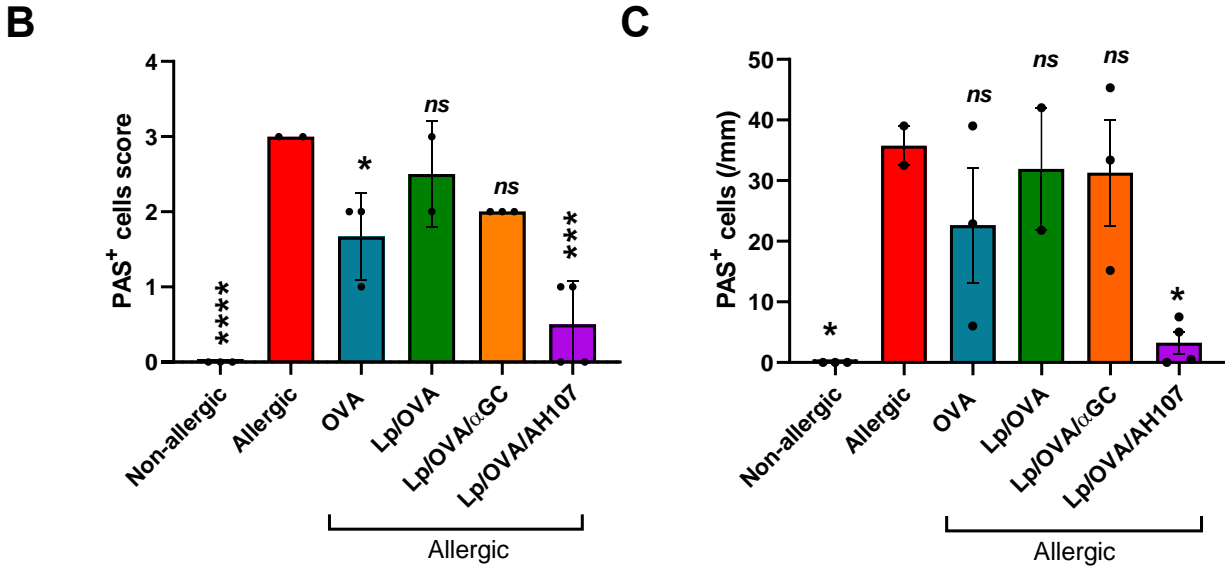


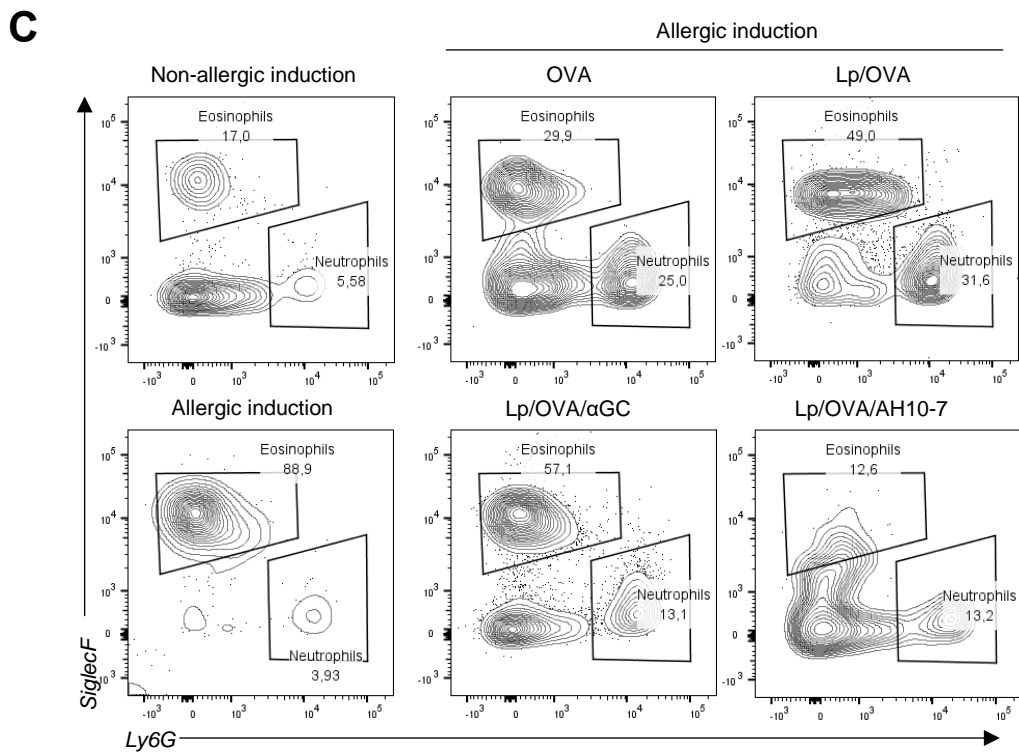
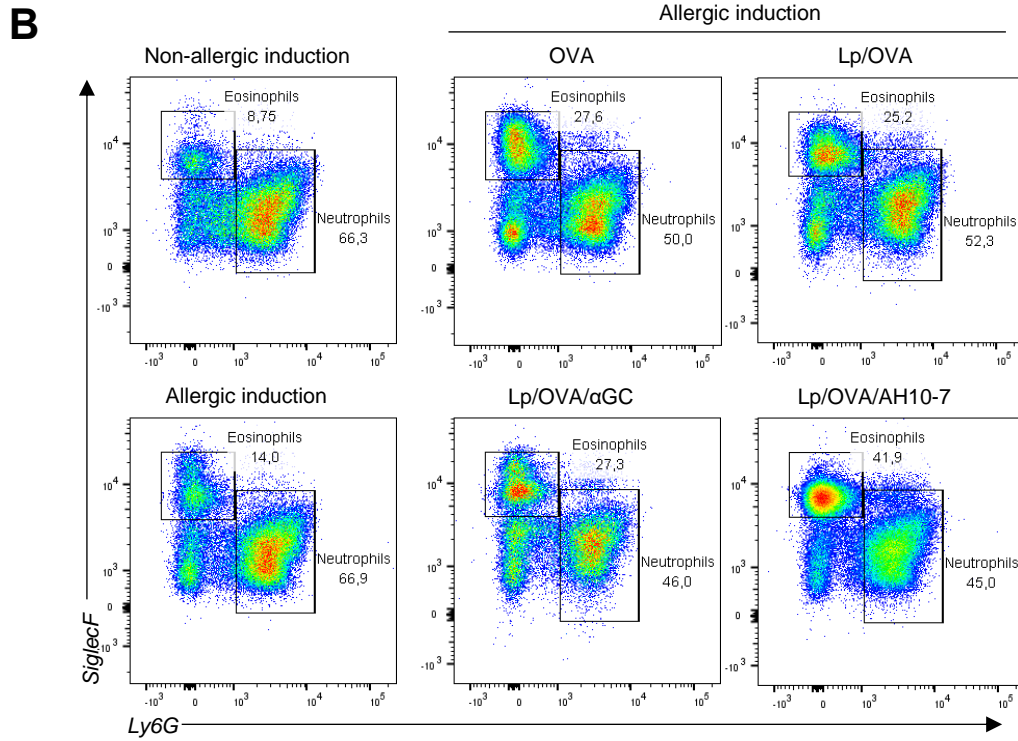
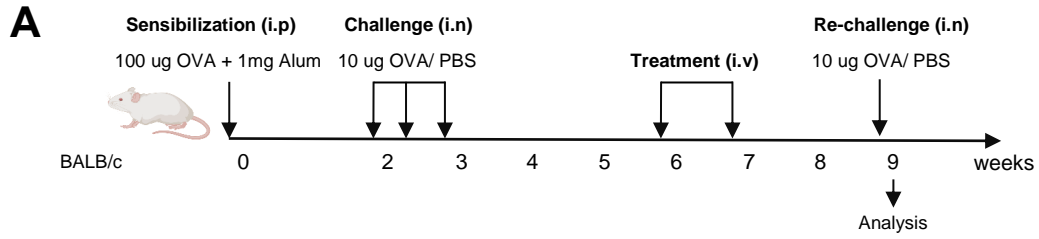
**Fig 16. Mucus secretion in lung tissue from mice with OVA-induced allergy treated with liposomes containing OVA and  $\alpha$ -GalCer or AH10-7, in a prophylactic scenery.** BALB/c mice ( $n = 4$ ) were sensitized with 100  $\mu\text{g}$  of OVA in 1mg of Alum. At 21, 24, and 28 days, the mice were re-challenge with an intranasal dose of 10  $\mu\text{g}$  of OVA in PBS. Liposomal preparations and controls were administered at 8 and 1 day before immunization with OVA / Alum. Lungs were collected 24 hours after the last i.n. challenge and the PAS stain was carried out to identification of goblet cells and mucus production at 40 X **(A)**. Representative microscopic photos of bronchiole stained with PAS. Fuchsia-red staining indicates the presence of goblet cells or mucus. Black scale bars represent 100  $\mu\text{m}$ . **(B)** Percentage of PAS<sup>+</sup> cells score in the bronchi and bronchiole. **(C)** Number of PAS<sup>+</sup> cells were counted and normalized by area of basement membrane. Each point represents results obtained from 1 individual mouse. The bars represent the mean  $\pm$  standard error of the mean. Asterisks indicate a statistical difference between allergic induced-mice and treated allergic induced-mice. <sup>ns</sup>,  $p > 0.05$ ; \*,  $p < 0.5$ ; \*\*\*,  $p < 0.001$ ; and \*\*\*\*  $p < 0.0001$  (ANOVA with Sidak post-test for multiple comparisons).

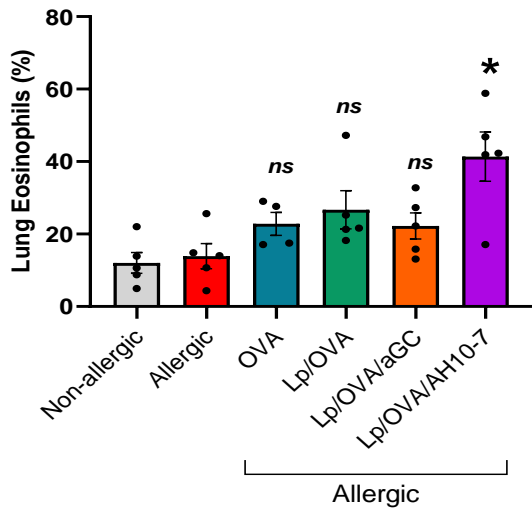
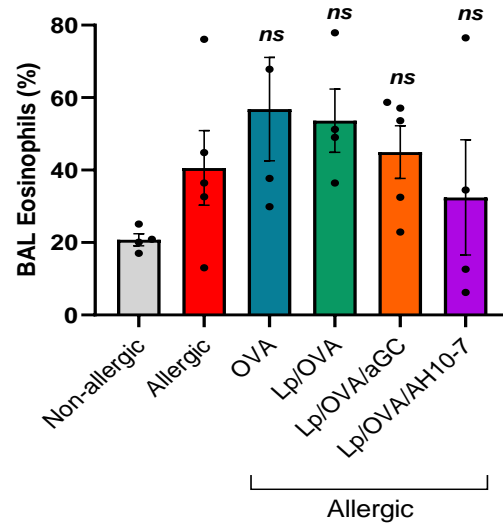
### Determination of the antiallergic effect of $\alpha$ -GalCer analogs contained into liposomes in a therapeutic scenery.

For this purpose, female BALB/c mice ( $n = 5$ ) were sensitized with 100  $\mu\text{g}$  of OVA in 1mg of Inject<sup>TM</sup>Alum. After two weeks, mice were challenged intranasally with three doses of 10  $\mu\text{g}$  of OVA in PBS. Following the immunization scheme established in this

study for NKT10 cell induction (two doses from 4  $\mu\text{g}$  of glycolipid and 1  $\mu\text{g}$  of  $\alpha\text{-GalCer}$ , separated by seven days), liposomal preparations (and controls) were administered three weeks after the last i.n. challenge. In the ninth week, mice were re-challenged with an intranasal dose of 10  $\mu\text{g}$  of OVA in PBS (Fig. 17A). Symptoms of allergic inflammation were evaluated 24 hours after the last i.n. challenge. As a result, we observed an increase of eosinophils in the lung parenchyma and the titer of allergen-specific IgE in allergic mice treated with Lp/OVA/AH10-7 (Fig. 17B and D, Fig. 18). On the other hand, it was not appreciated a significant decrease in the frequency of eosinophils in the bronchoalveolar lavage (Fig. 17C y E) and the titer of allergen-specific IgE (Fig. 18) from the mice with allergic induction and treated with Lp/OVA/ $\alpha\text{-GC}$ , Lp/OVA, and soluble OVA.

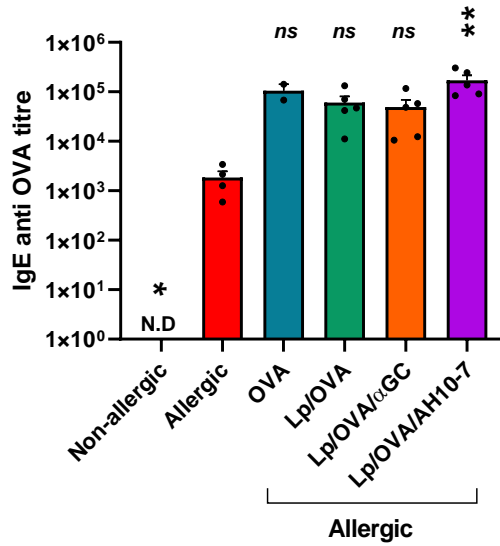
Immune tolerance to self-antigens and innocuous non-self-antigens is essential to protect the host against chronic inflammatory diseases and tissue damage [55]. B cells can regulate immune responses through their surface molecules and the secretion of cytokines. Regulatory B (Breg) cells are characterized by their immunosuppressive capacity, often mediated through IL-10 secretion [96]. Interestingly, we could appreciate a non-significant expansion of IL-10-producing regulatory B cells (B10 cells) in mediastinal lymph nodes from mice with OVA-induced allergy treated Lp/OVA/AH10-7 (Fig. 19). Since this expansion was not statistically significant, it is necessary for future experiments to verify the expansion of B10 cells induced by liposomes containing OVA and AH10-7. However, the results obtained in this experiment lead us to prove other immunization regimens to target iNKT cells with glycolipid activators of iNKT cells contained in liposomes in a therapeutic schedule.



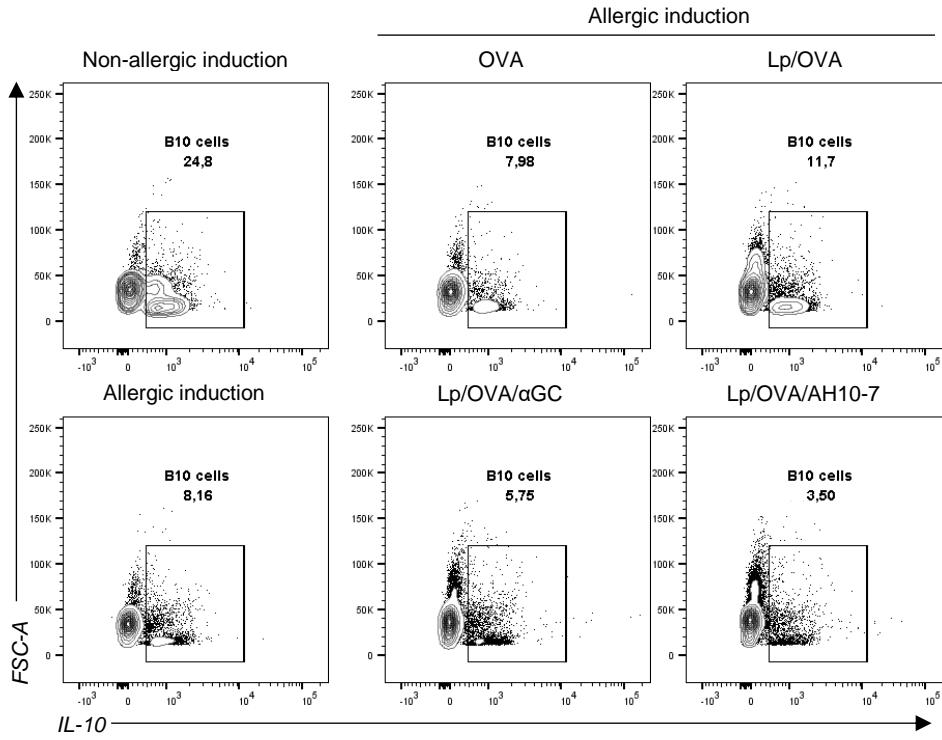
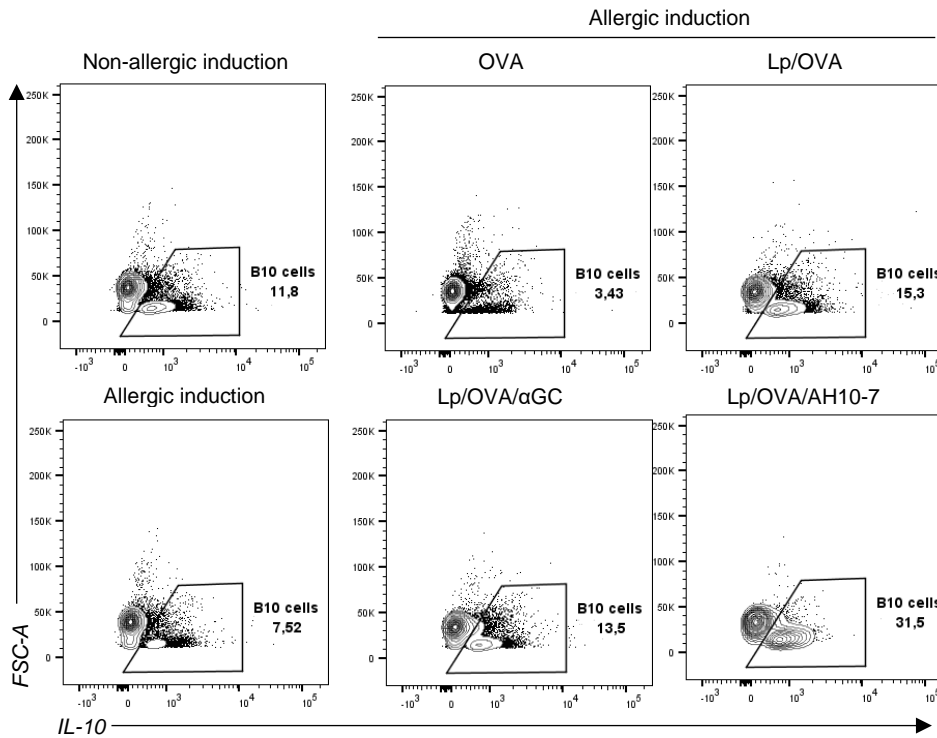
**D****E**

**Figure 17. Eosinophil recruitment in lung and bronchoalveolar lavage (BAL) from mice with OVA-induced allergy treated with liposomes containing OVA and glycolipids ( $\alpha$ -GalCer or AH10-7), in a therapeutic scenery.** Protocol for the obtention of mice with OVA-allergic induction and treated liposomes containing  $\alpha$ -GalCer or AH10-7 and OVA. BALB/c mice ( $n = 5$ ) were sensitized with 100  $\mu$ g of OVA in 1mg of Alum. After two weeks, mice were challenged intranasally with three doses of 10  $\mu$ g of OVA in PBS. Liposomal preparations (and controls) were administered three weeks after the last i.n. challenge. In the ninth week, mice were re-challenge with an intranasal dose of 10  $\mu$ g of OVA in PBS. **(B)** y **(C)** Representative flow cytometry graphs with the population of eosinophils (CD45<sup>+</sup>, CD11c<sup>-</sup>, CD11b<sup>+</sup>, CD24<sup>+</sup>, MHCII<sup>-/low</sup>, Ly6G<sup>-</sup> and SiglecF<sup>+</sup> cells) in lungs, and eosinophils (CD45<sup>+</sup>, CD11c<sup>-</sup>, Ly6G<sup>-</sup> and SiglecF<sup>+</sup> cells) in BAL. Charts **(D)** and **(E)** show the summary of the % of eosinophils in the BAL and lung, respectively. The bars represent the mean  $\pm$  standard error of the mean. Asterisks indicate significant differences compared with the allergic group. ns,  $p > 0.05$  and \*,  $p < 0.5$  (Mann-Whitney test).





**Figure 18. Levels of allergen-specific IgE in mice with OVA-induced allergy treated with liposomes containing OVA and glycolipids ( $\alpha$ -GalCer or AH10-7), in a therapeutic scenery.** BALB/c mice ( $n = 5$ ) were sensitized with 100  $\mu$ g of OVA in 1mg of Alum. After two weeks, mice were challenged intranasally with three doses of 10  $\mu$ g of OVA in PBS. Liposomal preparations (and controls) were administered three weeks after the last i.n. challenge. In the ninth week, mice were re-challenge with an intranasal dose of 10  $\mu$ g of OVA in PBS. The anti-OVA IgE titer is shown, defined as the cut-off point to determine the titer, twice the absorbance average of the pre-immune group. The bars represent the mean and standard error of the mean. Asterisks indicate the statistical difference between allergic induced mice and treated allergic induced mice. ns,  $p > 0.05$ ; \*,  $p < 0.05$ ; and \*\*,  $p < 0.01$  (Kruskal-Wallis test).

**A****B**

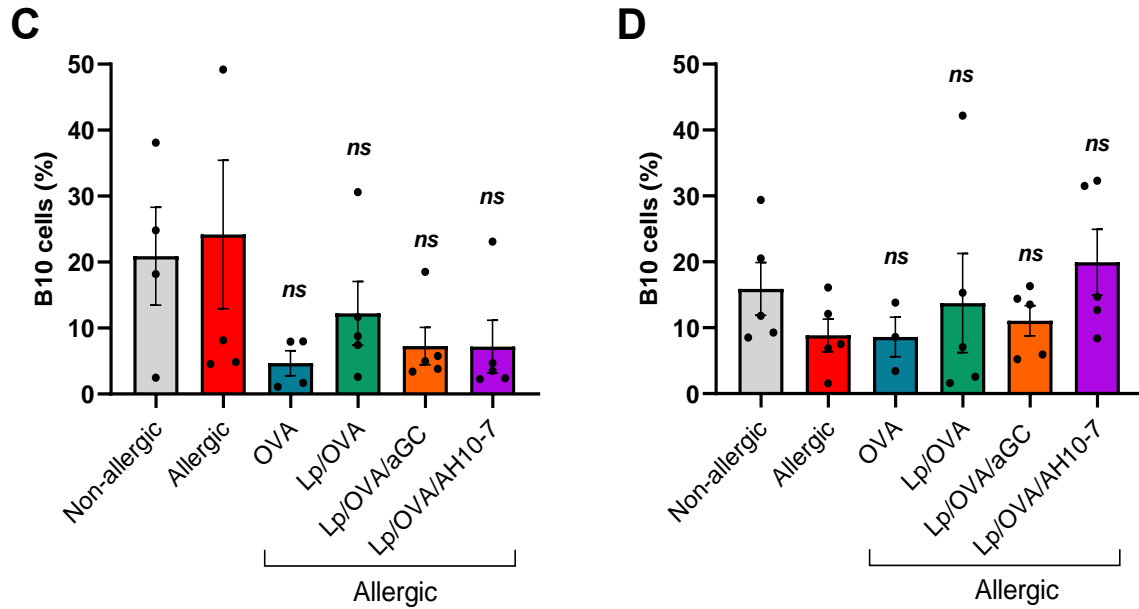


**Figure 19. IL-10-producing regulatory B cells (B10 cells) in mediastinal lymph nodes and spleen from mice with OVA-induced allergy treated with liposomes containing OVA and the and glycolipids ( $\alpha$ -GalCer or AH10-7), in a therapeutic scenery.** BALB/c mice ( $n = 5$ ) were sensitized with 100  $\mu\text{g}$  of OVA in 1mg of Alum. After two weeks, mice were challenged intranasally with three doses of 10  $\mu\text{g}$  of OVA in PBS. Liposomal preparations (and controls) were administered three weeks after the last i.n. challenge. In the ninth week, mice were re-challenge with an intranasal dose of 10  $\mu\text{g}$  of OVA in PBS. **(A)** y **(B)** Representative flow cytometry graphs with the population of IL-10-producing regulatory B cells (B10 cells) ( $\text{CD45}^+$ ,  $\text{CD19}^+$ ,  $\text{IL10}^+$  cells) in the spleen and mediastinal lymph node, respectively. Charts **(C)** and **(D)** show the summary of the % of B10 cells in the spleen and mediastinal lymph node, respectively. The bars represent the mean  $\pm$  standard error of the mean. Asterisks indicate significant differences compared with the allergic group. *ns*,  $p > 0.05$  and \*,  $p < 0.5$  (ANOVA with Dunnett's multiple comparisons test or Kruskal-Wallis test).

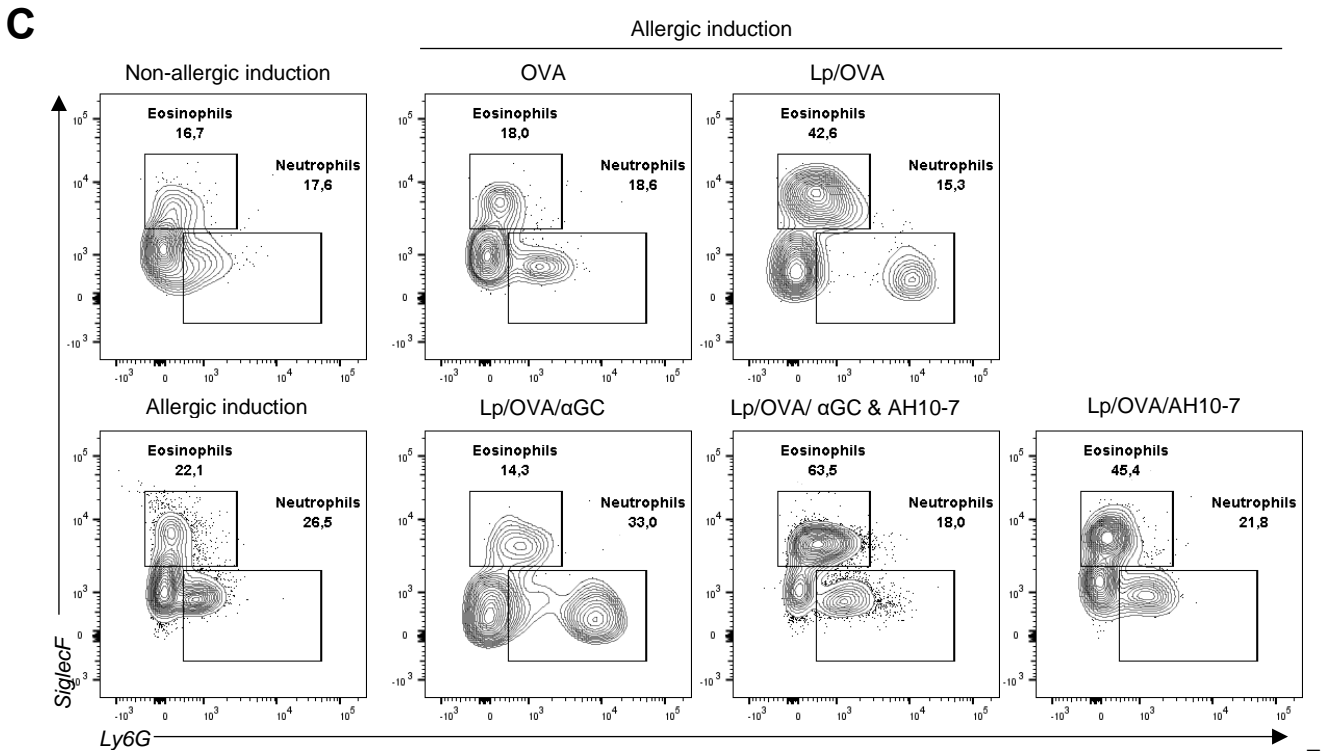
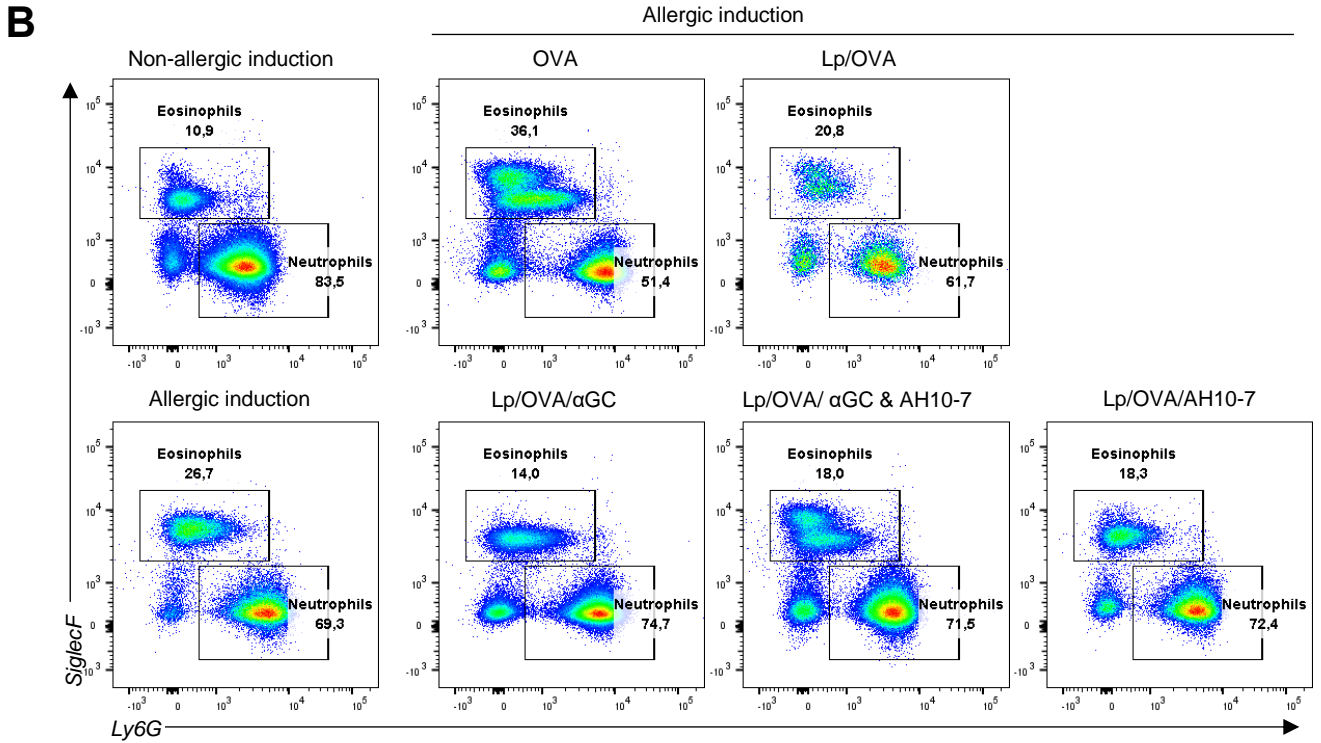
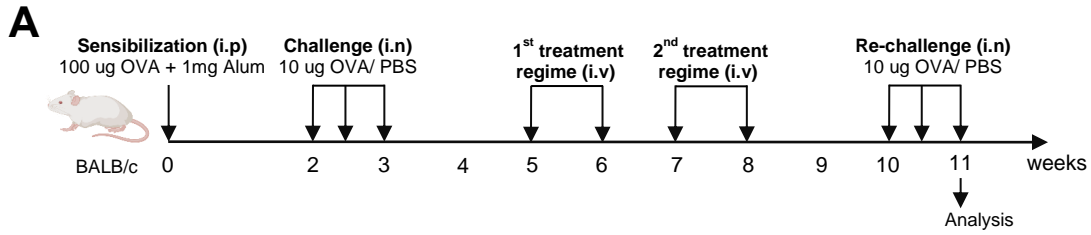
**Determination of the anti-inflammatory effect of  $\alpha$ -GalCer analogs contained into liposomes, in a therapeutic scenery, two treatment regimens.**

For this purpose, female BALB/c mice ( $n = 5$ ) were sensitized with 100  $\mu\text{g}$  of OVA in 1mg of Alum. After two weeks, mice were challenged intranasally with three doses of 10  $\mu\text{g}$  of OVA in PBS. Liposomal preparations (and controls) were administered two



weeks after the last i.n. challenge following a scheme of two immunization regimens (4 weekly doses). At the tenth week, mice were re-challenged with three intranasal doses of 10 µg of OVA in PBS. Symptoms of allergic inflammation were evaluated 24 hours after the last i.n. challenge (Fig. 20A).

As a result, we couldn't appreciate a significant decrease in the recruitment of eosinophil in lungs and BAL from mice with allergic mice and treated with two regimens of doses of liposomes containing OVA and α-GalCer (Lp/OVA/α-GC), liposomes containing OVA and AH10-7 (Lp/OVA/AH10-7) or mixed administration of liposomes containing OVA and AH10-7 & α-GalCer (Lp/OVA/AH10-7 & αGC) (Fig. 20B and D). Also, we couldn't appreciate a significant decrease in eosinophil recruitment in BAL of allergic mice treated with two regimens of doses of liposomes containing OVA (Lp/OVA) or soluble OVA. Caught our attention, that two of the five mice in this group died a day after i.v. challenge with soluble OVA. We could infer that the death of these mice was caused by an anaphylactic shock that occurred after the intravenous administration of soluble OVA. Anaphylactic shock is the most serious of all allergic reactions. This life-threatening condition is immunologically mediated by an antigen, for example, a heterogeneous protein that reacts to the specific IgE antibody [132]. However, to validate this hypothesis, it would be necessary to determine whether histamine levels and the allergen-specific IgE in the blood were high in these individuals. Additionally, it was not appreciated a significant decrease in the titer of allergen-specific IgE (Fig. 21) in allergic mice treated with two regimens of doses of Lp/OVA/α-GC, Lp/OVA/AH10-7, Lp/OVA/AH10-7 & αGC, Lp/OVA or soluble OVA.



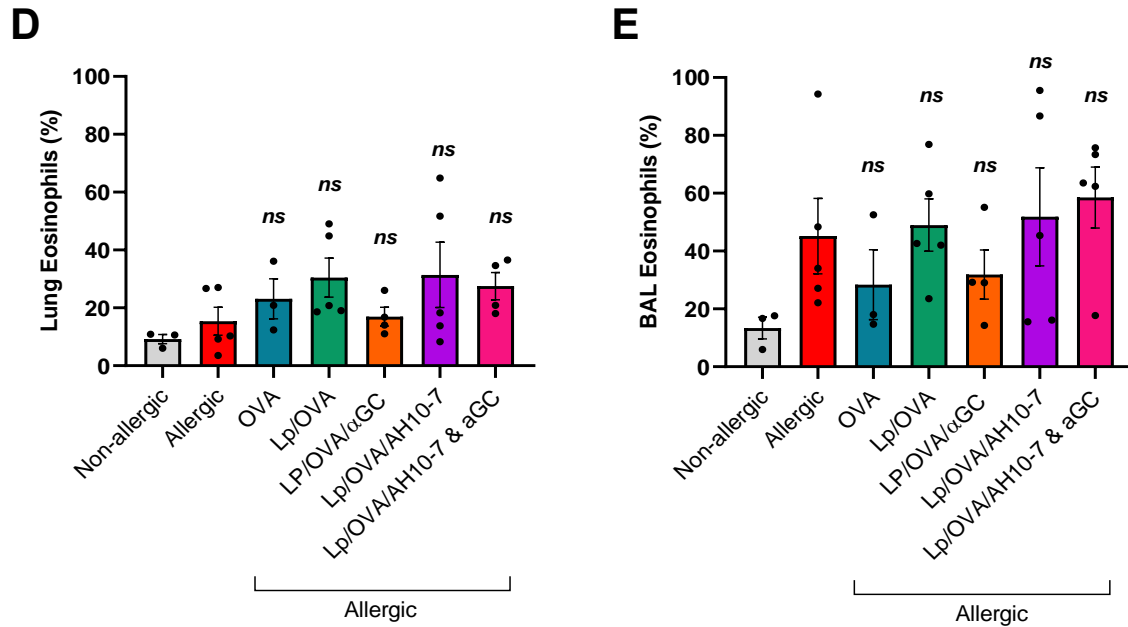
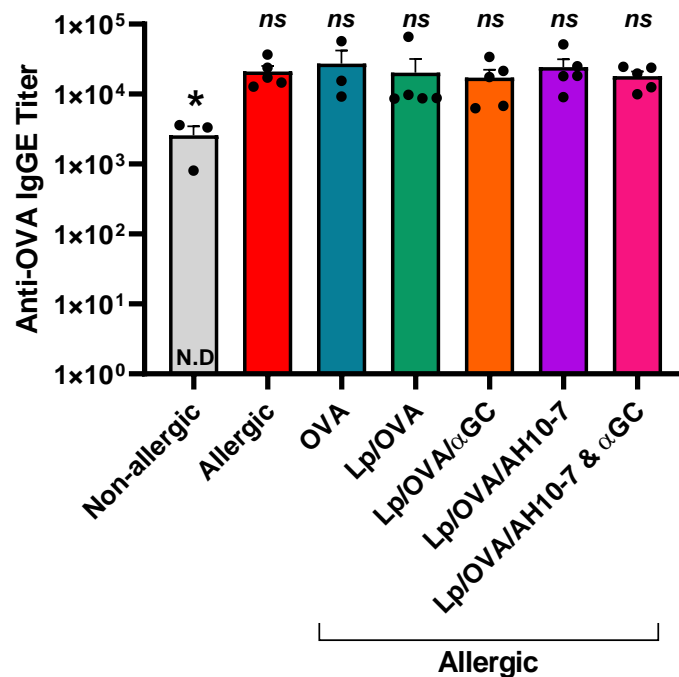


**Figure 20. Eosinophil recruitment in lungs and bronchoalveolar lavage (BAL) from mice treated with liposomes containing OVA and glycolipids ( $\alpha$ -GalCer or AH10-7), in a therapeutic scenery, two treatment regimens. (A) Protocol for the obtention of mice with OVA-allergic induction and treated liposomes containing  $\alpha$ -GalCer or AH10-7 and OVA. BALB/c mice ( $n = 5$ ) were sensitized with 100  $\mu$ g of OVA in 1mg of Alum. After two weeks, mice were challenged intranasally with three doses of 10  $\mu$ g of OVA in PBS. Liposomal preparations (and controls) were administered two weeks after the last i.n. challenge following a scheme of two immunization regimens (4 weekly doses). In the tenth week, mice were re-challenge with three intranasal doses of 10  $\mu$ g of OVA in PBS. (B) y (C) Representative flow cytometry graphs with the population of eosinophils ( $CD45^+$ ,  $CD11c^-$ ,  $CD11b^+$ ,  $CD24^+$ ,  $MHCII^{-/low}$ ,  $Ly6G^-$  and  $SiglecF^+$  cells) in lungs, and eosinophils ( $CD45^+$ ,  $CD11c^-$ ,  $CD24^+$ ,  $MHCII^{-/low}$ ,  $Ly6G^-$  and  $SiglecF^+$  cells) in BAL. Charts (D) and (E) show the summary of the % of eosinophils in the BAL and lung, respectively. The bars represent the mean  $\pm$  standard error of the mean. Asterisks indicate significant differences compared with the allergic group. <sup>ns</sup>,  $p > 0.05$  and \*,  $p < 0.5$  (Mann-Whitney test).**

On the other hand, we could appreciate a non-significant expansion of IL-10-producing regulatory B cells (B10 cells) in mediastinal lymph nodes from mice with OVA-induced allergy treated with two regimens of doses of liposomes containing OVA and  $\alpha$ -GalCer (Lp/OVA/ $\alpha$ GC) (Fig. 22). Since this increase was not statistically significant compared to the allergic mice group, these results are considered preliminary. It is necessary to repeat these experimental conditions to validate them thoroughly. Interestingly, we observed a significant reduction of infiltration of inflammatory cells and mucus secretion in lung tissue from allergic mice treated with two regimens of doses of liposomes containing OVA and  $\alpha$ -GalCer (Lp/OVA/ $\alpha$ -GC) (Fig. 23, Fig. 24). In this experimental group, Lp/OVA/ $\alpha$ GC-treated mice had minimal alveolar space loss due to inflammatory infiltration, and no extensive foci of inflammatory cells in the bronchi or bronchioles were observed.

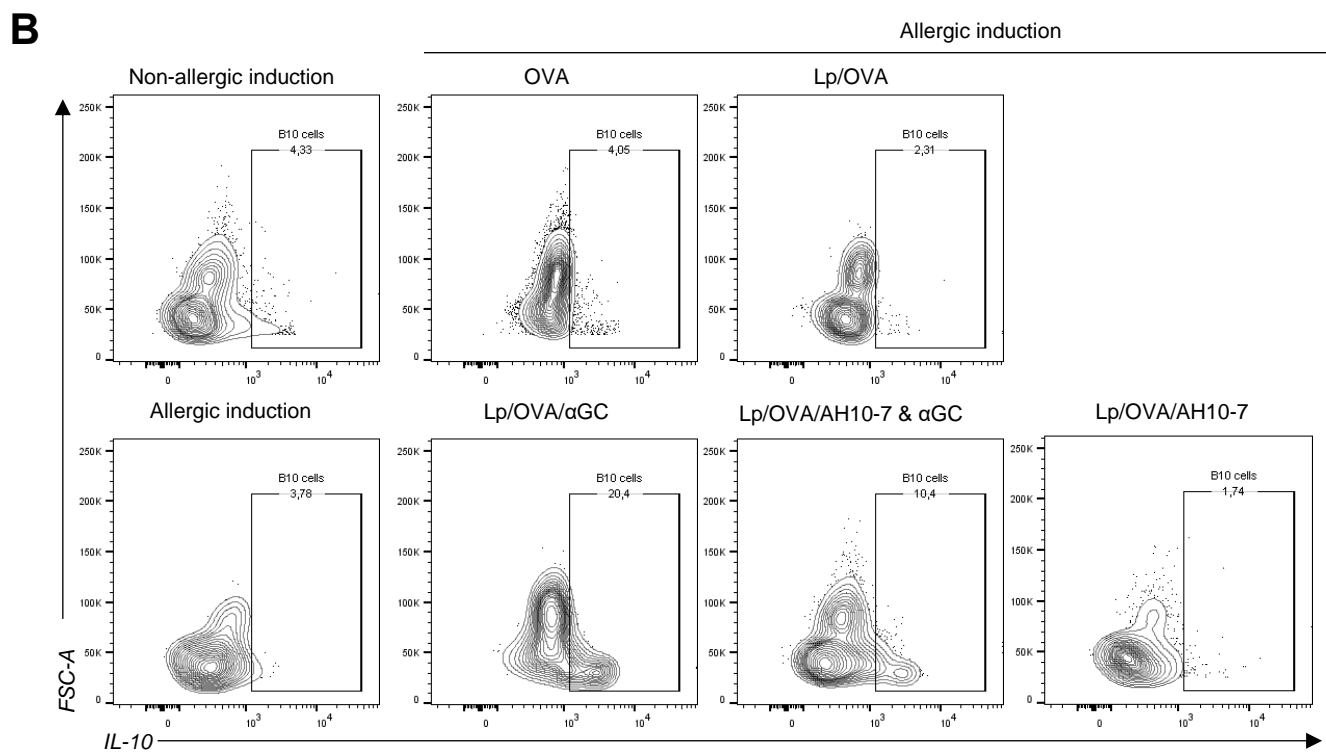
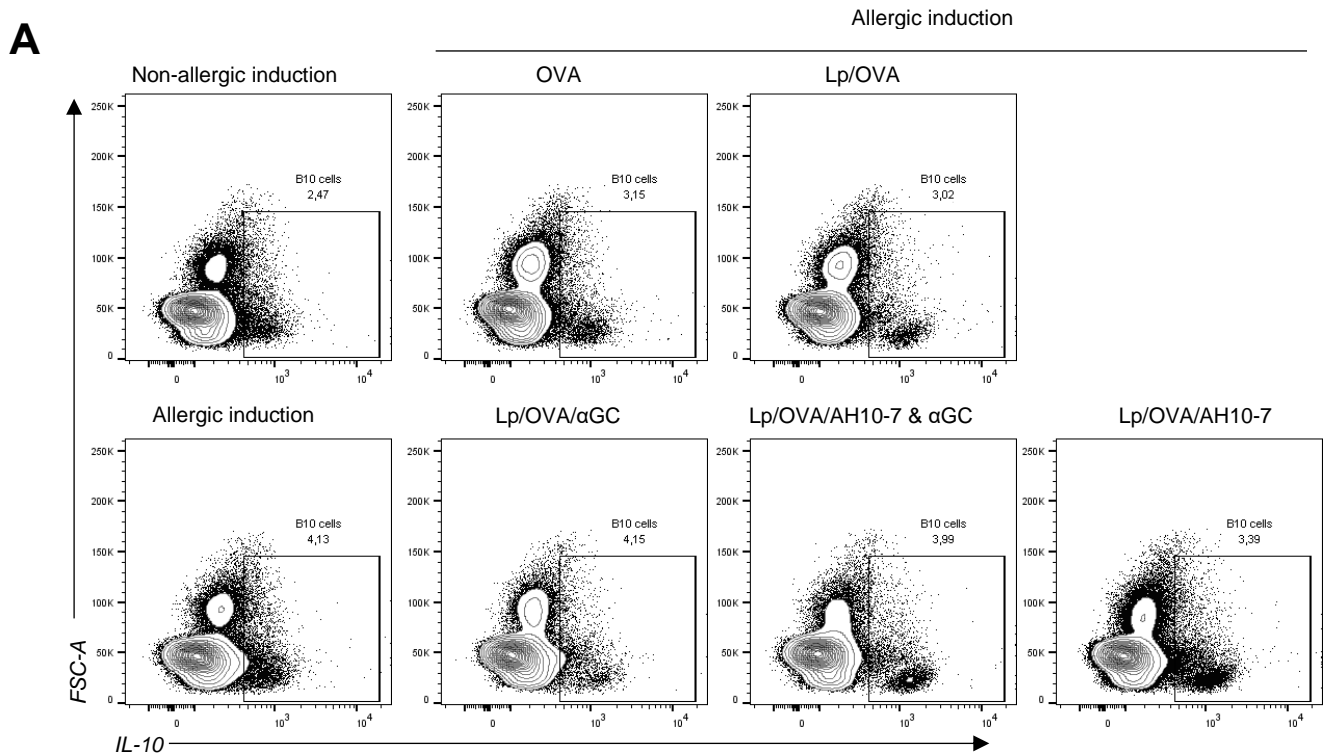
On the other side, in the group of allergic mice treated with liposomes containing OVA and AH10-7 (Lp/OVA/AH10-7), an increase in the numbers and extension of foci of mononuclear inflammatory infiltrate has been observed, both in the alveoli, the bronchioles, and bronchi. Also, it was possible to observe a reduction of the alveolar spaces and the thickening of alveolar septa (compared to non-allergic mice). In addition, red blood cells were present in the alveolar spaces, and a similar number to allergy-induced mice with PAS-positive cells was observed (Fig. 23, Fig. 24). Besides, in the group of allergic mice treated with liposomes containing OVA and AH10-7 &  $\alpha$ -GalCer (Lp/OVA/  $\alpha$ GC & AH10-7), more significant alveolar space and minor extension of the foci of mononuclear inflammatory infiltrate compared to Lp/OVA/AH10-7 was observed (Fig. 23, Fig. 24). Also, there were fewer foci of inflammatory cells in the

submucosa of the bronchioles, increasing in the bronchi. Finally, in the mice treated with liposomes Lp/OVA and soluble OVA, there were no extensive foci of inflammatory infiltrate in the alveoli, and the alveolar spaces were preserved. However, in these groups' small foci of inflammatory cell infiltrate were observed in the submucosa of the bronchioles. In addition, these experimental groups had PAS-positive cell levels like allergy-induced mice (Fig. 23, Fig. 24).



**Figure 21. Levels of allergen-specific IgE in mice with OVA-induced allergy treated with liposomes containing OVA and glycolipids ( $\alpha$ -GalCer or AH10-7), in a therapeutic scenery, two treatment regimens.** BALB/c mice ( $n = 5$ ) were sensitizing with 100  $\mu$ g of OVA in 1mg of Alum. After 2 weeks, mice were challenged intranasally with three doses of 10  $\mu$ g of OVA in PBS. Liposomal preparations (and controls) were administered two weeks after the last i.n. challenge following a scheme of two immunization regimens (4 weekly doses). In the tenth week, mice were re-challenge with three intranasal doses of 10  $\mu$ g of OVA in PBS. **(A)** Plots of absorbance vs. the logarithm of the reciprocal of serum dilution. **(B)** The log of the anti-OVA IgE titer is shown, defined as the cut-off point to determine the titer, twice the absorbance average of the pre-immune group. The bars represent the mean. Asterisks indicate

statistical difference between allergic-induced mice and treated allergic-induced mice.  
 $ns, p > 0.05$  (Kruskal-Wallis test).



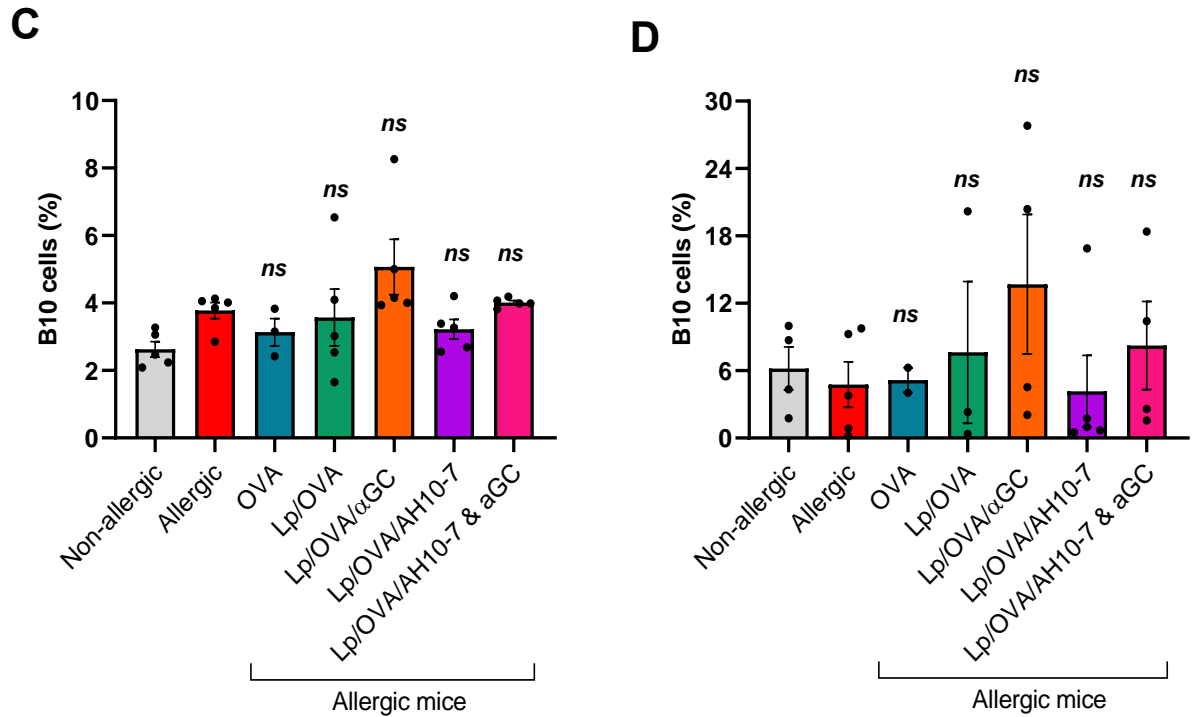


**Figure 22. IL-10-producing regulatory B cells (B10 cells) in mediastinal lymph nodes and spleen from mice with OVA-induced allergy treated with liposomes containing OVA and the and glycolipids ( $\alpha$ -GalCer or AH10-7), in a therapeutic scenery, two treatment regimens.** BALB/c mice ( $n = 5$ ) were sensitized with  $100 \mu\text{g}$  of OVA in  $1\text{mg}$  of Alum. After two weeks, mice were challenged intranasally with three doses of  $10 \mu\text{g}$  of OVA in PBS. Liposomal preparations (and controls) were administered two weeks after the last i.n. challenge following a scheme of two immunization regimens (4 weekly doses). In the tenth week, mice were re-challenge with three intranasal doses of  $10 \mu\text{g}$  of OVA in PBS. **(A)** and **(B)** Representative flow cytometry graphs with the population of IL-10-producing regulatory B cells (B10 cells) ( $\text{CD45}^+$ ,  $\text{CD19}^+$ ,  $\text{IL10}^+$  cells) in the spleen and mediastinal lymph node, respectively. Charts **(C)** and **(D)** show the summary of the % of B10 cells in the spleen and mediastinal lymph node, respectively. The bars represent the mean  $\pm$  standard error of the mean. Asterisks indicate significant differences compared with the allergic group.  $^{ns}$ ,  $p > 0.05$  and  $^*$ ,  $p < 0.5$  (Kruskal-Wallis test).

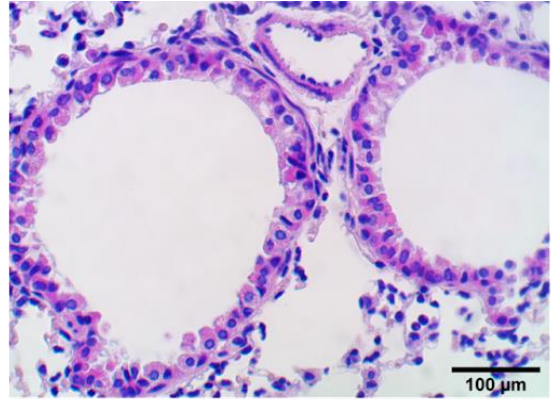
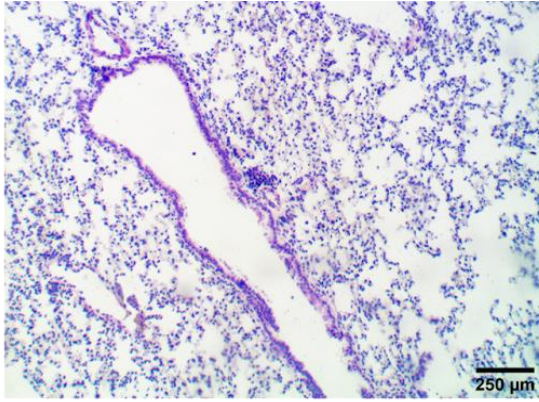


**A**

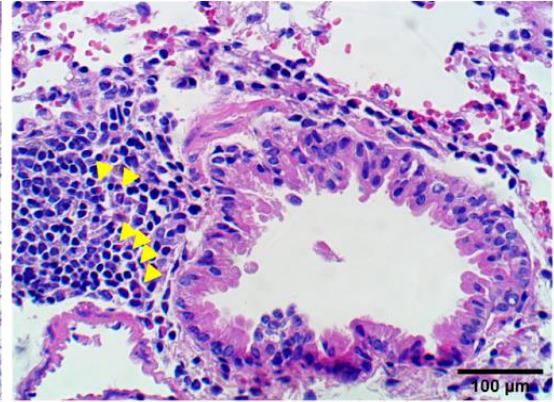
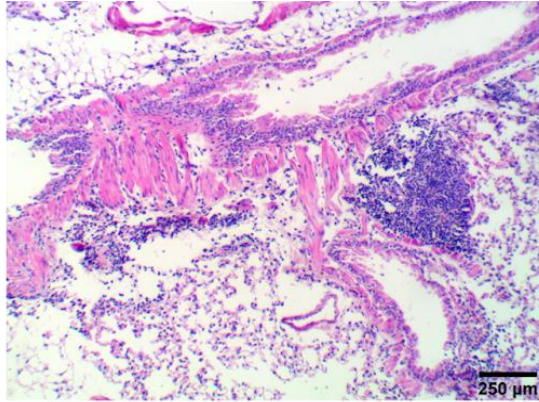
**Bronchi**

**Bronchiole**

**Non-allergic mice**

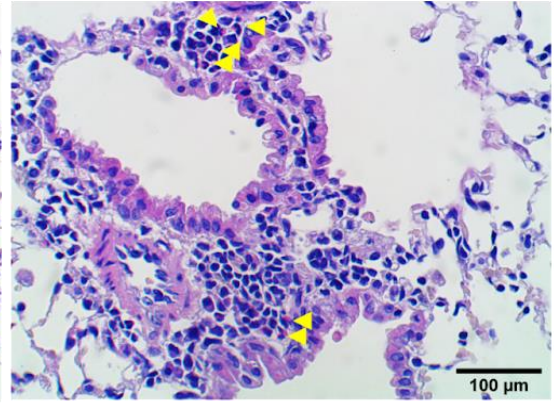
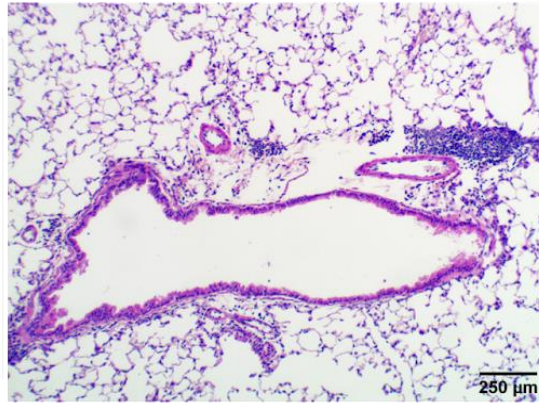


**Allergic mice**

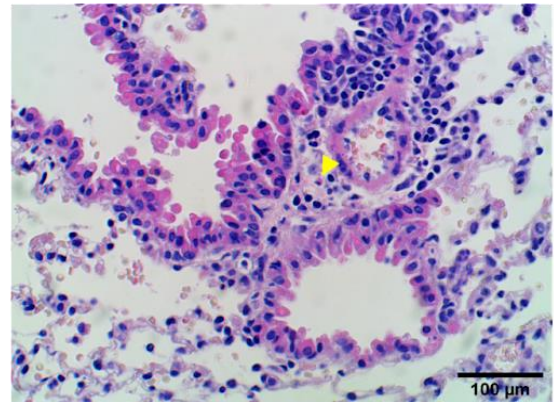
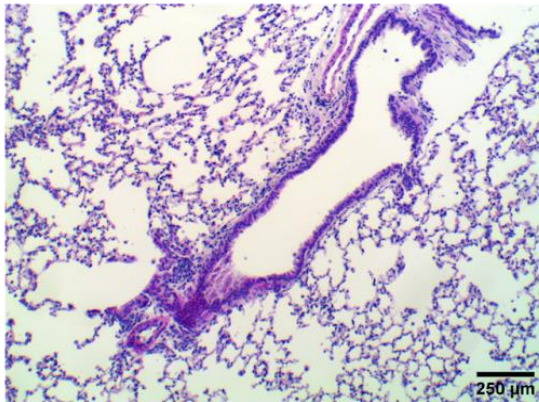


**Allergic mice**

**OVA**



**Lp/OVA**



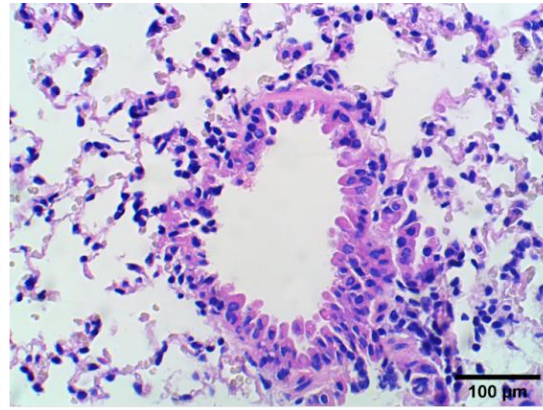
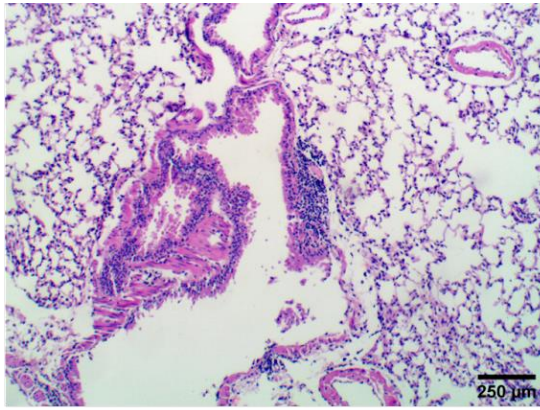


Allergic mice

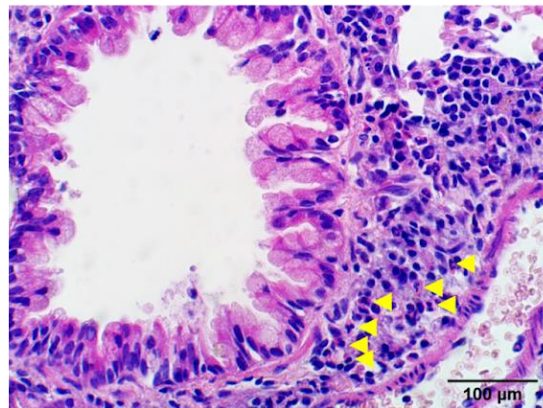
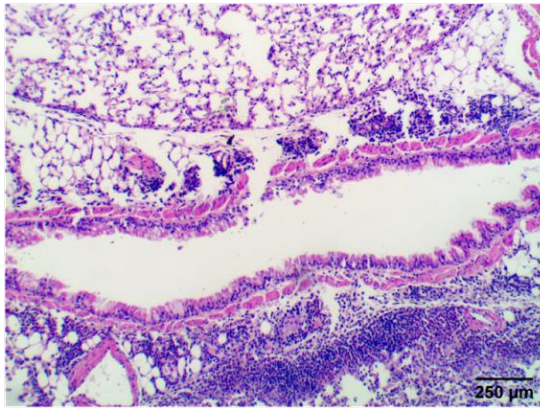
Bronchi

Bronchiole

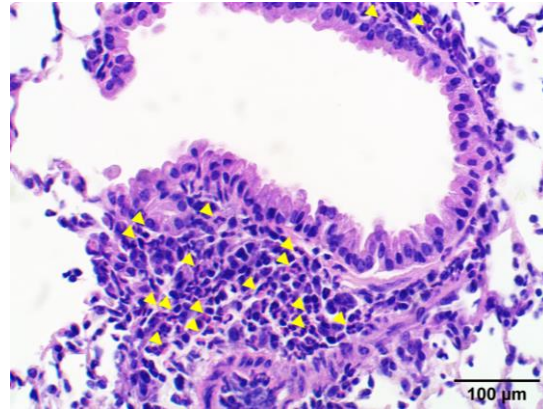
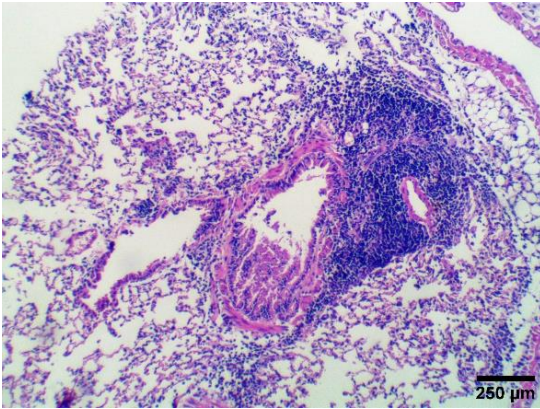
Lp/OVA/ $\alpha$ GC

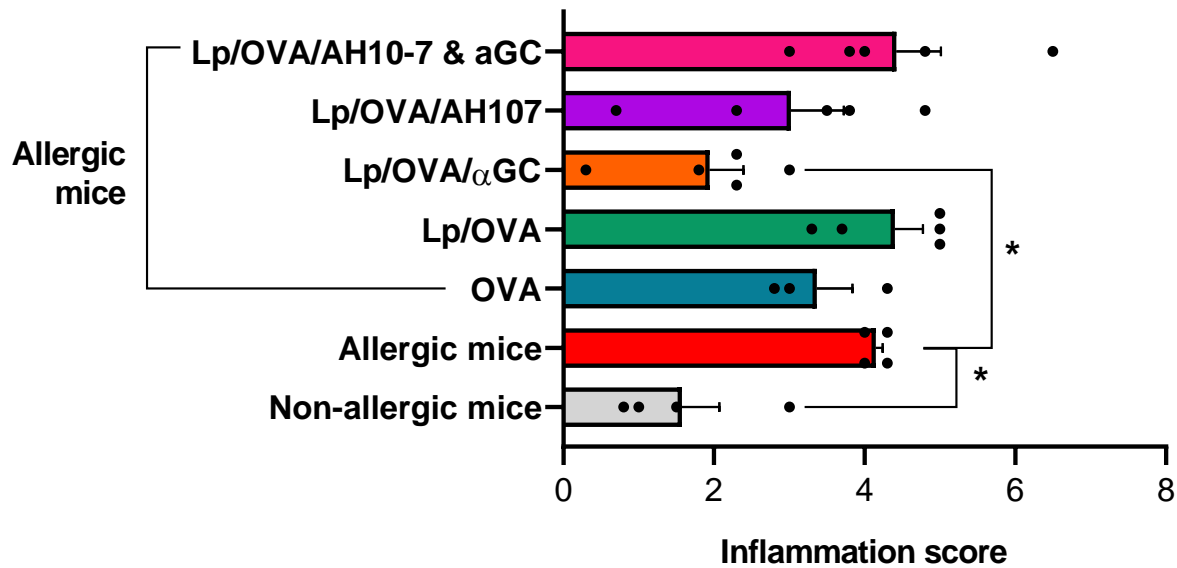


Lp/OVA/AH10-7



Lp/OVA/ $\alpha$ GC & AH10-7



**B**

**Figure 23. Infiltration of inflammatory cells in lung tissue from mice with OVA-induced allergy treated with liposomes containing OVA and glycolipids ( $\alpha$ -GalCer or AH10-7), in a therapeutic scenery, two treatment regimens.** BALB/c mice ( $n = 5$ ) were sensitized with 100  $\mu\text{g}$  of OVA in 1mg of Alum. After two weeks, mice were challenge intranasally with three doses of 10  $\mu\text{g}$  of OVA in PBS. Liposomal preparations (and controls) were administered two weeks after the last i.n. challenge following a scheme of two immunization regimens (4 weekly doses). In the tenth week mice were re-challenge with three intranasal doses of 10  $\mu\text{g}$  of OVA in PBS. Lungs were collected 24 hours after the last i.n. challenge and stained for histopathology analyses using hematoxylin & eosin to identify lung infiltrate at 40 X. **(A)** Representative microscopic photos of bronchi and bronchioles stained with hematoxylin & eosin. Yellow arrows indicate eosinophils in peribronchial and perivascular inflammatory foci. Black scale bars in the bronchi represent 250  $\mu\text{m}$  and in the bronchiole 100  $\mu\text{m}$  **(B)**. Inflammation scores. Each point represents results obtained from 1 individual mouse. The bars represent the mean  $\pm$  standard error of the mean. Asterisks indicate a statistical difference between allergic induced-mice and treated allergic induced-mice. ns,  $p > 0.05$ ; \*,  $p < 0.5$ ; (ANOVA with Dunnet post-test for multiple comparisons).



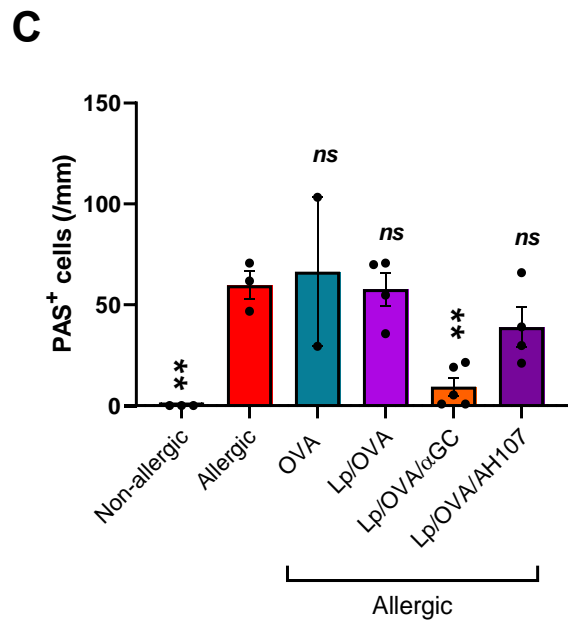
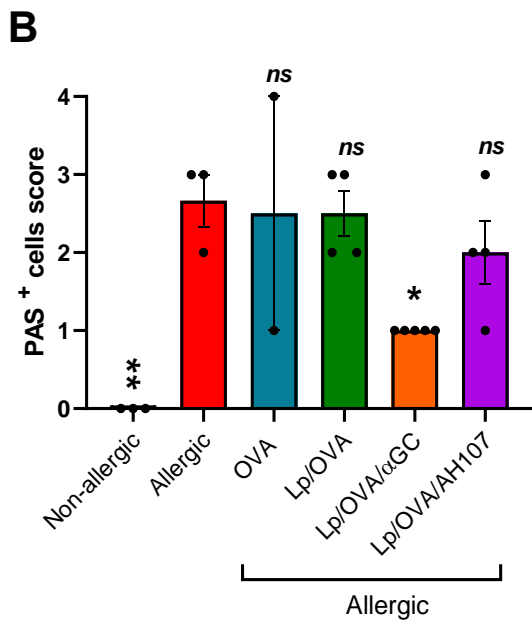
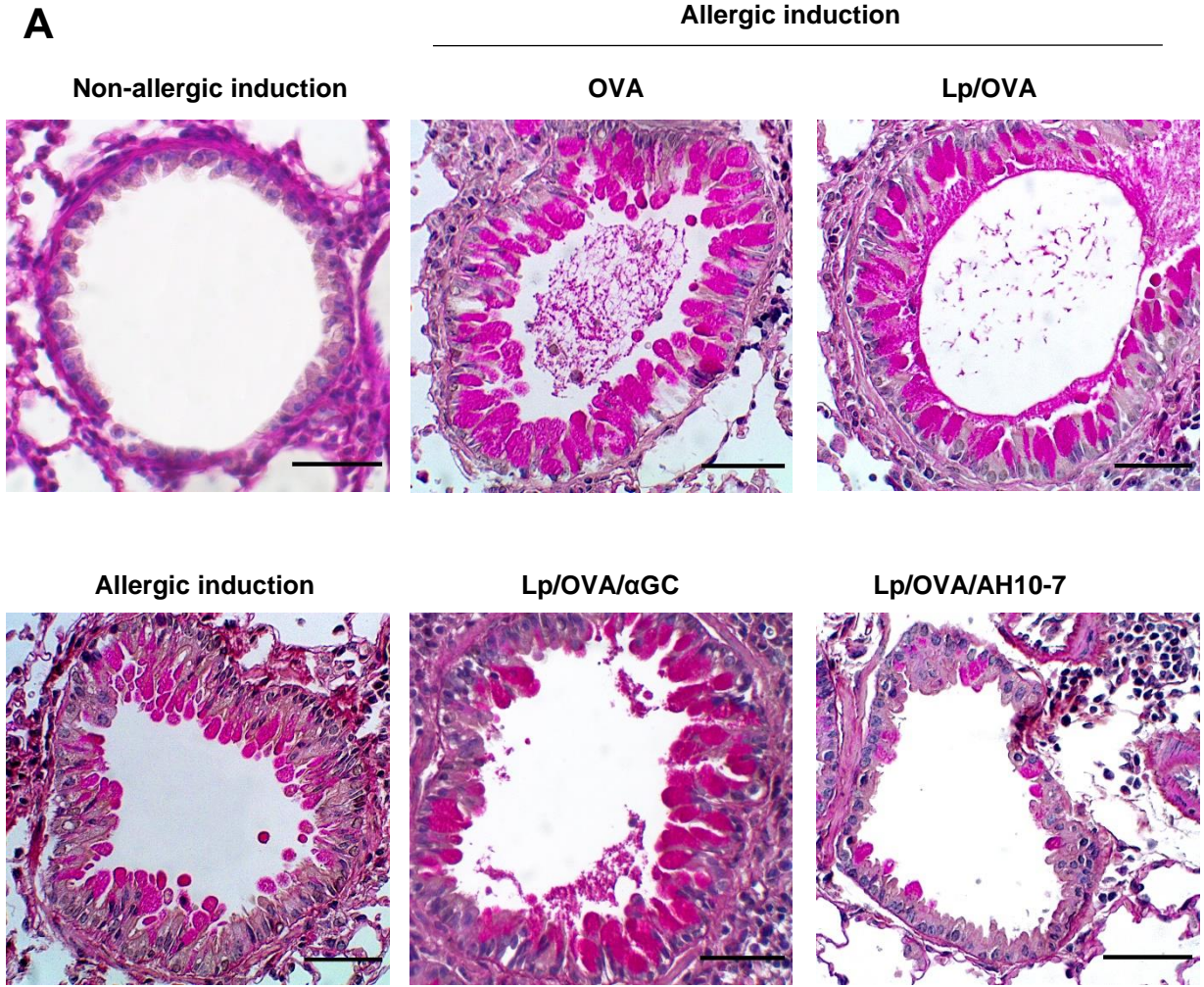


**Fig 24. Mucus secretion in lung tissue from mice with OVA-induced allergy treated with liposomes containing OVA and glycolipids ( $\alpha$ -GalCer or AH10-7), in a therapeutic scenery, two treatment regimens.** BALB/c mice (n = 5) were sensitized with 100  $\mu$ g of OVA in 1mg of Alum. After two weeks, mice were challenge intranasally with three doses of 10  $\mu$ g of OVA in PBS. Liposomal preparations (and controls) were administered two weeks after the last i.n. challenge following a scheme of two immunization regimens (4 weekly doses). In the tenth week mice were re-challenge with three intranasal doses of 10  $\mu$ g of OVA in PBS. Lungs were collected 24 hours after the last i.n. challenge and the PAS stain was carried out to identification of goblet cells and mucus production at 40 X **(A)**. Representative microscopic photos of bronchiole stained with PAS. Fuchsia-red staining indicates the presence of goblet cells or mucus. Black scale bars represent 100  $\mu$ m.**(B)** Percentage of PAS<sup>+</sup> cells score in the bronchi and bronchiole. **(C)** Number of PAS<sup>+</sup> cells were counted and normalized by area of basement membrane. Each point represents results obtained from 1 individual mouse. The bars represent the mean  $\pm$  standard error of the mean. Asterisks indicate a statistical difference between allergic induced-mice and treated allergic induced-mice. <sup>ns</sup>, p >0.05; \*, p <0.5; \*\*\*, p <0.001; and \*\*\*\* p <0.0001 (ANOVA with Sidak post-test for multiple comparisons).

***SPECIFIC AIM 3: To determine if the differential activation of iNKT cells with different  $\alpha$ -GalCer analogs in liposomes will increase the expansion of Breg, leading to prevention or reduction of allergic asthma, in hCD1d-KI C57BL6 with induced allergy by the human allergen HDM.***

#### **Obtention of OVA induced-allergic hCD1d-KI mice**

It was recently found that using humanized mice models, such as hCD1d-KI mice, is a relevant strategy for developing NKT cell-based immunotherapies [79]. In this project, we would like to target iNKT cells to treat allergic inflammation, but the particularity of our study falls upon the use of hCD1d-KI mice. To assess this objective, we tried to develop an OVA-induced mouse model of asthma [107] using C57BL/6J hCD1d-KI mice. Briefly, i.p. immunization with 100  $\mu$ g OVA in 1 mg of Inject<sup>TM</sup>Alum followed by

i.n. challenge with 10  $\mu$ g OVA at days 14, 17, and 21 post-immunizations lead to a severe allergic response. We also administered i.p and i.n PBS (allergen vehicle) as a negative control of the asthma-induced mouse model. 24 hours after the last OVA i.n. challenge (day 22), the allergic response was evaluated by determining the recruitment of eosinophils (CD11c<sup>-</sup>, CD3<sup>-</sup>, CD19<sup>-</sup>, CD11b<sup>-</sup>, Ly6G<sup>-</sup> and SiglecF<sup>+</sup> cells) into the lungs and BAL by FACS. As a result, we obtained that, the group of mice with OVA-induced allergy did not show a significant allergic response (Fig. 25). This condition led us to explore other models of allergic asthma induced in C57BL/6J hCD1d-KI mice.

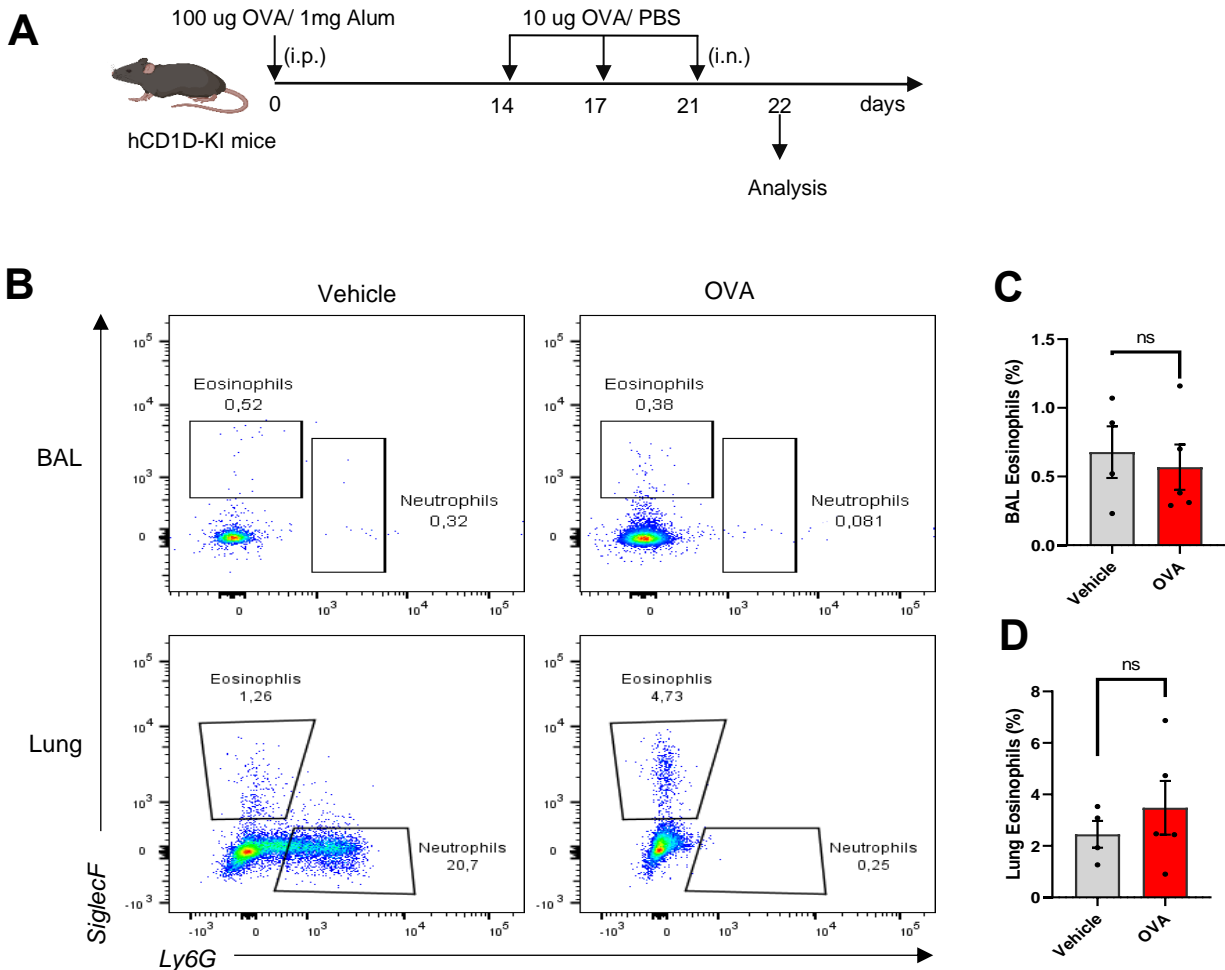


**Figure 25. Obtain of OVA-induced allergy model in C57BL/6J hCD1d-KI mice. (A)** C57BL/6J hCD1d-KI mice (n=4) were sensitized with 100 µg OVA in 1mg Alum. At 21, 24 and 28 days the mice were intranasal challenged with 10 µg OVA in PBS. **(B)** Representative flow cytometry graphs are shown with the eosinophil population (CD11c<sup>-</sup>, CD3<sup>-</sup>, CD19<sup>-</sup>, CD11b<sup>-</sup>, Ly6G<sup>-</sup> and SiglecF<sup>+</sup> cells) in bronchoalveolar lavage (BAL) and lung. Graphs **(C)** and **(D)** show the summary of the % of eosinophils in the BAL and lung, respectively. The bars represent the mean ± standard error of the mean. Asterisks indicate significant differences. ns, p >0.05; (Unpaired t test).

### **Obtention of HDM induced-allergic hCD1d-KI mice**

The limits of the use of OVA as an experimental allergen; besides the lowest effect of airway hyperreactivity in C57BL/6J [133]. For these reasons, we continued our study using a house dust mite (HDM)-induced mouse model of asthma. For the acute allergic HDM model, C57BL/6J hCD1d-KI mice were sensitized i.n. with 1 µg of HDM in 10 µL of PBS followed by i.n. challenged on days 7 to 11 with 10 µg in 10 µL of PBS. We also administered i.n. PBS (allergen vehicle) as a negative control of the asthma-induced mouse model [134, 135]. Mice were sacrificed on day 14. The allergic response was evaluated by determining the recruitment of eosinophils (CD11c<sup>-</sup>, CD3<sup>-</sup>, CD19<sup>-</sup>, CD11b<sup>-</sup>, Ly6G<sup>-</sup>, and SiglecF<sup>+</sup> cells) into the lungs and BAL by FACS. We could not obtain a severe allergic response in the lung and the BAL of mice challenged with HDM (Fig. 26). Consequently, it is necessary to improve the obtention of the HDM induced-allergic model in hCD1D-KI mice, maybe in trying to induce allergy in hCD1d-KI mice with a BALBc mice background, to evaluate the possible expansion of regulatory B cells induced by differential activation of iNKT cells with different α-GalCer analogs contained in liposomes in hCD1d-KI mice with allergic asthma.

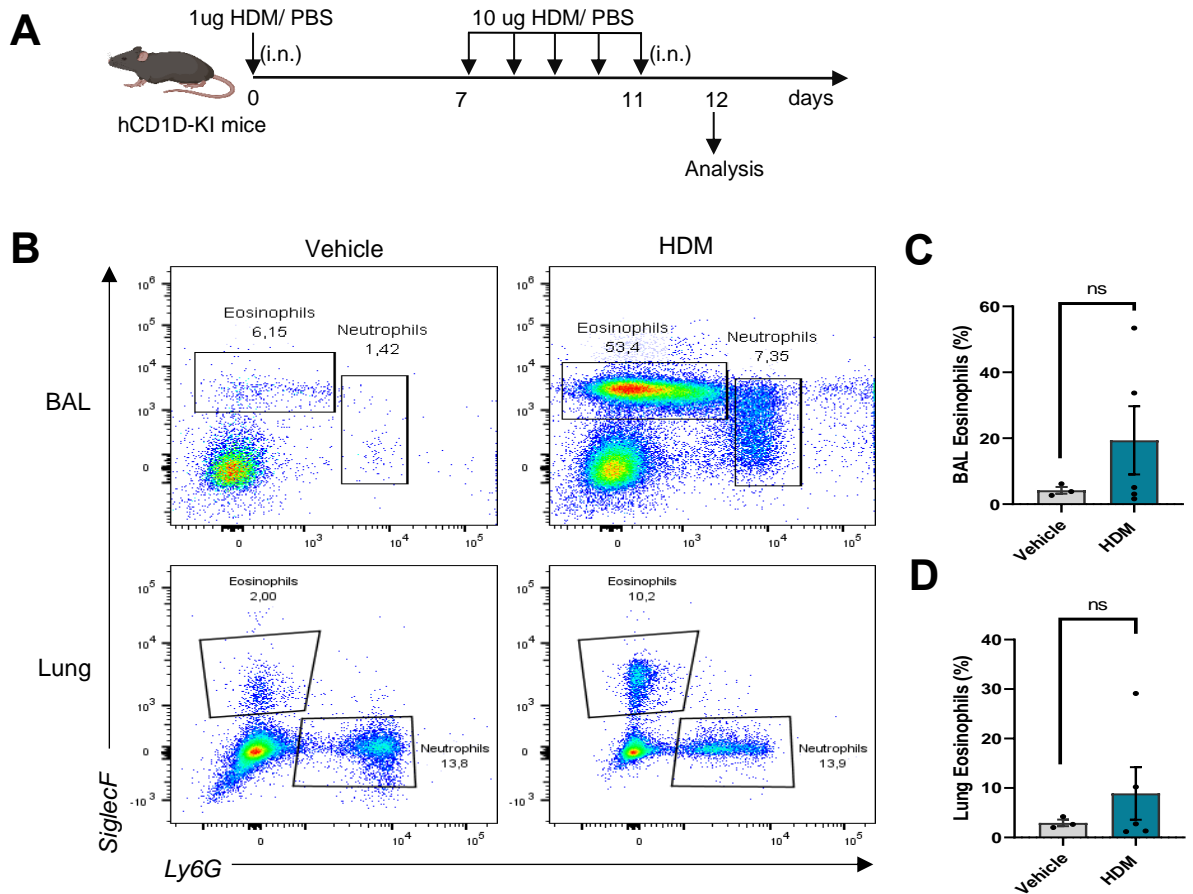


**Figure 26. Obtain the HDM-induced allergy model in C57BL/6J hCD1d-KI mice.** (A) C57BL/6J hCD1d-KI mice (n = 5) were intranasally sensitized with 1 µg HDM dissolved in PBS. From the 7th to the 11th day after sensitization, mice were daily re-challenge with 10 µg HDM dissolved in PBS. (B) Representative flow cytometry graphs are shown with the eosinophil population (CD11c-, CD3-, CD19-, CD11b-, Ly6G- and SiglecF+ cells) in bronchoalveolar lavage (BAL) and lung. Graphs (C) and (D) show the summary of the % of eosinophils in the BAL and lung, respectively. The bars represent the mean ± standard error of the mean. Asterisks indicate significant differences. ns, p >0.05; (Unpaired t test with Welch's correction).

## DISCUSSION

iNKT cells constitutively display a partially activated phenotype, enabling them to rapidly-produce cytokines following activation. Using a nearly monospecific T cell receptor, they recognize glycolipid antigens presented by CD1d in a conserved manner, but their activation can catalyze a spectrum of polarized immune responses [17]. The possibility of modulating the function of regulatory cells activating iNKT reveals a new strategy to induce the tolerance required to protect from allergic inflammation. Since iNKT cells can be differentially activated by  $\alpha$ -GalCer analogs, which can generate more restricted patterns of cytokines (pro-inflammatory, anti-inflammatory, or regulatory- skewed response). It was essential to address whether this differential activation can influence the crosstalk between iNKT and regulatory immune cells. Thus, in this project, we evaluated the expansion and suppressive function of regulatory (Breg and Treg) cells promoted by the differential activation of iNKT cells with  $\alpha$ -GalCer analogs contained in liposomes in a partially humanized murine model for NKT cell responses with allergic asthma.

It has been recognized that the induction of iNKT-cell unresponsiveness often occurs with strong glycolipid agonists after repeated administration, and the administration of high doses of  $\alpha$ -GalCer induces liver toxicity [124, 126-130]. An effective way of avoiding both anergy and liver toxicity is the incorporation of glycolipid agonists in liposomes. In this study, we obtained  $\alpha$ -GalCer or  $\alpha$ -GalCer analogs (OCH and AH10-7) into stearylated octaarginine-modified liposomes following the method described by Nakamura, *et al.* (2013).



STEM is an essential method for characterizing the size and shape of nanoparticles as it can directly visualize single particles and even their inner architecture [113]. In these micrographs, we can visualize the liposomes obtained with a spheric shape and non-regular edges (Fig 4). Additionally, any change in liposome forms was not observed when the protein was integrated into the liposome; the liposomes' sizes in the stained image give 100 nm to 200 nm values. However, the size of the liposomes would not represent the real value in the solution. The spreading of the liposomes on the carbon film (present in the STEM) and the crushing of these vesicles could change the diameter of the visible liposomes in the micrograph [113]. This evidence allows us to explain why in the case of some evaluated micrographs (data not shown), liposomes were with a diameter greater than 200 nm, and the edges were not very defined.

On the other hand, the morphology of the liposomes could be affected by negative staining in the STEM. The main problem in negative staining of liposomes is that these can change morphology during the process. This problem is due to the interaction of the lipids with the carbon surface and/or changes in ionic strength and osmolarity during the staining and air drying [136]. Liposomes can change their shape and, in extreme cases, completely lose integrity and spread out onto the carbon film [136]. In some of the evaluated micrographs (data not shown), we observed liposomes that form worm-like micelles and tubes at high concentrations. Often these problems can be resolved by diluting the liposome preparation and/or varying the standard negative stain procedure to reduce the time liposomes interact with carbon film and increase drying speed [113, 136].

Additionally, the characteristic spherical morphology of liposomes can be affected due to the water-soluble substance entrapped in the aqueous core of the liposome. For example, liposomes containing the doxorubicin crystal slightly change liposome morphology to an oval shape [137]. Also, it has been observed that when liposomes are loaded with a boronated drug, WSP (Water Soluble Phenanthridine), WSP crystals can deform, even perforate, the lipid bilayer and destroy the vesicle [138]. However, there are some cases of liposomes that contain ovalbumin (OVA) [139] or liposomes that encapsulate the fusion protein (Ag85B–ESAT-6) [140], where there is no evidence of change in liposome morphology. According to this evidence, the inclusion of OVA and the glycolipids ( $\alpha$ -GalCer, OCH, or AH10-7) did not change the liposome's spherical shapes in all the liposomes obtained.

Interestingly, we observed different intensities in the negative staining. For instance, some liposomes have a stain depth, while others do not. Scarff *et al.* (2018) detailed that the intensity of negative staining was influenced by multiple factors such as hydrophilicity of the grid surface, evenness of the carbon layer, the amount of stain applied to the grid, the length of time stain is in contact with the grid before blotting, the extent of blotting and the time it takes for the grid to completely dry [141]. Based on the factors mentioned above, it is likely that since the liposome preparations were processed on different days, this may introduce some variabilities in the intensity of negative staining of the liposomes.

The charge acquired by a particle or molecule in a given medium is its zeta potential and has often been used to characterize colloidal drug delivery systems. [142]. The inclusion of a protein can modify the zeta potential of loaded liposomes. It has been

observed that the integration of protamine sulfate (a group of simple proteins that yield basic amino acids) into lipoparticles can increase the zeta potential of these liposomes' constructs [143]. At pH 7.0, OVA carry a net negative charge (isoelectric point = 4.5) [144, 145]. As expected, adding negative charged OVA into liposomes containing  $\alpha$ -GalCer or  $\alpha$ -GalCer analogs (OCH and AH10-7) decreased the zeta potentials of these liposomes (Fig. 6A).

The presence of a charge on the surface induces electrostatic repulsion among liposomes that prevents their aggregation [146]. Probably, a decrease of zeta potential in OVA-loaded liposomes containing  $\alpha$ -GalCer or  $\alpha$ -GalCer analogs (OCH and AH10-7) (Fig. 6A) could be related to the formation of aggregated liposomes with different sizes; hence it can be explained that OVA-loaded liposomes are polydisperse systems with a polydispersity index greater than 0.7 (Fig. 6D).

Zeta potential depends on diverse parameters, including liposome composition, temperature, pH, conductivity (ionic strength), and solvent (viscosity). Small changes in any of these parameters can dramatically affect the zeta potential values [122]. On the other hand, octaarginine (R8) is a cell-penetrating peptide that can be useful for delivering various molecules to cells [147]. The octaarginine is attached to the liposomal surface by conjugation with a stearyl moiety, resulting stearylated R8 (STR-8). We observed that the zeta potential of liposomes and OVA-contained liposomes with STR-8 was positive. As expected, the liposomes and OVA-contained liposomes vesicles without STR-8 had negative zeta potential values (Fig. 6B). Harashima *et. al.* (2008) reported that liposomes composed by the lipids: DOPE, EPC, and cholesteryl hemisuccinate (CHEMS) without STR-8, the zeta potential were  $-37.6 \pm 10.6$  mV;

contrarily liposomes with STR-8 the zeta potential was  $57.2 \pm 3.4$  mV [148]. On the other hand, Miura *et al.* (2017) obtained OVA-contained liposomes composed of EPC, Cho, and CHEMS, and STR-8 had a zeta potential of  $52 \pm 4$  mV, and these liposomes without STR-8 had a zeta potential of  $-37 \pm 11$  mV [149]. The surface charge is a crucial factor contributing to the immunoregulatory effect of liposomes [150]. Vangasseri *et al.* (2006) found a group of cationic liposomes with a positive charge, such as 1,2-dioleoyl-3-trimethylammonium propane (DOTAP) and N-[1-(2,3-dioleoyloxy) propyl]-N,N,N-trimethylammonium chloride (DOTMA), that significantly induced DC maturation by upregulating the expression of CD80 and CD86. In contrast, zwitterionic and anionic liposomes, which have a net-zero or negative charge, did not affect DC maturation and activation [151].

The liposomes' size and size distribution (polydispersity) are significant in their physicochemical characterization. In most cases, the mean of liposomes' size obtained measured by NTA, takes values from 100 nm to 250 nm (Fig 5), and the polydispersity index of the liposomes containing  $\alpha$ -GalCer or  $\alpha$ -GalCer analogs (OCH and AH10-7) was smaller or equal to 0.4 (Fig 6D). The control of these parameters is critical for the biological activity of the liposomes. For instance, liposomes of a diameter larger than 150 nm are phagocytosed by specialized immune system cells, such as macrophages and DC [152]. Nakamura, *et al.* (2013) demonstrated that *in vivo* stimulation of iNKT cells with  $\alpha$ GalCer/R8-Lip of 273 nm was higher than stimulation with  $\alpha$ GalCer/R8-Lip of 311 nm [107]. Besides, one report indicated that the efficiency of cellular uptake of latex particles by DC decreased from 300 to 400 nm [153]. Thus, the appropriate range of liposomes sizes to enhance cellular uptake efficiency could be from 150 to 300 nm.

On the other hand, the spleen is a major target lymphatic organ for immunization via intravenous administration and contains high antigen-presenting cells. Nakamura, et al. (2013) demonstrated that  $\alpha$ GalCer/R8-Lip with a size of 273 nm led to the accumulation of  $\alpha$ GC/R8-Lip in the spleen (not in the liver). In addition, Takara, et al. (2012) showed that large-sized liposomes (300 nm) accumulate more efficiently in the spleen compared to small-sized liposomes (100 nm) [154].

Finally, the Z-average size of  $\beta$ -GalCer or  $\alpha$ -GalCer analogs (OCH and AH10-7) contained into liposomes takes values from 100 nm to 250 nm (Fig. 6C). Interestingly,  $\alpha$ -GalCer or  $\alpha$ -GalCer analogs (OCH and AH10-7) included in OVA-contained liposomes take  $\geq 500$  nm. This last result of the analysis of particle size determined by DLS caught our attention because it differs from the results of the size of the liposomes obtained by the NTA technique. NTA measures the hydrodynamic diameters of submicron particles based on their Brownian motions. Unlike DLS, the NTA software can identify and track individual particles in a recorded video; thus, the size and number of particles in a polydisperse sample can be more detailed [155]. NTA has better peak resolution than DLS, and it is less affected by a few large particles, making it more suitable for sizing and counting polydisperse submicron particles in a sample [156]. Considering that the liposomes that encapsulate OVA become polydisperse systems with a high polydispersity index (Fig 6D), we preferred to take the NTA values as more suitable to characterize the size of the obtained liposomes that encapsulate OVA.

The clinical response to soluble  $\alpha$ -GalCer is varied depending on the therapeutic approach used, such as the direct injection of  $\alpha$ -GalCer and cell therapies using  $\alpha$ GC-loaded DC. While  $\alpha$ -GalCer has few effects *in vivo* direct treatments, it appears effective

in *ex vivo* cell therapies [157-160]. These results suggest that antigen-presenting cells did not take soluble  $\alpha$ -GalCer efficiently. Hence, to induce an effective immune response by the systemic administration of  $\alpha$ -GalCer, it will be necessary to control the disposition and cellular uptake of  $\alpha$ -GalCer with the currently available delivery systems. A promising alternative for delivery of glycolipid activators of iNKT cells is the use of liposomes. This work evaluated the antigenic potency of  $\alpha$ -GalCer and  $\alpha$ -GalCer analogs (OCH or AH10-7) contained in liposomes. We found that BMDC pulsed with  $\alpha$ -GalCer OCH, and AH10-7 incorporated in liposomes (or in OVA-contained liposomes) efficiently activated iNKT cells hybridoma. However, a different response was observed between the iNKT cells hybridoma activated by BMDC pulsed with the various glycolipids. For instance, the truncated sphingosine analog, OCH, showed the lowest activation level of iNKT cells hybridoma. This result could be related to this ligand's extremely low affinity or avidity for iNKT cell TCR [161, 162]. On the other hand, we observed that the highest activation of iNKT cells hybridoma was obtained with AH10-7. The compound, AH10-7, which combines a sphinganine base with a C6''-hydrocinnamoyl moiety, has the anticipated effect of enhancing iNKT cell activation when presented by hCD1d [72].

This study identified NKT10 cells in hCD1d-KI mice (a partially humanized murine model for NKT cell responses) (Fig. 8B). This iNKT cell subset was reported in spleen and subcutaneous white adipose tissue from C57BL/6 and in peripheral blood mononuclear cells from healthy human donors [22], but never in hCD1d-KI mice. This result opens an opportunity for research to distinguish the optimal experimental condition for NKT10 cell expansion. According to this objective, we evaluated different

experimental conditions, such as immunization schemes, glycolipid activators of iNKT cells, and the uses of glycolipid delivery systems. Firstly, we induced an expansion of NKT10 cells in hCD1d-KI mice in a short immunization scheme. In this sense, a significant expansion of NKT10 cells was observed in hCD1d-KI mice treated with  $\alpha$ -GalCer at seven days, similar to the development of NKT10 cells reported during the immunization scheme of 30 days [124]. In addition, significant proliferation of NKT10 cells was not detected in mice treated with OCH or AH10-7 (Fig. 8). However, in the group of mice treated with AH10-7 at 7 days, we can observe a slight increase of NKT10 cells.

It has been found that the ability of  $\alpha$ GalCer to expand NKT10 cells in vivo was shared in some Th1-biasing antigens [74, 163]. In contrast, a Th2-biasing iNKT cell antigen, or cytokine-driven iNKT cell activation due to TLR engagement or infections, did not induce NKT10 cell expansion [163]. We could appreciate a slight increase of NKT10 cells in the group of mice treated with Th1-biasing iNKT cell antigen: AH10-7, with an immunization scheme of two doses separated by seven days (Fig. 10). However, we could not find this ability in C4" amide linked derivatives of  $\alpha$ -GalCer such as AH10-3 and AH10-1 (Fig. 10). Saavedra-Avila *et. al.* (2020) synthesized and tested  $\alpha$ -GalCer variants with amide-linked phenyl alkane substitution in the C4" – position of the galactose ring included in these variants AH10-3 and AH10-1. They found that only a few groups of variants (which it is not included AH10-3 and AH10-1) have a solid ability to activate iNKT cells and increase serum IFN $\gamma$  production levels, which correlates with substantial antitumor activity in hCD1d-KI mice [76].

Interestingly, AH10-7 could strongly induce Th1 cytokines and promote an antitumor response in wild-type and hCD1d-KI mice [72]. According to our results and what has been described by other investigations, we can affirm that there is a greater probability of inducing regulatory iNKT cells only with glycolipids that generate a robust Th1-type response. Until now, only the expansion of NKT10 cells has been evaluated without considering different factors that can enhance the immune response beyond simple antigenic stimulation. We refer to strategies that optimize the release and availability of antigens, as in the case of liposomal preparations. In this sense, we could observe that incorporating the glycolipid ligands ( $\alpha$ -GalCer, OCH, and AH10-7) into liposomes remarkably increased the expansion of NKT10 cells, which was superior in the group of mice treated with AH10-7 incorporated in liposomes (Fig. 11). This result was very relevant for this study; then, we would like to differentially activate iNKT cells with  $\alpha$ -GalCer analogs, which expand NKT10 cells and elicit a regulatory- skewed response. Therefore, we demonstrated that AH10-7 in liposomes could be an excellent candidate for therapies targeting iNKT cells to treat allergic inflammation, based on  $\alpha$ -GalCer's limited therapeutic efficacy in asthma and allergies [60-62].

We demonstrated that liposomes containing AH10-7 and OVA induced an antiallergic effect in BALB/c mice with OVA-induced allergy in a prophylactic scenery. In this sense, we observed a significant decrease in the inflammatory score and the number of mucus-producing cells in the lungs of mice with allergic induction treated with Lp/OVA/AH10-7 (Fig. 15 and 16), as well as a reduction of a significant reduction in the recruitment eosinophil in lungs (Fig. 13B y D). After this promising result, we decided to evaluate the expansion of regulatory B cells promoted by the differential activation



of iNKT cells with  $\alpha$ -GalCer analogs contained in liposomes in a partially humanized murine model for NKT cell responses to allergic asthma. For this purpose, we induced OVA-induced allergy in BALBc mice. Following the immunization scheme established in this study for NKT10 cell induction (two doses from 4  $\mu$ g of glycolipid and 1  $\mu$ g of  $\alpha$ -GalCer, separated by seven days), liposomal preparations (and controls) were administered. Interestingly, we could not appreciate a significant expansion of IL-10-producing regulatory B cells (B10 cells) in mediastinal lymph nodes from mice with OVA-induced allergy treated with liposomes containing OVA and the  $\alpha$ -GalCer analog: AH10-7 (Fig. 19B). Some evidence indicates that the  $\alpha$ -GalCer before allergen sensitization promotes iNKT cell-mediated induction of Treg cells, preventing Th2 cell responses in murine asthma [164]. Hence, the expansion and suppression of Treg cells could be an alternative pathway for the prevention of the inflammation observed when liposomes containing AH10-7 and OVA were administered.

This last result leads us to prove other immunization regimens to improve the antiallergic effect of liposomes containing glycolipid activators of iNKT cells. We tried a scheme of two immunization regimens (4 weekly doses). We observed a complete decrease in lung inflammation and goblet cells hyperplasia in mice with OVA-induced allergy treated with two regimens of doses of liposomes containing OVA the  $\alpha$ -GalCer (Lp/OVA/ $\alpha$ GC) (Fig. 15 and 16). Additionally, we could not observe a significant expansion of B10 cells in mediastinal lymph nodes from mice with OVA-induced allergy treated with two regimens of doses of Lp/OVA/ $\alpha$ GC. Thus, the suppression of the allergic response observed could be mediated by other regulatory cells such as Treg or myeloid-derived suppressor cells (MDSCs) (Fig. 27). There is an increasing amount

of evidence supporting the involvement of this heterogeneous group of immature myeloid cells can suppress the immune response in lung diseases like asthma [165, 166]. Recent studies demonstrate that glycolipid-activated iNKT cells cooperate with MDSCs in protecting mice against the development of EAE [167]. Finally, we must not forget the role of NKT10 cells in suppressing the immune response in the context of autoimmune diseases such as EAE [22]. Thus, evaluating the allergic response in IL-10 knock-out mice with OVA-induced allergy and treated with Lp/OVA/AH10-7 or Lp/OVA/ $\alpha$ GC would be extremely attractive, for demonstrate the role of NKT10 in preventing or suppressing lung inflammation.

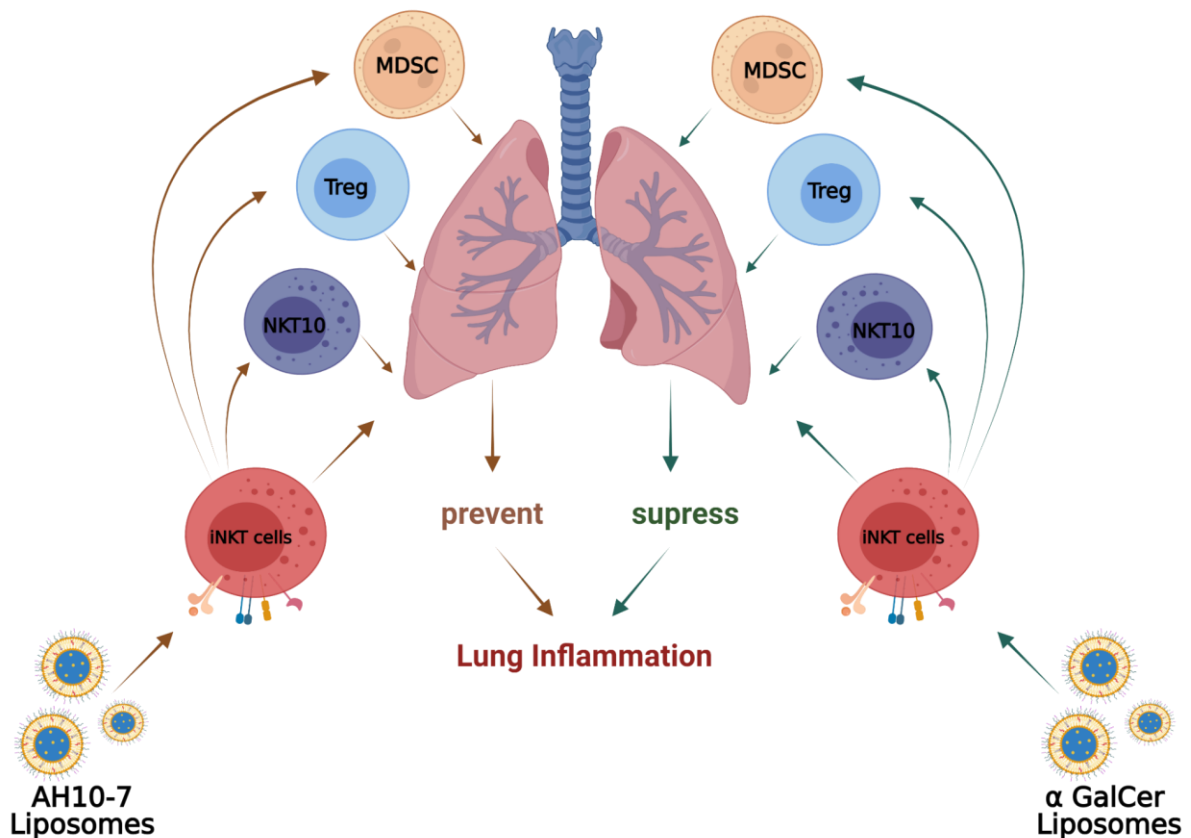


**Figure 27. Model proposal on the differential activation of iNKT cells with glycolipids ( $\alpha$ -GalCer and AH10-7) contained in liposomes, which could expand**

**NKT10 cells and other regulatory cells such as regulatory T cells (Treg) or myeloid-derived suppressor cells (MDSCs) which led to prevent or suppress immune inflammation.**

Additionally, in this project, we wanted to evaluate the expansion and the suppressive function of regulatory (Breg) cells promoted by the differential activation of iNKT cells with  $\alpha$ -GalCer analogs contained in liposomes in hCD1d-KI mice with allergic asthma. At this point, we identified a good candidate for the activation of iNKT, which induces an antiallergic effect (AH10-7). Our next step was the induction of allergic asthma in hCD1d-KI mice. For that purpose, we developed an OVA-induced mouse model of asthma in hCD1d-KI mice. We observed that it was tricky to induce an OVA model in hCD1d-KI mice (C57BL/6J background) that generates airway hyperreactivity (Fig. 24). Mice do not spontaneously develop asthma. The nature of the acute inflammatory model may be influenced by the choice of mouse strain, the allergen, and the sensitization and challenge protocol [168]. The uses OVA as an experimental allergen; besides the common effect of airway hyperreactivity in C57BL/6J, it is not a relevant allergen in humans, the allergen is not affecting the epithelial cells as a relevant allergen, the sensitization is often needed to be together with adjuvant (Inject®Alum) and often through i.p. injections which not a natural way of allergy [133]. For these reasons, we continued our study using house dust mite (HDM), a clinically relevant allergen given through the airways from the start. The protocol is easy, short, and strongly responds to the main asthmatic parameters [134, 135, 169]. Finally, we didn't obtain a severe allergic response in the lung and the BAL of mice challenged with HDM (Fig. 25). Consequently, its necessary to improve the obtention of HDM induced-allergic model in hCD1D-KI mice, maybe in BALBc mice background.

## CONCLUSIONS

1. We **identified** for the first-time **expansion of NKT10 cells in hCD1d-KI mice** through stimulation with  $\alpha$ -GalCer.
2. There was a **significant expansion of NKT10 cells in hCD1d-KI mice treated with  $\alpha$ -GalCer at 7 days**; very similar to the expansion of NKT10 cells reported at 30 days.
3. The **incorporation of glycolipids into stearylated octaarginine-modified liposomes effectively induced in vitro activation of iNKT cells** hybridoma and remarkably increased the in vivo expansion of NKT10 cells.
4. **The glycolipid antigen AH10-7 contained into liposomes could be an excellent candidate** for therapies that target NKT10 cells.
5. Our results demonstrated that **liposomes containing AH10-7 and OVA (Lp/OVA/AH10-7) induce an anti-allergic effect in BALB/c mice with OVA-induced allergy in a prophylactic scenery**. Particularly, we observed a significant decrease in the inflammatory score and in the number of mucus-producing cells in the lungs of mice with allergic induction treated with Lp/OVA/AH10-7.
6. We observed a **complete decrease of lung inflammation and goblet cells hyperplasia in mice with OVA-induced allergy treated with two regimens of doses of liposomes containing OVA the  $\alpha$ -GalCer**.
7. We could appreciate that it is tricky to induce an OVA-model in hCD1d-KI mice (C57BL/6J background). Additionally, we didn't obtain a severe allergic response in the lung and the BAL of mice challenged with HDM. Consequently, **its necessary to improve the obtention of HDM induced-allergic model in hCD1D-KI mice, maybe in BALBc mice background**.

## **PUBLICATIONS & PARTICIPATION IN SCIENTIFIC MEETINGS**

García-Betancourt, R., Gutiérrez-Vera, C., Palacios, P., Schneider, D., Schäfer, C., Santibáñez, A., Pérez-Baño A., González S., Flores, G., Falcón, R. Riveros, A., Carreño, L. ***“Induction of regulatory iNKT cells with glycolipid incorporated into liposomes in a humanized model for iNKT cells”*** (2022) manuscript in preparation.

Participation with the poster: *“Induction of regulatory iNKT cells with glycolipids encapsulated into liposomes, in a humanized model for iNKT cells.”* **IV Annual Meeting ASOCHIN 2021** (CHILE, 2021).

3<sup>rd</sup> place award with the poster: *“Induction of regulatory iNKT cells with glycolipids encapsulated into liposomes, in a humanized model for iNKT cells.”* **I Congress of Postgraduate Students Campus Dr. Eloisa Díaz, University of Chile** (CHILE, 2020).

Participation with the poster: *“Induction of regulatory iNKT cells with glycolipids encapsulated into liposomes, in a humanized model for iNKT cells.”* **III Annual Meeting ASOCHIN 2020** (CHILE, 2020).

Participation with the poster: *“Modulation of regulatory B cells and T cells through activation of iNKT cells with glycolipids encapsulated into liposomes.”* **XXIV Latin American Congress of Microbiology** (CHILE, 2018)

## REFERENCES

1. Taniguchi, M., et al., *The regulatory role of Valpha14 NKT cells in innate and acquired immune response*. Annu Rev Immunol, 2003. **21**: p. 483-513.
2. Gumperz, J.E., et al., *Functionally distinct subsets of CD1d-restricted natural killer T cells revealed by CD1d tetramer staining*. J Exp Med, 2002. **195**(5): p. 625-36.
3. Godfrey, D.I., et al., *NKT cells: what's in a name?* Nat Rev Immunol, 2004. **4**(3): p. 231-7.
4. Bendelac, A., P.B. Savage, and L. Teyton, *The biology of NKT cells*. Annu Rev Immunol, 2007. **25**: p. 297-336.
5. Arase, H., N. Arase, and T. Saito, *Interferon gamma production by natural killer (NK) cells and NK1.1+ T cells upon NKR-P1 cross-linking*. J Exp Med, 1996. **183**(5): p. 2391-6.
6. Carreño, L.J., Shalu, and S.A. Porcelli, *Optimizing NKT cell ligands as vaccine adjuvants*. Immunotherapy, 2014. **6**(3): p. 309-320.
7. Bricard, G. and S.A. Porcelli, *Antigen presentation by CD1 molecules and the generation of lipid-specific T cell immunity*. Cell Mol Life Sci, 2007. **64**(14): p. 1824-40.
8. Dellabona, P., et al., *An invariant V alpha 24-J alpha Q/V beta 11 T cell receptor is expressed in all individuals by clonally expanded CD4-8- T cells*. J Exp Med, 1994. **180**(3): p. 1171-6.
9. Lantz, O. and A. Bendelac, *An invariant T cell receptor alpha chain is used by a unique subset of major histocompatibility complex class I-specific CD4+ and CD4-8- T cells in mice and humans*. J Exp Med, 1994. **180**(3): p. 1097-106.
10. Bendelac, A., et al., *CD1 recognition by mouse NK1+ T lymphocytes*. Science, 1995. **268**(5212): p. 863-5.
11. Kawano, T., et al., *CD1d-restricted and TCR-mediated activation of valpha14 NKT cells by glycosylceramides*. Science, 1997. **278**(5343): p. 1626-9.
12. Burdin, N., et al., *Selective ability of mouse CD1 to present glycolipids: alpha-galactosylceramide specifically stimulates V alpha 14+ NK T lymphocytes*. J Immunol, 1998. **161**(7): p. 3271-81.
13. Kinjo, Y., et al., *Natural killer T cells recognize diacylglycerol antigens from pathogenic bacteria*. Nat Immunol, 2006. **7**(9): p. 978-86.
14. Brigl, M. and M.B. Brenner, *How invariant natural killer T cells respond to infection by recognizing microbial or endogenous lipid antigens*. Semin Immunol, 2010. **22**(2): p. 79-86.
15. Kinjo, Y., et al., *Invariant natural killer T cells recognize glycolipids from pathogenic Gram-positive bacteria*. Nature Immunology, 2011. **12**(10): p. 966-974.
16. De Libero, G. and L. Mori, *Recognition of lipid antigens by T cells*. Nat Rev Immunol, 2005. **5**(6): p. 485-96.
17. Brennan, P.J., et al., *Invariant natural killer T cells recognize lipid self antigen induced by microbial danger signals*. Nat Immunol, 2011. **12**(12): p. 1202-11.
18. Saroha, A., et al., *Critical Role for Very-Long Chain Sphingolipids in Invariant Natural Killer T Cell Development and Homeostasis*. Front Immunol, 2017. **8**: p. 1386.
19. Kumar, A., et al., *Natural Killer T Cells: An Ecological Evolutionary Developmental Biology Perspective*. Front Immunol, 2017. **8**: p. 1858.
20. Coquet, J.M., et al., *Diverse cytokine production by NKT cell subsets and identification of an IL-17-producing CD4-NK1.1- NKT cell population*. Proc Natl Acad Sci U S A, 2008. **105**(32): p. 11287-92.
21. Crosby, C.M. and M. Kronenberg, *Tissue-specific functions of invariant natural killer T cells*. Nat Rev Immunol, 2018. **18**(9): p. 559-574.
22. Sag, D., et al., *IL-10-producing NKT10 cells are a distinct regulatory invariant NKT cell subset*. Journal of Clinical Investigation, 2014. **124**(9): p. 3725-3740.
23. Constantinides, M.G. and A. Bendelac, *Transcriptional regulation of the NKT cell lineage*. Current Opinion in Immunology, 2013. **25**(2): p. 161-167.
24. Lee, Y.J., et al., *Steady-state production of IL-4 modulates immunity in mouse strains and is determined by lineage diversity of iNKT cells*. Nature Immunology, 2013. **14**(11): p. 1146-1154.
25. Das, R., D.B. Sant'Angelo, and K.E. Nichols, *Transcriptional control of invariant NKT cell development*. 2010. **238**(1): p. 195-215.
26. Wingender, G., D. Sag, and M. Kronenberg, *NKT10 cells: a novel iNKT cell subset*. Oncotarget, 2015. **6**(29): p. 26552-3.

27. Lynch, L., et al., *Regulatory iNKT cells lack expression of the transcription factor PLZF and control the homeostasis of T(reg) cells and macrophages in adipose tissue*. *Nat Immunol*, 2015. **16**(1): p. 85-95.
28. Stetson, D.B., et al., *Constitutive cytokine mRNAs mark natural killer (NK) and NK T cells poised for rapid effector function*. *J Exp Med*, 2003. **198**(7): p. 1069-76.
29. Matsuda, J.L., et al., *Natural killer T cells reactive to a single glycolipid exhibit a highly diverse T cell receptor beta repertoire and small clone size*. *Proc Natl Acad Sci U S A*, 2001. **98**(22): p. 12636-41.
30. Brigl, M., et al., *Mechanism of CD1d-restricted natural killer T cell activation during microbial infection*. *Nat Immunol*, 2003. **4**(12): p. 1230-7.
31. Carnaud, C., et al., *Cutting edge: Cross-talk between cells of the innate immune system: NKT cells rapidly activate NK cells*. *J Immunol*, 1999. **163**(9): p. 4647-50.
32. Fujii, S., et al., *Innate Valpha14(+) natural killer T cells mature dendritic cells, leading to strong adaptive immunity*. *Immunol Rev*, 2007. **220**: p. 183-98.
33. Kitamura, H., et al., *alpha-galactosylceramide induces early B-cell activation through IL-4 production by NKT cells*. *Cell Immunol*, 2000. **199**(1): p. 37-42.
34. Nair, S. and M.V. Dhodapkar, *Natural Killer T Cells in Cancer Immunotherapy*. *Front Immunol*, 2017. **8**: p. 1178.
35. Schmidt, S., et al., *Natural killer cells as a therapeutic tool for infectious diseases - current status and future perspectives*. *Oncotarget*, 2018. **9**(29): p. 20891-20907.
36. Khan, A., et al., *Prophylactic Sublingual Immunization with Mycobacterium tuberculosis Subunit Vaccine Incorporating the Natural Killer T Cell Agonist Alpha-Galactosylceramide Enhances Protective Immunity to Limit Pulmonary and Extra-Pulmonary Bacterial Burden in Mice*. *Vaccines (Basel)*, 2017. **5**(4).
37. Noto Llana, M., et al., *Activation of iNKT Cells Prevents Salmonella-Enterocolitis and Salmonella-Induced Reactive Arthritis by Downregulating IL-17-Producing  $\gamma\delta$ T Cells*. *Front Cell Infect Microbiol*, 2017. **7**: p. 398.
38. Juno, J.A., Y. Keynan, and K.R. Fowke, *Invariant NKT cells: regulation and function during viral infection*. *PLoS Pathog*, 2012. **8**(8): p. e1002838.
39. Zhao, L., et al., *[NKT cells and graft-versus-host disease-review]*. *Zhongguo Shi Yan Xue Ye Xue Za Zhi*, 2013. **21**(5): p. 1345-50.
40. Hongo, D., et al., *Tolerogenic interactions between CD8(+) dendritic cells and NKT cells prevent rejection of bone marrow and organ grafts*. *Blood*, 2017. **129**(12): p. 1718-1728.
41. Hongo, D., et al., *Interactions between NKT cells and Tregs are required for tolerance to combined bone marrow and organ transplants*. *Blood*, 2012. **119**(6): p. 1581-9.
42. Novak, J. and A. Lehen, *Mechanism of regulation of autoimmunity by iNKT cells*. *Cytokine*, 2011. **53**(3): p. 263-70.
43. Uchida, T., et al., *Repeated administration of alpha-galactosylceramide ameliorates experimental lupus nephritis in mice*. *Sci Rep*, 2018. **8**(1): p. 8225.
44. Oleinika, K., et al., *CD1d-dependent immune suppression mediated by regulatory B cells through modulations of iNKT cells*. *Nature Communications*, 2018. **9**(1).
45. Paget, C. and F. Trottein, *Role of type 1 natural killer T cells in pulmonary immunity*. *Mucosal Immunol*, 2013. **6**(6): p. 1054-67.
46. Tsao, C.C., et al., *Repeated Activation of Lung Invariant NKT Cells Results in Chronic Obstructive Pulmonary Disease-Like Symptoms*. *PLoS One*, 2016. **11**(1): p. e0147710.
47. Finn, P.W. and T.D. Bigby, *Innate Immunity and Asthma*. *Proceedings of the American Thoracic Society*, 2009. **6**(3): p. 260-265.
48. Akuthota, P., H. Wang, and P.F. Weller, *Eosinophils as antigen-presenting cells in allergic upper airway disease*. *Current Opinion in Allergy & Clinical Immunology*, 2010. **10**(1): p. 14-19.
49. He, J.S., et al., *Biology of IgE production: IgE cell differentiation and the memory of IgE responses*. *Curr Top Microbiol Immunol*, 2015. **388**: p. 1-19.
50. Conner, E.R. and S.S. Saini, *The immunoglobulin E receptor: expression and regulation*. *Curr Allergy Asthma Rep*, 2005. **5**(3): p. 191-6.
51. Galli, S.J., S. Nakae, and M. Tsai, *Mast cells in the development of adaptive immune responses*. *Nat Immunol*, 2005. **6**(2): p. 135-42.

52. Mudde, G.C., et al., *IgE: an immunoglobulin specialized in antigen capture?* Immunol Today, 1990. **11**(12): p. 440-3.
53. Fahy, J.V., *Type 2 inflammation in asthma — present in most, absent in many.* Nature Reviews Immunology, 2015. **15**(1): p. 57-65.
54. Kay, A.B., *Allergy and allergic diseases. Second of two parts.* N Engl J Med, 2001. **344**(2): p. 109-13.
55. Larché, M., C.A. Akdis, and R. Valenta, *Immunological mechanisms of allergen-specific immunotherapy.* Nat Rev Immunol, 2006. **6**(10): p. 761-71.
56. Berzins, S.P., M.J. Smyth, and A.G. Baxter, *Presumed guilty: natural killer T cell defects and human disease.* Nat Rev Immunol, 2011. **11**(2): p. 131-42.
57. Yamada, D., et al., *Efficient Regeneration of Human V $\alpha$ 24(+) Invariant Natural Killer T Cells and Their Anti-Tumor Activity In Vivo.* Stem Cells, 2016. **34**(12): p. 2852-2860.
58. Kobayashi, E., et al., *KRN7000, a novel immunomodulator, and its antitumor activities.* Oncol Res, 1995. **7**(10-11): p. 529-34.
59. Im, J.S., et al., *Kinetics and cellular site of glycolipid loading control the outcome of natural killer T cell activation.* Immunity, 2009. **30**(6): p. 888-98.
60. Nie, H., et al., *Invariant NKT Cells Act as an Adjuvant to Enhance Th2 Inflammatory Response in an OVA-Induced Mouse Model of Asthma.* 2015. **10**(4): p. e0119901.
61. Akbari, O., et al., *Essential role of NKT cells producing IL-4 and IL-13 in the development of allergen-induced airway hyperreactivity.* Nat Med, 2003. **9**(5): p. 582-8.
62. Akbari, O., et al., *ICOS/ICOSL Interaction Is Required for CD4+ Invariant NKT Cell Function and Homeostatic Survival.* 2008. **180**(8): p. 5448-5456.
63. Venkataswamy, M.M. and S.A. Porcelli, *Lipid and glycolipid antigens of CD1d-restricted natural killer T cells.* Seminars in Immunology, 2010. **22**(2): p. 68-78.
64. Arora, P., et al., *A rapid fluorescence-based assay for classification of iNKT cell activating glycolipids.* J Am Chem Soc, 2011. **133**(14): p. 5198-201.
65. Kopecky-Bromberg, S.A., et al., *Alpha-C-galactosylceramide as an adjuvant for a live attenuated influenza virus vaccine.* 2009. **27**(28): p. 3766-3774.
66. Schmiege, J., et al., *Superior Protection against Malaria and Melanoma Metastases by a C-glycoside Analogue of the Natural Killer T Cell Ligand  $\alpha$ -Galactosylceramide.* Journal of Experimental Medicine, 2003. **198**(11): p. 1631-1641.
67. Padte, N.N., et al., *A glycolipid adjuvant, 7DW8-5, enhances CD8+ T cell responses induced by an adenovirus-vectored malaria vaccine in non-human primates.* PLoS One, 2013. **8**(10): p. e78407.
68. Forestier, C., et al., *Improved Outcomes in NOD Mice Treated with a Novel Th2 Cytokine-Biasing NKT Cell Activator.* 2007. **178**(3): p. 1415-1425.
69. Miyamoto, K., S. Miyake, and T. Yamamura, *A synthetic glycolipid prevents autoimmune encephalomyelitis by inducing TH2 bias of natural killer T cells.* Nature, 2001. **413**(6855): p. 531-4.
70. Aspeslagh, S., et al., *Galactose-modified iNKT cell agonists stabilized by an induced fit of CD1d prevent tumour metastasis.* The EMBO Journal, 2011. **30**(11): p. 2294-2305.
71. Aspeslagh, S., et al., *Enhanced TCR Footprint by a Novel Glycolipid Increases NKT-Dependent Tumor Protection.* 2013. **191**(6): p. 2916-2925.
72. Chennamadhavuni, D., et al., *Dual Modifications of  $\alpha$ -Galactosylceramide Synergize to Promote Activation of Human Invariant Natural Killer T Cells and Stimulate Anti-tumor Immunity.* Cell Chemical Biology, 2018. **25**(5): p. 571-584.e8.
73. Carreño, L.J., N.A. Saavedra-Ávila, and S.A. Porcelli, *Synthetic glycolipid activators of natural killer T cells as immunotherapeutic agents.* 2016. **5**(4): p. e69.
74. Birkholz, A.M., et al., *A Novel Glycolipid Antigen for NKT Cells That Preferentially Induces IFN- Production.* 2015. **195**(3): p. 924-933.
75. Wingender, G., et al., *Selective Conditions Are Required for the Induction of Invariant NKT Cell Hyporesponsiveness by Antigenic Stimulation.* The Journal of Immunology, 2015. **195**(8): p. 3838-3848.
76. Saavedra-Avila, N.A., et al., *Amide-Linked C4"-Saccharide Modification of KRN7000 Provides Potent Stimulation of Human Invariant NKT Cells and Anti-Tumor Immunity in a Humanized Mouse Model.* ACS Chemical Biology, 2020. **15**(12): p. 3176-3186.



77. Godfrey, D.I., et al., *NKT cells: facts, functions and fallacies*. Immunol Today, 2000. **21**(11): p. 573-83.
78. Fernandez, C.S., et al., *In-vivo stimulation of macaque natural killer T cells with  $\alpha$ -galactosylceramide*. Clin Exp Immunol, 2013. **173**(3): p. 480-92.
79. Wen, X., et al., *Human CD1d knock-in mouse model demonstrates potent antitumor potential of human CD1d-restricted invariant natural killer T cells*. 2013. **110**(8): p. 2963-2968.
80. Venkataswamy, M.M., et al., *Improving Mycobacterium bovis bacillus Calmette-Guèrin as a vaccine delivery vector for viral antigens by incorporation of glycolipid activators of NKT cells*. PLoS One, 2014. **9**(9): p. e108383.
81. Yu, K.O.A. and S.A. Porcelli, *The diverse functions of CD1d-restricted NKT cells and their potential for immunotherapy*. 2005. **100**(1): p. 42-55.
82. Jiang, X., et al., *Mechanism of NKT Cell-Mediated Transplant Tolerance*. American Journal of Transplantation, 2007. **7**(6): p. 1482-1490.
83. Im, J.S., et al., *Expression of CD1d Molecules by Human Schwann Cells and Potential Interactions with Immunoregulatory Invariant NK T Cells*. 2006. **177**(8): p. 5226-5235.
84. Sakuishi, K., et al., *Invariant NKT Cells Biased for IL-5 Production Act as Crucial Regulators of Inflammation*. The Journal of Immunology, 2007. **179**(6): p. 3452-3462.
85. Vignali, D.A.A., L.W. Collison, and C.J. Workman, *How regulatory T cells work*. Nature Reviews Immunology, 2008. **8**(7): p. 523-532.
86. Robinson, D.S., *Regulatory T cells and asthma*. Clin Exp Allergy, 2009. **39**(9): p. 1314-23.
87. Setoguchi, R., et al., *Homeostatic maintenance of natural Foxp3+ CD25+ CD4+ regulatory T cells by interleukin (IL)-2 and induction of autoimmune disease by IL-2 neutralization*. The Journal of Experimental Medicine, 2005. **201**(5): p. 723-735.
88. Sakaguchi, S., *Naturally arising Foxp3-expressing CD25+CD4+ regulatory T cells in immunological tolerance to self and non-self*. Nat Immunol, 2005. **6**(4): p. 345-52.
89. Furtado, G.U.C., et al., *Interleukin 2 Signaling Is Required for CD4+ Regulatory T Cell Function*. Journal of Experimental Medicine, 2002. **196**(6): p. 851-857.
90. Papiernik, M., *Regulatory CD4 T cells: expression of IL-2R alpha chain, resistance to clonal deletion and IL-2 dependency*. International Immunology, 1998. **10**(4): p. 371-378.
91. Malek, T.R., et al., *CD4 Regulatory T Cells Prevent Lethal Autoimmunity in IL-2R $\beta$ -Deficient Mice*. Immunity, 2002. **17**(2): p. 167-178.
92. Cava, A.L., L.V. Kaer, and S. Fu Dong, *CD4+CD25+ Tregs and NKT cells: regulators regulating regulators*. Trends in Immunology, 2006. **27**(7): p. 322-327.
93. Liu, R., et al., *Cooperation of Invariant NKT Cells and CD4+CD25+ T Regulatory Cells in the Prevention of Autoimmune Myasthenia*. 2005. **175**(12): p. 7898-7904.
94. Braza, F., et al., *Regulatory functions of B cells in allergic diseases*. Allergy, 2014. **69**(11): p. 1454-1463.
95. Van De Veen, W., et al., *Role of regulatory B cells in immune tolerance to allergens and beyond*. Journal of Allergy and Clinical Immunology, 2016. **138**(3): p. 654-665.
96. Mauri, C. and A. Bosma, *Immune Regulatory Function of B Cells*. Annual Review of Immunology, 2012. **30**(1): p. 221-241.
97. Tian, J., et al., *Lipopolysaccharide-Activated B Cells Down-Regulate Th1 Immunity and Prevent Autoimmune Diabetes in Nonobese Diabetic Mice*. 2001. **167**(2): p. 1081-1089.
98. Shen, P., et al., *IL-35-producing B cells are critical regulators of immunity during autoimmune and infectious diseases*. Nature, 2014. **507**(7492): p. 366-370.
99. Khan, A.R., et al., *PD-L1hi B cells are critical regulators of humoral immunity*. Nature Communications, 2015. **6**(1): p. 5997.
100. Elizabeth and C. Mauri, *Regulatory B Cells: Origin, Phenotype, and Function*. Immunity, 2015. **42**(4): p. 607-612.
101. Leadbetter, E.A., et al., *NK T cells provide lipid antigen-specific cognate help for B cells*. Proceedings of the National Academy of Sciences, 2008. **105**(24): p. 8339-8344.
102. Barral, P., et al., *B cell receptor-mediated uptake of CD1d-restricted antigen augments antibody responses by recruiting invariant NKT cell help in vivo*. Proceedings of the National Academy of Sciences, 2008. **105**(24): p. 8345-8350.
103. Almishri, W., J. Deans, and M.G. Swain, *Rapid activation and hepatic recruitment of innate-like regulatory B cells after invariant NKT cell stimulation in mice*. 2015. **63**(4): p. 943-951.

104. Pillai, A.B., et al., *Host natural killer T cells induce an interleukin-4-dependent expansion of donor CD4+CD25+Foxp3+ T regulatory cells that protects against graft-versus-host disease*. 2009. **113**(18): p. 4458-4467.
105. Vomhof-Dekrey, E.E., et al., *Cognate interaction with iNKT cells expands IL-10-producing B regulatory cells*. 2015. **112**(40): p. 12474-12479.
106. Scanlon, S.T., et al., *Airborne lipid antigens mobilize resident intravascular NKT cells to induce allergic airway inflammation*. *The Journal of Experimental Medicine*, 2011. **208**(10): p. 2113-2124.
107. Nakamura, T., et al., *The nanoparticulation by octaarginine-modified liposome improves  $\alpha$ -galactosylceramide-mediated antitumor therapy via systemic administration*. *Journal of Controlled Release*, 2013. **171**(2): p. 216-224.
108. Lutz, M.B., et al., *An advanced culture method for generating large quantities of highly pure dendritic cells from mouse bone marrow*. *J Immunol Methods*, 1999. **223**(1): p. 77-92.
109. Rivas, M.N., et al., *MyD88 is critically involved in immune tolerance breakdown at environmental interfaces of Foxp3-deficient mice*. *J Clin Invest*, 2012. **122**(5): p. 1933-47.
110. Kujur, W., et al., *Caerulomycin A inhibits Th2 cell activity: a possible role in the management of asthma*. *Scientific Reports*, 2015. **5**(1): p. 15396.
111. Mäkelä, M.J., et al., *The failure of interleukin-10-deficient mice to develop airway hyperresponsiveness is overcome by respiratory syncytial virus infection in allergen-sensitized/challenged mice*. *Am J Respir Crit Care Med*, 2002. **165**(6): p. 824-31.
112. Thapa, P., et al., *Nanoparticle formulated alpha-galactosylceramide activates NKT cells without inducing anergy*. *Vaccine*, 2009. **27**(25-26): p. 3484-3488.
113. Baxa, U., *Imaging of Liposomes by Transmission Electron Microscopy*. *Methods Mol Biol*, 2018. **1682**: p. 73-88.
114. Tanaka, N., *Imaging of Scanning Transmission Electron Microscopy (STEM)*. 2017, Springer Japan. p. 161-166.
115. Yeap, S.P., et al., *On Size Fractionation of Iron Oxide Nanoclusters by Low Magnetic Field Gradient*. *The Journal of Physical Chemistry C*, 2014. **118**(41): p. 24042-24054.
116. Ito, T., et al., *Comparison of Nanoparticle Size and Electrophoretic Mobility Measurements Using a Carbon-Nanotube-Based Coulter Counter, Dynamic Light Scattering, Transmission Electron Microscopy, and Phase Analysis Light Scattering*. *Langmuir*, 2004. **20**(16): p. 6940-6945.
117. Carvalho, P.M., et al., *Application of Light Scattering Techniques to Nanoparticle Characterization and Development*. *Frontiers in Chemistry*, 2018. **6**.
118. Singh, P., et al., *Particle size analyses of polydisperse liposome formulations with a novel multispectral advanced nanoparticle tracking technology*. *International Journal of Pharmaceutics*, 2019. **566**: p. 680-686.
119. Koppel, D.E., *Analysis of Macromolecular Polydispersity in Intensity Correlation Spectroscopy: The Method of Cumulants*. *The Journal of Chemical Physics*, 1972. **57**(11): p. 4814-4820.
120. Danaei, M., et al., *Impact of Particle Size and Polydispersity Index on the Clinical Applications of Lipidic Nanocarrier Systems*. *Pharmaceutics*, 2018. **10**(2).
121. Nobbman, U. *Polydispersity – what does it mean for DLS and chromatography?* 2017 [cited 28-01-2022]; Available from: <https://www.materials-talks.com/polydispersity-what-does-it-mean-for-dls-and-chromatography/>.
122. Smith, M.C., et al., *Zeta potential: a case study of cationic, anionic, and neutral liposomes*. *Analytical and Bioanalytical Chemistry*, 2017. **409**(24): p. 5779-5787.
123. Clarke, S.R., et al., *Characterization of the ovalbumin-specific TCR transgenic line OT-I: MHC elements for positive and negative selection*. *Immunol Cell Biol*, 2000. **78**(2): p. 110-7.
124. Parekh, V.V., *Glycolipid antigen induces long-term natural killer T cell anergy in mice*. 2005. **115**(9): p. 2572-2583.
125. Laurent, X., et al., *Switching invariant natural killer T (iNKT) cell response from anticancerous to anti-inflammatory effect: molecular bases*. *J Med Chem*, 2014. **57**(13): p. 5489-508.
126. Uldrich, A.P., et al., *NKT Cell Stimulation with Glycolipid Antigen In Vivo: Costimulation-Dependent Expansion, Bim-Dependent Contraction, and Hyporesponsiveness to Further Antigenic Challenge*. *The Journal of Immunology*, 2005. **175**(5): p. 3092-3101.
127. Salio, M., et al., *Modulation of human natural killer T cell ligands on TLR-mediated antigen-presenting cell activation*. 2007. **104**(51): p. 20490-20495.

128. Sullivan, B.A., *Activation or anergy: NKT cells are stunned by  $\alpha$ -galactosylceramide*. Journal of Clinical Investigation, 2005. **115**(9): p. 2328-2329.
129. Natori, T., et al., *Agelasphins, novel antitumor and immunostimulatory cerebroside from the marine sponge Agelas mauritianus*. Tetrahedron, 1994. **50**(9): p. 2771-2784.
130. Osman, Y., et al., *Activation of hepatic NKT cells and subsequent liver injury following administration of  $\alpha$ -galactosylceramide*. Eur J Immunol, 2000. **30**(7): p. 1919-28.
131. Rogers, D.F., *Airway goblet cell hyperplasia in asthma: hypersecretory and anti-inflammatory?* Clinical & Experimental Allergy, 2002. **32**(8): p. 1124-1127.
132. Hieda, Y., et al., *An experimental model of death from anaphylactic shock with compound 48/80 and postmortem changes in levels of histamine in blood*. Forensic Sci Int, 1990. **45**(1-2): p. 159-69.
133. Fuchs, B. and A. Braun, *Improved mouse models of allergy and allergic asthma--chances beyond ovalbumin*. Curr Drug Targets, 2008. **9**(6): p. 495-502.
134. Plantinga, M., et al., *Conventional and Monocyte-Derived CD11b+ Dendritic Cells Initiate and Maintain T Helper 2 Cell-Mediated Immunity to House Dust Mite Allergen*. Immunity, 2013. **38**(2): p. 322-335.
135. Deckers, J., et al., *Epicutaneous sensitization to house dust mite allergen requires IRF4-dependent dermal dendritic cells*. 2017.
136. Baxa, U., *Preparation of Liposomes for Negative Staining TEM*. Microscopy and Microanalysis, 2020. **26**(S2): p. 2090-2091.
137. Franken, L.E., E.J. Boekema, and M.C.A. Stuart, *Transmission Electron Microscopy as a Tool for the Characterization of Soft Materials: Application and Interpretation*. Advanced Science, 2017. **4**(5): p. 1600476.
138. Almgren, M., K. Edwards, and G. Karlsson, *Cryo transmission electron microscopy of liposomes and related structures*. Colloids and Surfaces A: Physicochemical and Engineering Aspects, 2000. **174**(1): p. 3-21.
139. Gao, J.-Q., et al., *Effective transcutaneous immunization by antigen-loaded flexible liposome in vivo*. International Journal of Nanomedicine, 2011: p. 3241.
140. Davidsen, J., et al., *Characterization of cationic liposomes based on dimethyldioctadecylammonium and synthetic cord factor from M. tuberculosis (trehalose 6,6'-dibehenate)—A novel adjuvant inducing both strong CMI and antibody responses*. Biochimica et Biophysica Acta (BBA) - Biomembranes, 2005. **1718**(1-2): p. 22-31.
141. Scarff, C.A., et al., *Variations on Negative Stain Electron Microscopy Methods: Tools for Tackling Challenging Systems*. Journal of Visualized Experiments, 2018(132).
142. Clogston, J.D. and A.K. Patri, *Zeta Potential Measurement*, in *Characterization of Nanoparticles Intended for Drug Delivery*, S.E. McNeil, Editor. 2011, Humana Press: Totowa, NJ. p. 63-70.
143. Yeh, M.-K., et al., *The comparison of protein-entrapped liposomes and lipoparticles: preparation, characterization, and efficacy of cellular uptake*. International Journal of Nanomedicine, 2011: p. 2403.
144. Stein, P.E., et al., *Crystal structure of ovalbumin as a model for the reactive centre of serpins*. Nature, 1990. **347**(6288): p. 99-102.
145. Pereira, M.M., et al., *Single-step purification of ovalbumin from egg white using aqueous biphasic systems*. Process Biochemistry, 2016. **51**(6): p. 781-791.
146. González-Rodríguez, M.L. and A.M. Rabasco, *Charged liposomes as carriers to enhance the permeation through the skin*. Expert Opin Drug Deliv, 2011. **8**(7): p. 857-71.
147. Gupta, B., T.S. Levchenko, and V.P. Torchilin, *Intracellular delivery of large molecules and small particles by cell-penetrating proteins and peptides*. Adv Drug Deliv Rev, 2005. **57**(4): p. 637-51.
148. Nakamura, T., et al., *Efficient MHC Class I Presentation by Controlled Intracellular Trafficking of Antigens in Octaarginine-modified Liposomes*. Molecular Therapy, 2008. **16**(8): p. 1507-1514.
149. Miura, N., et al., *Modifying Antigen-Encapsulating Liposomes with KALA Facilitates MHC Class I Antigen Presentation and Enhances Anti-tumor Effects*. Molecular Therapy, 2017. **25**(4): p. 1003-1013.
150. Ma, Y., et al., *The role of surface charge density in cationic liposome-promoted dendritic cell maturation and vaccine-induced immune responses*. Nanoscale, 2011. **3**(5): p. 2307-14.
151. Vangasseri, D.P., et al., *Immunostimulation of dendritic cells by cationic liposomes*. Molecular Membrane Biology, 2006. **23**(5): p. 385-395.

152. Bozzuto, G. and A. Molinari, *Liposomes as nanomedical devices*. International Journal of Nanomedicine, 2015: p. 975.
153. Reece, J.C., et al., *Uptake of HIV and latex particles by fresh and cultured dendritic cells and monocytes*. Immunol Cell Biol, 2001. **79**(3): p. 255-63.
154. Takara, K., et al., *Size-controlled, dual-ligand modified liposomes that target the tumor vasculature show promise for use in drug-resistant cancer therapy*. Journal of Controlled Release, 2012. **162**(1): p. 225-232.
155. Saveyn, H., et al., *Accurate particle size distribution determination by nanoparticle tracking analysis based on 2-D Brownian dynamics simulation*. Journal of Colloid and Interface Science, 2010. **352**(2): p. 593-600.
156. Tran Le, T., et al., *Determination of heat-induced effects on the particle size distribution of casein micelles by dynamic light scattering and nanoparticle tracking analysis*. International Dairy Journal, 2008. **18**(12): p. 1090-1096.
157. Giaccone, G., et al., *A phase I study of the natural killer T-cell ligand alpha-galactosylceramide (KRN7000) in patients with solid tumors*. Clin Cancer Res, 2002. **8**(12): p. 3702-9.
158. Schneiders, F.L., et al., *Clinical experience with  $\alpha$ -galactosylceramide (KRN7000) in patients with advanced cancer and chronic hepatitis B/C infection*. 2011. **140**(2): p. 130-141.
159. Chang, D.H., et al., *Sustained expansion of NKT cells and antigen-specific T cells after injection of  $\alpha$ -galactosyl-ceramide loaded mature dendritic cells in cancer patients*. 2005. **201**(9): p. 1503-1517.
160. Ishikawa, A., *A Phase I Study of  $\alpha$ -Galactosylceramide (KRN7000)-Pulsed Dendritic Cells in Patients with Advanced and Recurrent Non-Small Cell Lung Cancer*. Clinical Cancer Research, 2005. **11**(5): p. 1910-1917.
161. Oki, S., et al., *The clinical implication and molecular mechanism of preferential IL-4 production by modified glycolipid-stimulated NKT cells*. 2004. **113**(11): p. 1631-1640.
162. Im, J.S., et al., *Kinetics and Cellular Site of Glycolipid Loading Control the Outcome of Natural Killer T Cell Activation*. Immunity, 2009. **30**(6): p. 888-898.
163. Wingender, G., et al., *Selective Conditions Are Required for the Induction of Invariant NKT Cell Hyporesponsiveness by Antigenic Stimulation*. J Immunol, 2015. **195**(8): p. 3838-48.
164. Chen, Q., et al.,  *$\alpha$ -Galactosylceramide treatment before allergen sensitization promotes iNKT cell-mediated induction of Treg cells, preventing Th2 cell responses in murine asthma*. Journal of Biological Chemistry, 2019. **294**(14): p. 5438-5455.
165. van Geffen, C., et al., *Myeloid-Derived Suppressor Cells Dampen Airway Inflammation Through Prostaglandin E2 Receptor 4*. Front Immunol, 2021. **12**: p. 695933.
166. Kolahian, S., et al., *The emerging role of myeloid-derived suppressor cells in lung diseases*. European Respiratory Journal, 2016. **47**(3): p. 967-977.
167. Parekh, V.V., et al., *Activated Invariant NKT Cells Control Central Nervous System Autoimmunity in a Mechanism That Involves Myeloid-Derived Suppressor Cells*. The Journal of Immunology, 2013. **190**(5): p. 1948-1960.
168. Nials, A.T. and S. Uddin, *Mouse models of allergic asthma: acute and chronic allergen challenge*. Disease Models and Mechanisms, 2008. **1**(4-5): p. 213-220.
169. Johnson, J.R., et al., *Continuous Exposure to House Dust Mite Elicits Chronic Airway Inflammation and Structural Remodeling*. American Journal of Respiratory and Critical Care Medicine, 2004. **169**(3): p. 378-385.

## APPENDIX

### Certificate of the Institutional Animal Care and Use Committee



Santiago, 10 de Enero de 2020

Certificado N°: **20342-MED-UCH**

#### CERTIFICADO

El Comité Institucional de Cuidado y Uso de Animales (CICUA) de la Universidad de Chile, certifica que en el Protocolo **CBA 1036**, del Proyecto de Investigación titulado: **“Modulación de células B y T reguladoras a través de la activación diferencial de células iNKT con glicolípidos contenidos en los liposomas”**, del Investigador **Richard García Betancourt**, Tesista del Programa de Doctorado en Ciencias Biomédicas, ICBM, Facultad de Medicina, Universidad de Chile y como Investigador Responsable y Patrocinador al Académico **Leandro Carreño Márquez**, Profesor Asociado, Programa de Inmunología, ICBM, Facultad de Medicina, Universidad de Chile, no se plantean acciones en sus procedimientos que contravengan las normas de Bioética de manejo y cuidado de animales, así mismo la metodología experimental planteada satisface lo estipulado en el Programa Institucional de Cuidado y Uso de Animales de la Universidad de Chile.


Ambos Investigadores se han comprometido a la ejecución de este proyecto dentro de las especificaciones señaladas en el protocolo revisado y autorizado por el CICUA, a mantener los procedimientos experimentales planteados y a no realizar ninguna modificación sin previa aprobación por parte de este Comité.

Se otorga la presente certificación para el uso de un total de **404** ratones según el siguiente desglose: **256** ratones Mus musculus cepa C57BL/6 hCD1d Knock-in, y **148** ratones Mus musculus cepa C57BL/6 hCD1d Knock-out, provenientes del Bioterio Central, Facultad de Medicina, Universidad de Chile, desde Enero de 2020 a Marzo de 2021, tiempo estimado de ejecución del estudio, el cual será financiado por **Fondocyt Nro. 1160336; Proyecto ICGEB crp-ch17-06-ec; Instituto Milenio de Inmunología e Inmunoterapia.**

*El CICUA de la Universidad de Chile, forma parte de la Vicerrectoría de Investigación y Desarrollo, y está constituido por 53 miembros: 5 médicos veterinarios, 39 académicos (12 de ellos médicos veterinarios), y 9 miembros no asociados a la academia o investigación, y que cuentan con experiencia en bioética relacionada a mantención y uso de animales. El certificado que emite el Comité procede de la aprobación del “Protocolo de Manejo y Cuidado de Animales” después de un estudio acucioso y de la acogida de los investigadores de las observaciones exigidas por el Comité.*

  
Ronald Vargas Casanova  
Director  
CICUA – VID  
Universidad de Chile



  
Dr. Emilio Herrera Videla  
Presidente  
CICUA - VID  
Universidad de Chile

Comité Institucional de Cuidado y Uso de Animales (CICUA)  
Vicerrectoría de Investigación y Desarrollo (VID) – Universidad de Chile

<http://www.uchile.cl/portal/investigacion/152120/comite-institucional-de-cuidado-y-uso-de-animales-cicua>  
email: [coordinador.cicua@uchile.cl](mailto:coordinador.cicua@uchile.cl)